Dissertation

submitted to the

combined Faculties for the Natural Sciences and for Mathematics

of the

Ruperto-Carola University of Heidelberg, Germany

for the degree of

Doctor in Natural Sciences

Presented by:

Shahrouz Ghafoory, Master of Immunology

Born in Kermanshah, Iran

Oral-examination:

Gene expression recovery during an acute toxic damage in the liver

Referees:

Prof. Dr. Stefan Wölfl, IPMB, Heidelberg University, Germany

Prof. Dr. Steven Dooley, Mannheim Medicine Faculty, Heidelberg University, Germany

List of publications:

Zonation of nitrogen and glucose metabolism gene expression upon acute liver damage in mouse.

Ghafoory S, Breitkopf-Heinlein K, Li Q, Scholl C, Dooley S, Wölfl S.

PLoS One. 2013 Oct 17;8(10):e78262. doi: 10.1371/journal.pone.0078262. eCollection 2013.

PMID:24147127

Bone morphogenetic protein-9 induces epithelial to mesenchymal transition in hepatocellular carcinoma cells.

Li Q, Gu X, Weng H, **Ghafoory S**, Liu Y, Feng T, Dzieran J, Li L, Ilkavets I, Kruithof-de Julio M, Munker S, Marx A, Piiper A, Augusto Alonso E, Gretz N, Gao C, Wölfl S, Dooley S, Breitkopf-Heinlein K.

Cancer Sci. 2013 Mar;104(3):398-408. doi: 10.1111/cas.12093. Epub 2013 Feb 13.

PMID:23281849

A fast and efficient polymerase chain reaction-based method for the preparation of in situ hybridization probes.

Ghafoory S, Breitkopf-Heinlein K, Li Q, Dzieran J, Scholl C, Dooley S, Wölfl S.

Histopathology. 2012 Aug;61(2):306-13. doi: 10.1111/j.1365-2559.2012.04237.x. Epub 2012 Mar 28.

PMID:22458731

Table of content

1.1 Summary

Specific structures and cell types in the organization of the liver are the key for its variant functions, like protein production, glucose homeostasis and detoxification. In the present work, liver damage from an acute toxic injury caused by intraperitoneal injection of a mixture of CCl_4 and mineral oil in Balb/c mice and its subsequent recovery was studied using different methods to investigate specific cellular functions in the liver. The analysis by *in situ* hybridization and RT-qPCR showed how expression of liver specific enzymes and proteins in mouse hepatocytes is changed over a period of 6 days following injection. The genes investigated included Albumin, Arginase, Glutaminase2, Glutamine synthetase, Glucose-6-phosphatase, Glycogen synthase2, Gapdh, Cyp2e1 and Glucagon receptor genes. Interestingly, a significant change in gene expression of enzymes involved in nitrogen and glucose metabolism and their local distribution in different areas of the liver were observed following CCl_4 injury. Cyp2e1, an essential metabolizing enzyme in CCl_4 metabolism, was strongly expressed in the pericentral zone during recovery. In comparison to hepatocytes in livers from untreated mice, liver cells from treated animals displayed distinct gene expression profiles in the damaged area around the pericentral vein during the analyzed time course and showed a complete recovery with strong albumin production at day 6 post CCl_4 injection. The results obtained indicate that despite of the severe damage, liver cells in the damaged area do not simply die but instead locally adjust gene expression to deal with the damage effect and thereby ensure survival.

In order to optimize the preparation of cRNA hybridization probes and enable the rapid synthetize of the large number of probes used in this study, a new rapid method for antisense cRNA preparation was established. The development of this rapid and efficient protocol for the generation of labeled cRNA probes was an important pre-requisite for the project. The new protocol is based on the preparation of DNA templates *in vitro* by PCR using primers that include RNA polymerase promoter sequences and size based purification of PCR fragments containing the target gene specific cDNA and promoter elements for T7 and SP6 RNA-polymerase. Purified PCR fragment based *in vitro* transcription enables the preparation

of *in situ* hybridization probes, which can be used for the detection of the respective gene and visualization of the distribution of gene expression in tissue slices for any gene of interest. The optimized synthesis and purification protocols ensure high transcription efficiency and target specificity of the labeled cRNA and the obtained cRNA hybridization probes are compatible with established *in situ* hybridization protocols.

This study proved that with a single dose of CCl4 injection in mouse, liver pericentral hepatocytes are the main cell type responsible for neutralizing the toxic agent, and the main consequence of this damage is not simply to induce cell death due to apoptosis, but instead these damaged hepatocytes seem to reduce any unnecessary activities in favor of processes needed for recovery from damage.

1.2 Zusammenfassung

Innerhalb des Lebergewebes sorgen spezifische Strukturen und Zelltypen für die verschiedenen Funktionen wie Proteinproduktion, Glucose Homöostase und Detoxifizierung. In der vorliegenden Studie wurden unterschiedliche Verfahren zur Untersuchung spezifischer zellulärer Vorgänge innerhalb des Regenerierungsprozesses der Leber nach akuter Belastung durch intraperitonealer Injektion von CCl4 und Mineralöl in Balb/c Mäuse untersucht. Die Analyse mittels in situ Hybridisierung und RT-qPCR zeigte, wie sich die Expression leberspezifischer Enzyme und Protein in murinen Hepatozyten über einen Zeitraum von sechs Tagen nach der Injektion verhielt. Folgende Gene wurden in diesem Zusammenhang untersucht Albumin, Arginase, Glutaminase2, Glutamine-synthetase, Glucose-6-phosphatase, Glycogen synthase2, Gapdh, Cyp2e1 und Glucagon Rezeptor Gene. Interessanterweise wurden nach ClC4 Belastung signifikante Änderungen in der Genexpression von Enzymen, welche in den Stickstoff- und Glucose Stoffwechsel involviert sind und derer Verteilung innerhalb des Lebergewebes nachgewiesen. Cyp2e1, ein essenzielles metabolisierendes Enzym innerhalb des Stoffwechsels von CCl4,

wurde während der Regeneration des Lebergewebes stark erhöht innerhalb der perizentralen Zone exprimiert. Im Vergleich zu Hepatozyten von unbehandelten Mäusen zeigten die Leberzellen der Versuchstiere charakteristisch ausgeprägte Genexpressionprofile innerhalb des geschädigten Bereichs um die perizentrale Vene auf. Eine vollständige Wiederherstellung und hohe Albuminexpression konnte sechs Tage nach der CCl4 Behandlung nachgewiesen werden. Die erhaltenen Ergebnisse weisen darauf hin, dass trotz des enormen Schadens Leberzellen innerhalb der beschädigten Areale nicht sterben, sondern lokal ihre Genexpression ändern, um die Schädigung zu bewältigen und ihr Überleben zu sichern. Um die Herstellung und rapide Synthese von cRNA Hybridisierungsproben, welche innerhalb dieser Studie verwendet wurden, zu gewährleisten, wurde eine neue Methode zur Herstellung von antisenser cRNA etabliert. Die Entwicklung einer schnellen und effektiven Methode zur Herstellung von markierter cRNA stellte eine entscheidende Voraussetzung zum Gelingen des Projektes dar. Das neu etablierte Protokoll basiert auf der Herstellung von DNA Templates durch in vitro Transkription mittels PCR. Hierfür wurden Primer, welche die RNA Polymerase Promotor Sequenz beinhalten und größenabhängiger Aufreinigung von PCR Fragmenten, die die cDNA des Zielgenes und die Promotor für T7 und SP6 RNA-Polymerase enthalten, verwendet. Aufgereinigte PRC Fragmente, welche auf in vitro Transkription basieren, ermöglichen die Herstellung von in situ Hybridisierungsproben. Diese dienen dem Nachweis des entsprechenden Genes und der Visualisierung der Verteilung der Genexpression eines beliebigen Genes innerhalb des Gewebes. Die optimierten Protokolle zur Synthese und Aufreinigung sorgen für eine hohe Transkriptionseffektivität und Zielspezifität der markierten cRNA. Die erhaltenen cRNA Hybridisierungsproben sind vergleichbar mit etablierten in situ Hybridisierungsprotokollen. Innerhalb unserer Studien haben wir nachgewiesen, dass nach einer Einzelbehandlung von Mäusen mit CCl4 , perizentrale Hepatozyten den hauptverantwortliche Zelltyp zur Neutralisierung der toxischen Substanz darstellen. Des Weiteren haben wir aufgezeigt, dass infolge der Schädigung nicht einfach der Zelltod durch Apoptose eintritt, sondern dass die geschädigten Hepatozyten sämtliche anderen Aktivitäten einstellen, um sich von dem Schaden zu erholen.

2 Abbreviations:

AFP	Alpha-fetoprotein
Arg1	Arginase
aSma	alpha-smooth muscle actin
BP	Base pair
BSA	Bovine serum albumin
cDNA	Complementary deoxyribonucleic acid
cRNA	Complementary ribonucleic acid
DAPI	4',6-diamidino-2-phenylindole
DIG	Digoxigenin
DMEM	Dulbeccos modified eagel-medium
DNA	Deoxyribonucleic acid
DNase	Deoxyribonuclease
dNTPs	Deoxyribonucleoside triphosphates
EDTA	Ethylenediaminetetraacetic acid
EtOH	Ethanol
FCS	Fetal-calf serum
g	Gram
G6pc	Glucose-6-phosphatase
Gapdh	Glyceraldehyde-3-phosphate dehydrogenase
Gcgr	Glucagon receptor
Gls2	Glutaminase 2
Gys2	Glycogen synthase 2
Gs	Glutamine synthetase
Gpx4	Glutathione peroxidase 4

Gsh	Glutathion
Gssg	Glutathione disulfide
Gss	Glutathione synthetase
ISH	*In situ* hybridization
IHC	Immunohistochemistry
µg	Microgram
$NADP^+$	Nicotinamide adenine dinucleotide phosphate
PCR	Polymerase chain reaction
PPH	Periportal hepatocyte
PPC	Percentral hepatocyte
RNA	Ribonucleic acid
RNase	Ribonuclease
Rpm	Round per minute
RT	Room temperature
UTP	Uridintriphosphat

3. Introduction:

3.1 Liver:

The liver is a vital and complex organ in vertebrates and plays a key role in many metabolic processes. It is the largest visceral organ and gland in the body. The liver has been found to participate in more than 500 separate functions. A healthy human liver is reddish brown in color and weighs about 1.44-1.66 kg. It contains four lobes of unequal size. Terminology related to the liver contains the prefix "hepato-", the Greek term for liver. This organ's wide range of functions includes detoxification, plasma protein synthesis, and the storage of vitamins and carbohydrate like glycogen. It also participates in bile production (as a side effect of red blood cell death and hemoglobin degradation), which is necessary for lipid degradation in intestine [1]. The liver is one of the first lines of defense between the host and the external environment. It is exposed to blood-borne pathogens, many of which are thought to be derived from the gut [2]. Eighty percent of the liver's volume is occupied by parenchymal cells, commonly referred to as hepatocytes. Non-parenchymal cells constitute Sinusoidal hepatic endothelial cells, Kupffer cells, and hepatic stellate cells.

The hepatic artery and the portal vein are two blood vessels connected to the liver. The blood from the aorta carries by the hepatic artery, whereas digested nutrients from the entire gastrointestinal tract and also blood from the spleen and pancreas carries by the portal vein. Only20% of the liver blood is arterially derived, the remaining originates from the portal vein [3]. Further inside the liver these blood vessels subdivide into capillaries, which then with hepatocytes form lobules. Acinies (lobule) are the basic functional units in the liver. These units consist of two separated areas with different functions, an upstream unit region which

constructed of hepatocytes around the terminal hepatic arteriole and terminal portal vein (the periportal zone) and a downstream hepatocytes region around the central vein (the perivenous, pericentral, or centrilobularzone). Hepatocytes belonging to these two areas due to distinct enzyme expression are known to be unequally involved in a variety of different metabolic processes. The periportal hepatocytes have greater ability for urea synthesis, bile formation and glucose output, whereas hepatocytes in the pericentral area are more responsible for glutamine formation, glucose uptake, and xenobiotic metabolisms [4, 5] (Figure 1).

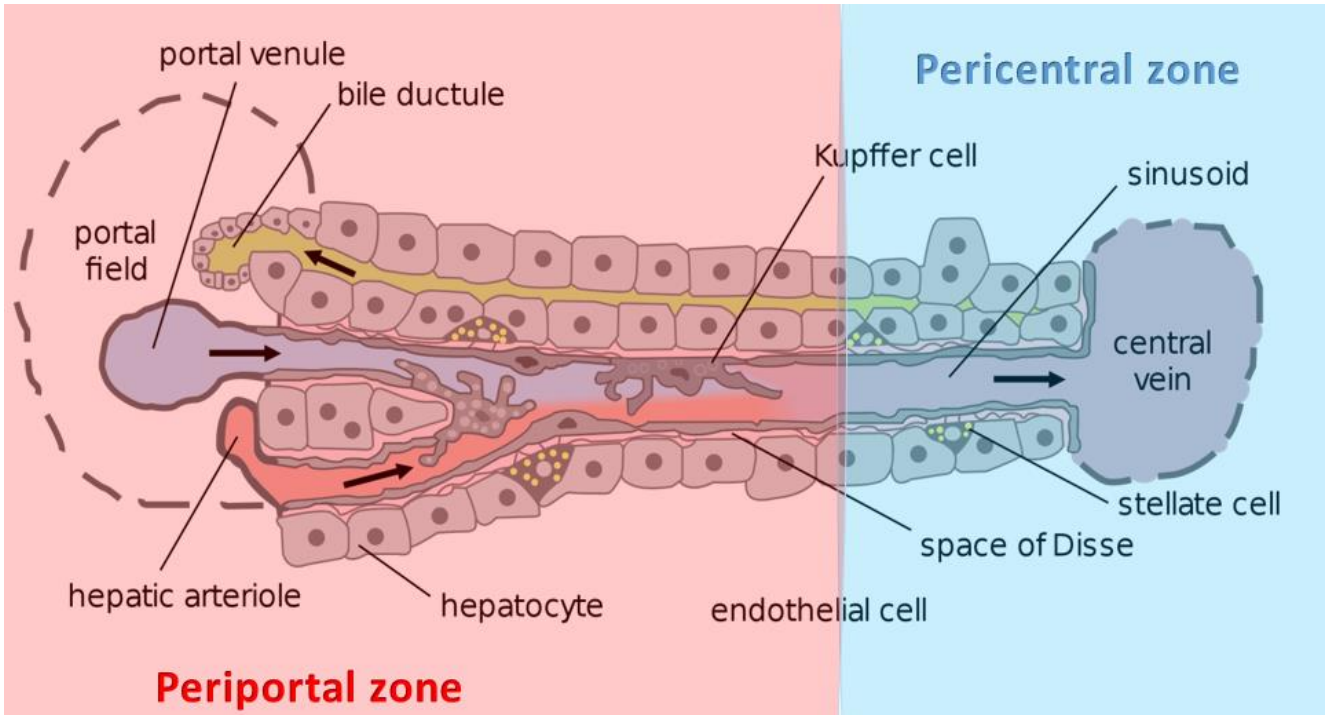

Figure 1: Illustration of part of a liver lobule (modified from Frevert U et al)

Based on the research article "Intravital Observation of *Plasmodium berghei* Sporozoite Infection of the Liver", PLoS Biology, doi:10.1371/journal.pbio.0030192.g011. Originally by Frevert U, Engelmann S, Zougbédé S, Stange J, Ng B, et al. Converted to SVG by Viacheslav Vtyurin who was hired to do so by User:Eug.

3.1.2 The liver functions in the body:

The liver performs several roles in the body:

Protein metabolism: Protein and amino acid synthesis, as well as degradation.

Carbohydrate metabolism: *Gluconeogenesis* (the synthesis of glucose from certain amino acids, lactate, or glycerol), *Glycogenolysis* (the breakdown of glycogen into glucose), and *Glycogenesis* (the formation of glycogen from glucose; muscle tissues can also do this).

Lipid metabolism: *Cholesterol synthesis*, *Lipogenesis*, and Triglycerides (fats) synthesis. Many other lipoproteins are also synthesized in the liver.

Coagulation factors synthesis: Factor I (fibrinogen), II (prothrombin), V, VII, IX, X, and XI, as well as protein C, protein S, and antithrombin (responsible for blood coagulation) are synthesized in the liver.

Lipid degradation: The liver produces and excretes bile, required for emulsifying fats and vitamin K absorption.

Hormone production: The liver is a major site of thrombopoietin (a glycoprotein hormone that regulates the production of platelets by bone marrow) and insulin-like growth factor 1 (IGF-1) production, as well as the degradation of insulin and other hormones.

Drug and toxic molecules modification: most medicines and toxic molecules are detoxified in the liver (drug metabolism). This sometimes results in toxication, when the metabolite is more toxic than the first one (CCl_4 neutralization).

Urea synthesis: The liver is the main source for producing urea.

Molecules storage: The liver stores glucose (in the form of glycogen), vitamin A, vitamin B12, vitamin K, iron, and copper.

Blood component producing: The liver produces Alpha fetal protein (AFP) in its embryonic state and Albumin (the major osmolar component of blood serum).

RBC producers: The liver is the main site of red blood cell production in the fetus (before the 32nd week of gestation) and is also responsible for immunological effects [1] .

3.1.3 Nitrogen metabolism:

The major by-product of proteins, amino acids and other nitrogen-containing molecules metabolisms is ammonia. Ammonia is a toxic and harmful molecule for cells and its physiological level should be maintained in a minimum level in the circulation. Liver (hepatocytes) is the only organ in the body that has the ability for urea synthesis from ammonia and this organ plays a central role in ammonia detoxification [6] (Figure 2).

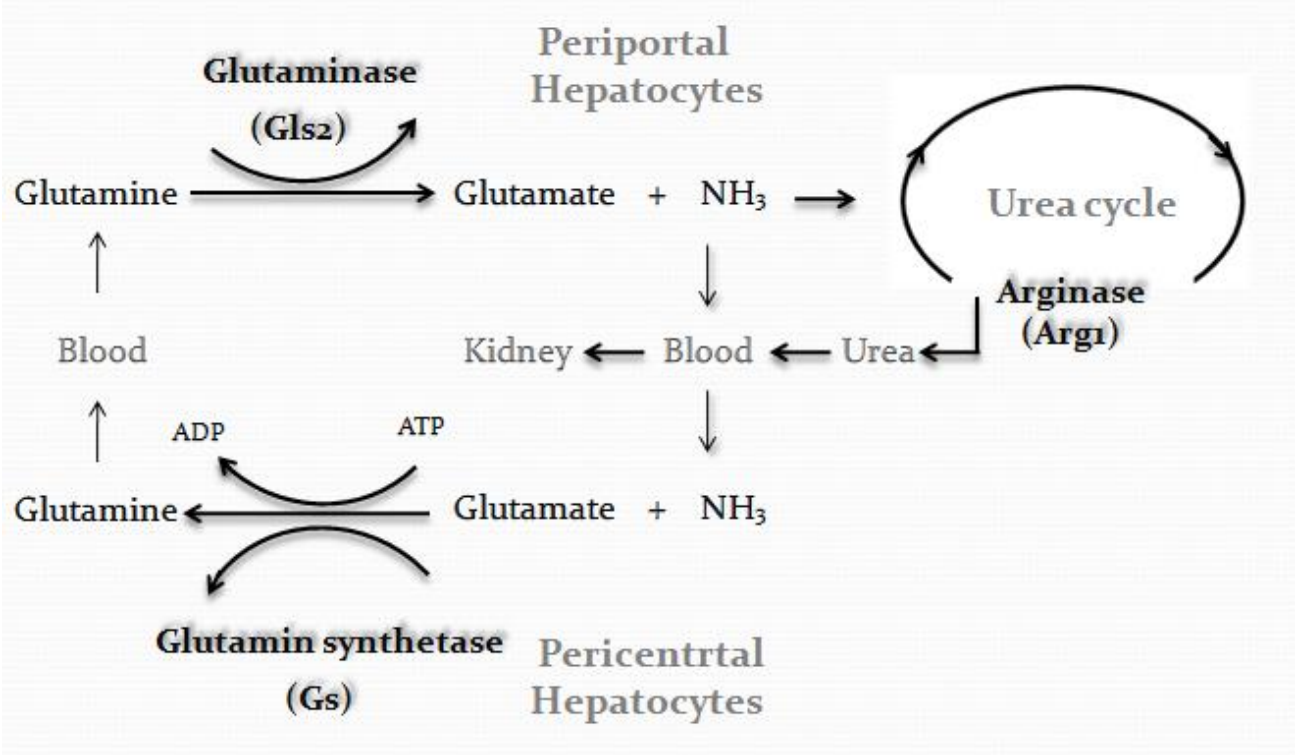

Figure2: Nitrogen cycle in the liver (modified from Ghafoory et al 2013)

In the liver anatomy, these two major ammonia detoxificating types of hepatocytes are separated within the liver lobules. In the periportal area hepatocytes with high capacity for urea synthesis are located, whereas other type of hepatocytes in the pericentral zone are the only cells in the liver responsible for glutamine synthesis (and ammonia detoxification by absorption from the circulation). In order to scavenge ammonia escaping from the periportal urea, these two ammonia detoxification systems are anatomically arranged in series [7]. Because ammonia's high toxicity glutamine is the most important amino acid for presenting nitrogen from other organs or tissues to the liver, of the nitrogen presented to the liver from other organs or tissues.The major sources for ammonia in the liver are also glutamine and glutamate. Periportal hepatocytes (PPH) are responsible for absorbing glutamine from circulation, the glutaminase enzyme hydrolyses glutamine into glutamate and ammonia in PPHs cytoplasm. In mitochondria of these cells, the toxic ammonia is introduced to the urea cycle and detoxification will done through urea conversion. There are five enzymes in the urea cycle. carbamoylphosphate synthetase I (CpsI), ornithine transcarbamylase (Otc), argininosuccinate synthetase (Ass), argininosuccinate lyase (Asl) and arginase. Arginase is a key enzyme in the urea cycle and catalyzes the last reaction in urea cycle is catalyzed by arginase, it is the key enzyme in converting arginine into urea and ornithine [8, 9] . Excess ammonia in the circulation is absorbed by 2-3 layer of hepatocytes around central vein (PCH) and in a reverse biochemical reaction glutamine is generated from ammonia and glutamate condensation. Glutamine synthetase is the enzyme which catalyze the reaction (Figure 2).

3.1.4 Carbohydrate metabolism:

The important molecule for energy storage in the body is glycogen which accumulates mainly in muscle and liver tissue [10]. Glycogen is a polysaccharide made from glucose, in this molecule many glucose molecules bound and form a chain, glycogen synthase catalysis this reaction by adding glucose-6-phosphate molecules one after the other in this chain [11] (Figure 3).

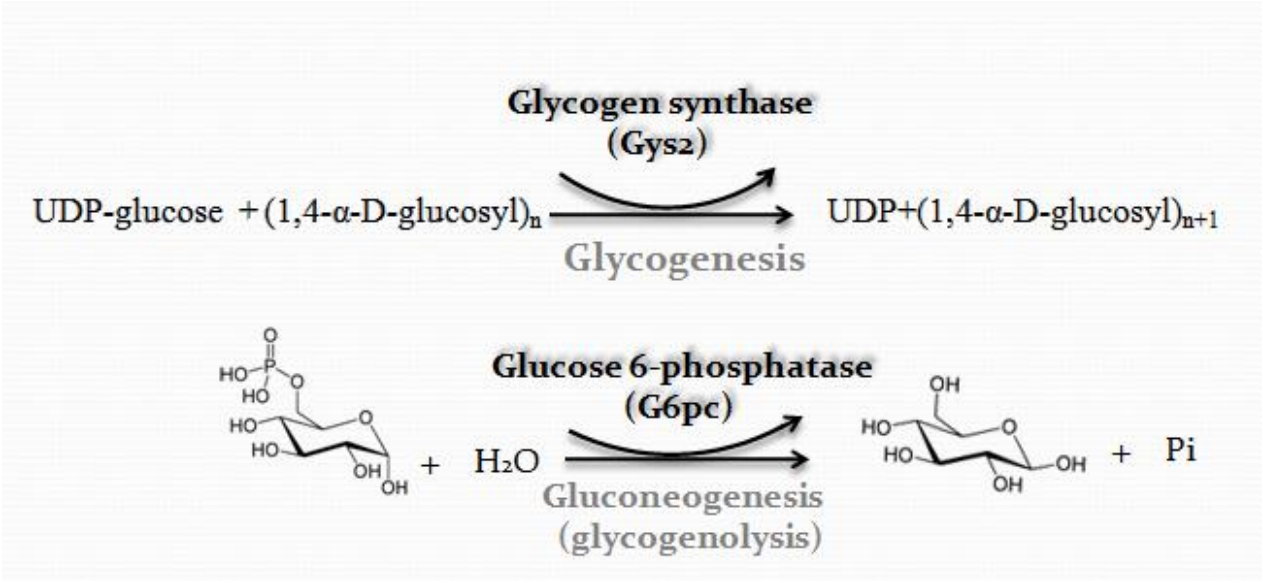

Figure 3: Glycogenesis and gluconeogenesis in the liver (modified from Ghafoory et al 2013)

Glycogen synthesis in the liver is either directly used the glucose absorbed from blood or through gluconeogenesis utilizing other precursors, like pyruvate, lactate or glutamine. It had been demonstrated, that glucose utilization and glycolysis is mostly found in perivenous hepatocytes, also known as pericentral hepatocytes (PCH), while gluconeogenesis is more taking place in periportal hepatocytes (PPH). Thus, both glycogen synthesis and glycolysis routes are almost taking place in different metabolic zones [12]. Glucose uptake is increased after meals (higher glucose level in the blood during absorptive phase) in PCHs, where glucose is converted to glycogen catalyzed by glycogen synthase 2 (Gys2). Between meals and in the post absorptive phase, first glycogen is degraded to glucose (Glycogenolysis) and later it is utilized in glycolysis leading to the production of lactate in the PCHs. Lactate is released from PCHs into circulation, it leaves the liver, and when it is brought back to the liver by the circulation, hepatocytes in the periportal zones can be taken it up and converted into glycogen via gluconeogenesis [5, 13, 14].

Glucose-6-phospate is the central metabolite in carbohydrate metabolism. It plays a key role for providing the connection between glycogenolysis, glycogen synthesis, glycolysis, and gluconeogenesis and also regulation of blood glucose level. Glucose-6-phospate is hydrolyzed by glucose-6-phosphatase (G6pc) into free glucose and a phosphate group [15]. By quantitative enzyme histochemical study had been shown in periportal hepatocytes glucose-6-phosphatase activity is much higher than in pericentral hepatocytes [11]. Another key enzyme in glycolysis is Glyceraldehyde 3-phosphate dehydrogenase (Gapdh). It is considered as "housekeeping" gene whichresponsible for conversion of glyceraldehyde-3-phosphate (G3p) to 1,3-biphosphoglycerate. It is important for energy production by glycolysis [16].

3.1.5 Liver damage:

The liver supports almost all other organs in the body and it is vital for survival. Its strategic location and multidimensional functions, prone it for many diseases. Detoxification and neutralization of medicine and molecules in the circulation is one of the most important of liver duty is. if the byproduct produces free radicals, detoxification of these molecules is a procedure can be harmful and induce injuries in liver hepatocytes,. In liver cells, free radicals can bind and react with different molecules (especially in cell organ construction).

The damage in cells can be various and directly depend on exposure repetition and dosage. The superfamily cytochrome P450 (CYPs) is a large and diverse group of enzymes (Table1). The *CYP* genes encode enzymes of the cytochrome *P*-450 superfamily. This group of proteins is expressed mainly in the liver and is active in the mono-oxygenation and hydroxylation of various xenobiotics, including drugs and alcohol, and also endogenous compounds such as steroids, bile

acids, prostaglandins, and leukotrienes. Their expression has a zonated pattern with high expression prevailing in the pericentral zone [17] . They are hemoproteins (cysteinato-heme enzymes) and containing a heme cofactor (Figure 4).

The prosthetic group is constituted of an in all of cysteinato-heme enzymes, iron(III) protoporphyrin- IX covalently linked to the protein by the sulfur atom of a proximal cysteine ligand [18]. Oxidation of organic substances are catalyzed by these enzymes Metabolic intermediates such as lipids and steroidal hormones and xenobiotic substances such as drugs and other toxic chemicals are their substrates. They involved in around 75% of drug metabolism and bioactivation of different metabolic reactions [19]. The most common reaction catalyzed by cytochromes P450 is mono oxygenase reaction During the reaction one atom of oxygen reduced to water and the other one is inserted into the aliphatic position of an organic substrate [19]. Change in active site conformation induced by substrate is the base and general mechanism for substrate metabolisms in this group of enzymes. By binding the substrate to the active site of the enzyme, change is induced in close proximity of heme group [18]. This conformational changes induce the electronic state changes in active site, an NADPH's electron is transfered by cytochrome P450 reductase (or another associated reductase) and ferric heme iron reduced to the ferrous state [20]. The heme iron can bind covalently to one atom of oxygen. The iron-oxygen covalent bindis relatively stable but can dissociate to an iron (III) and superoxide anion. Superoxide released from cytochromecan generate hydrogen peroxide which is harmful for cells [18]. .The mechanisms and carcinogenicity effects of hepatotoxic molecules can be studied by using these molecules *in vivo or in vitro*. The best and well-known toxic molecule is Carbon tetrachloride (CCl_4), it has been extensively used to study liver injury in animal models. Cytochrome p450 2e1 (Cyp2e1) in hepatocytes activates CCl_4 to generate the trichloromethyl radical, CCl_3*.

Family	Function	Members	Names
CYP1	drug and steroid (especially estrogen) metabolism	3 subfamilies, 3 genes, 1 pseudogene	CYP1A1, CYP1A2, CYP1B1
CYP2	drug and steroid metabolism	13 subfamilies, 16 genes, 16 pseudogenes	CYP2A6, CYP2A7, CYP2A13, CYP2B6, CYP2C8, CYP2C9, CYP2C18, CYP2C19, CYP2D6, CYP2E1, CYP2F1, CYP2J2, CYP2R1, CYP2S1, CYP2U1, CYP2W1
CYP3	drug and steroid (including testosterone) metabolism	1 subfamily, 4 genes, 2 pseudogenes	CYP3A4, CYP3A5, CYP3A7, CYP3A43
CYP4	arachidonic acid or fatty acid metabolism	6 subfamilies, 12 genes, 10 pseudogenes	CYP4A11, CYP4A22, CYP4B1, CYP4F2, CYP4F3, CYP4F8, CYP4F11, CYP4F12, CYP4F22, CYP4V2, CYP4X1, CYP4Z1
CYP5	thromboxane A_2 synthase	1 subfamily, 1 gene	CYP5A1
CYP7	bile acid biosynthesis 7-alpha hydroxylase of steroid nucleus	2 subfamilies, 2 genes	CYP7A1, CYP7B1
CYP8	varied	2 subfamilies, 2 genes	CYP8A1 (prostacyclin synthase), CYP8B1 (bile acid biosynthesis)
CYP11	steroid biosynthesis	2 subfamilies, 3 genes	CYP11A1, CYP11B1, CYP11B2
CYP17	steroid biosynthesis, 17-alpha hydroxylase	1 subfamily, 1 gene	CYP17A1
CYP19	steroid biosynthesis: aromatase synthesizes estrogen	1 subfamily, 1 gene	CYP19A1
CYP20	unknown function	1 subfamily, 1 gene	CYP20A1
CYP21	steroid biosynthesis	2 subfamilies, 1 gene, 1 pseudogene	CYP21A2
CYP24	vitamin D degradation	1 subfamily, 1 gene	CYP24A1
CYP26	retinoic acid hydroxylase	3 subfamilies, 3 genes	CYP26A1, CYP26B1 , CYP26C1
CYP27	varied	3 subfamilies, 3 genes	CYP27A1 (bile acid biosynthesis), CYP27B1 (vitamin D_3 1-alpha hydroxylase, activates vitamin D_3), CYP27C1 (unknown function)
CYP39	7-alpha hydroxylation of 24-hydroxycholesterol	1 subfamily, 1 gene	CYP39A1
CYP46	cholesterol 24-hydroxylase	1 subfamily, 1 gene	CYP46A1
CYP51	cholesterol biosynthesis	1 subfamily, 1 gene, 3 pseudogenes	CYP51A1 (lanosterol 14-alpha demethylase)

Table 1: Cytochromes P450 in humans (Modified from Nelson D 2003) Retrieved May 9, 2005

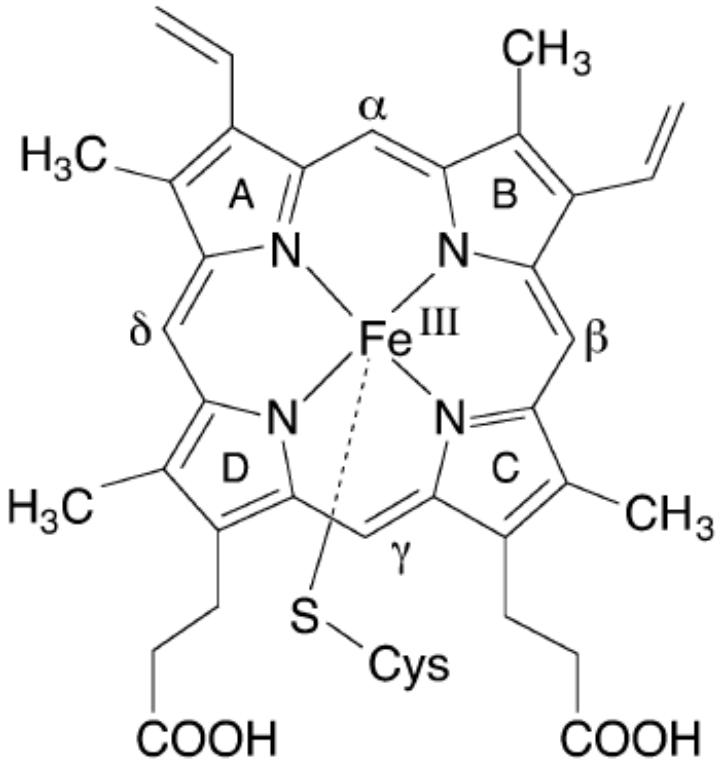

Figure 4: Prosthetic of cysteinato-heme enzymes: an iron- (III) protoporphyrin-IX linked with cysteine ligands (Uploaded from http: //drnelson.utmem.edu/ CytochromeP450 .html)

The reaction between this radical and various cellular molecules (e.g. nucleic acid, protein, lipid) or crucial cellular processes is harmful for hepatocytes (Figure 5)

In the oxygen excess presence, it can react with CCl_3* to form the trichloromethylperoxy radical CCl_3OO*, another highly reactive species. Under the aerobic conditions CCl_3OO* is formed very rapidly and in consequence lipid peroxidation proceed is start more faster with trichloromethylperoxy radical than trichloromethyl [21].

Damage is induced in cell membrane by attacking and destroying polyunsaturated fatty acids in response to lipid peroxidation (particular those associated with phospholipids). One of the most

important antioxidant molecules in hepatocytes is Glutathion (GSH) (Figure 6), a tripeptide composed of glutamin, cysteine, and glycine.

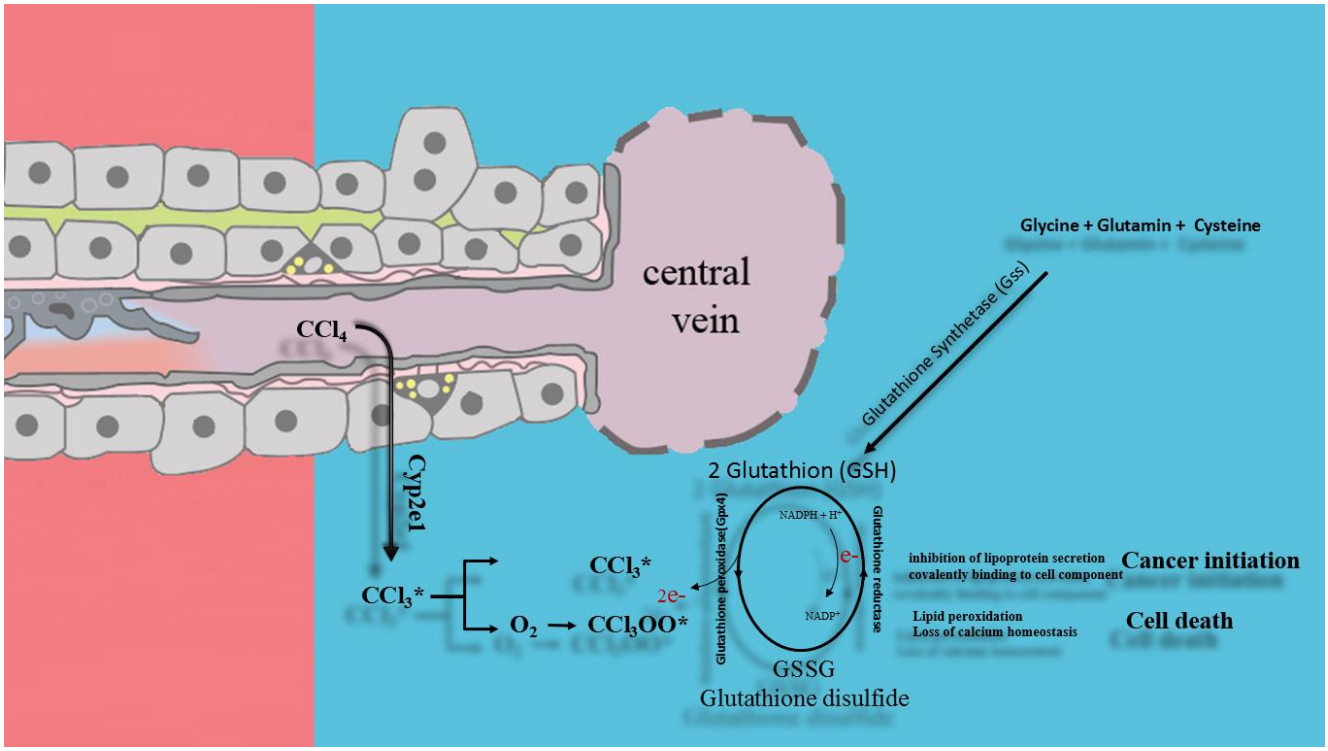

Figure 5: The mechanism of CCl_4 damage in hepatocytes

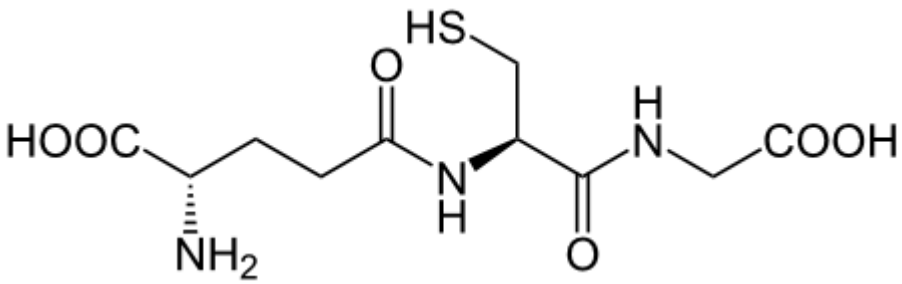

Figure 6: Glutathion (GSH) molecule (file from the Wikimedia Commons)

The sulfhydryl side chains of the cysteine residues can act as an electron donor in this process: two glutathione molecules form a disulfide bond (GSSG) and convert to glutathione disulfide (GSSG). Fig

This molecule is glutathione reductase substrate (GSR). To convert one molecule of GSSG to two GSH molecules, glutathione reductase requires NADPH as an electron donor. The ratio of GSH to GSSG is often used as a measure of cellular toxicity [22], Figure 7.

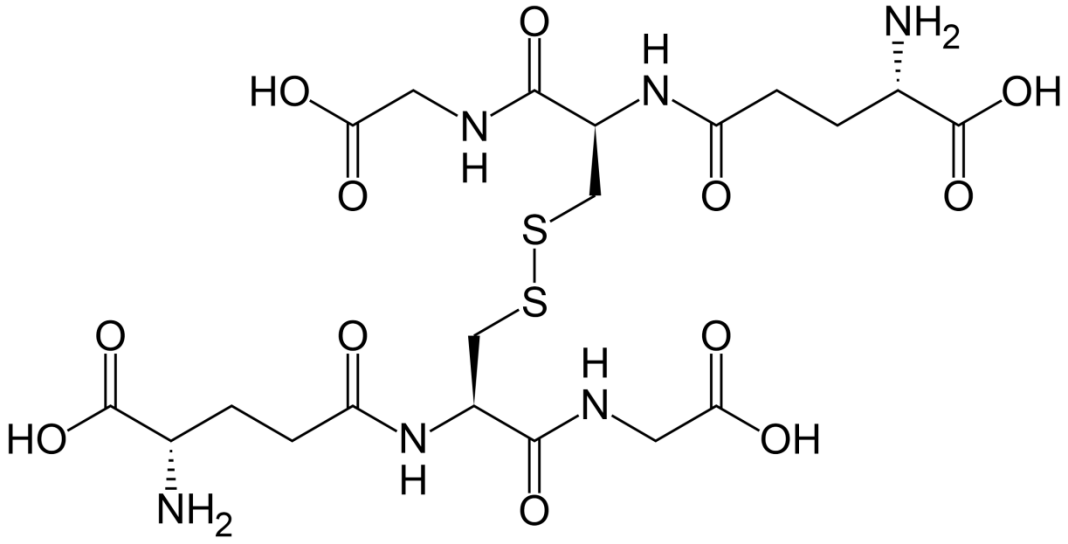

Figure 7: Glutathione disulfide (GSSG) This is a file from the Wikimedia Commons

In normal cells and tissues, more than 90% of the total glutathione is in the reduced form (GSH) and less than 10% has a disulfide form (GSSG). An increased GSSG to GSH ratio should be considered a symptom of oxidative stress [22]. The capacity of the liver to convert GSSG to GSH decreases with aging and, therefore, molecules responsible for lipid peroxidation are more likely accumulate to toxic levels after prolonged exposure or after a high dose administration.

The GSH/ GSSG ratio is decreased and CCl_4 mediated damage will lead to liver degeneration and could contribute to initiate hepatic cancer [17, 19, 23, 24].

It is well documented that antioxidants can prevent CCl_4 liver toxicity by inhibiting lipid peroxidation and increasing antioxidant enzyme activities [23, 25] . Cyp2e1 is predominantly expressed in pericentral hepatocytes (PCHs). Consequently, CCl_4 treatment leads to severe damage of PCHs, while periportal hepatocytes (PPHs) are not damaged [24, 26].It has been shown previously, that CCl_4 damage also influences nitrogen metabolism. Upon CCl_4 treatment, glutamine synthase activity was reduced, due to the damage of PCHs, and normal glutamine metabolism was disturbed, which resulted in impaired ammonia detoxification. Even so, periportal urea synthesis remained unchanged [27].

CCl_4 treatment also influences carbohydrate metabolism. Perfusion experiments with CCl_4 treated livers showed disturbed glycogen synthesis from exogenous glucose, while glycogen synthesis from gluconeogenesis was not impaired [28] Furthermore, treatment with CCl_4 also reduced the activity of glucose-6-phosphatase in isolated liver microsomes [29].

The aim of the present study was to analyze the effect of CCl_4 on the expression of important metabolizing enzymes in the different zones of liver acini in more detail, and to follow the course of expression over time, for 6 days after CCl_4 treatment. *In situ* hybridization was used on mouse liver sections to analyze gene expressions and distribution patterns of key enzymes (nitrogen and carbohydrate metabolisms).

3.2 In situ Hybridization:

3.2.1 History:

In cellular and molecular biology, hybridization establishes interactions between two complementary strands of nucleic acids to make a double-strand DNA or RNA complex. Under normal conditions, oligonucleotides from single strands of DNA or RNA will bind to a complementary strand, so two strands can bind to each other. In other words, using this technique allows for a visualization of the distribution of specific nucleic acid sequences in cells within a tissue section (*in situ*), or in the entire organ (whole mount ISH). ISH can also evaluate gene activity at the DNA or mRNA level Coghlan, Aldred [30], Gall and Pardue [31].

Among all different types of *in situ* hybridization, RNA ISH is used to visualize the localization of RNA (all kinds of RNA) expression within whole mounts, tissue sections, or cells. Since some types of tissue contain a range of different cell types with specialized functions, it is the preferred method for gene profiling studies. Any changes in gene expression and cellular function within the tissue can also be studied using this method. This technique was originally developed by Pardue and Gall, in 1969, Coghlan, Aldred [30] and at the same time independently by John et al. In the experiment which they developed it single strands DNA were bound with tritium-labeled RNA.

Radioisotopes labeled nucleic acids were the only source available in 1969 and molecular cloning was not possible. *In situ* hybridization was restricted to sequences like ribosomal RNAs, viral DNA, and mouse satellite DNA that could be isolated and purified by chemical methods.

Years later, improved radiolabeling techniques and nucleic acids molecular cloning changed this method dramatically. In 1985, Coghlan et al used these chemically synthesized radioactivity labeled oligonucleotides especially for mRNA detection [31]. Although *in situ* hybridization was widely applicable and the sensitivity of this technique was good, some problems associated with radioactive probes and the extensive time required for autoradiography made technique would

only be usable in a well-equipped laboratories techniques. These obstacles were removed by preparing nucleic acid probes labeled with stable nonradioactive molecules.

3.2.2 Non-radioactive *in situ* hybridization:

Non-radioactive *in situ* hybridization (ISH) is becoming increasingly popular because of the major advantages attached to this technique, when compared with the use of radioactively-labelled probes. Those advantages include longer half-life, higher safety, lower costs, and reproducibility due to the option of reusing the same probe, as well as a higher signal-to-noise ratio and better cellular resolution of the hybridization pattern [32].Among different modified oligonucleotides for *in situ* hybridization, Digoxigenin (Figure 8A) labeled nucleotides were introduced and developed by Roche in 1987 and the first ISH kit with nonradioactivenucleic acid for DNA detection was introduced to the market during the same year. Digoxigenin (DIG) is a steroid found exclusively in the flowers and leaves of the plants *Digitalis purpurea*, *Digitalis orientalis*, and *Digitalis lanata.* DIG is a high antigenicity

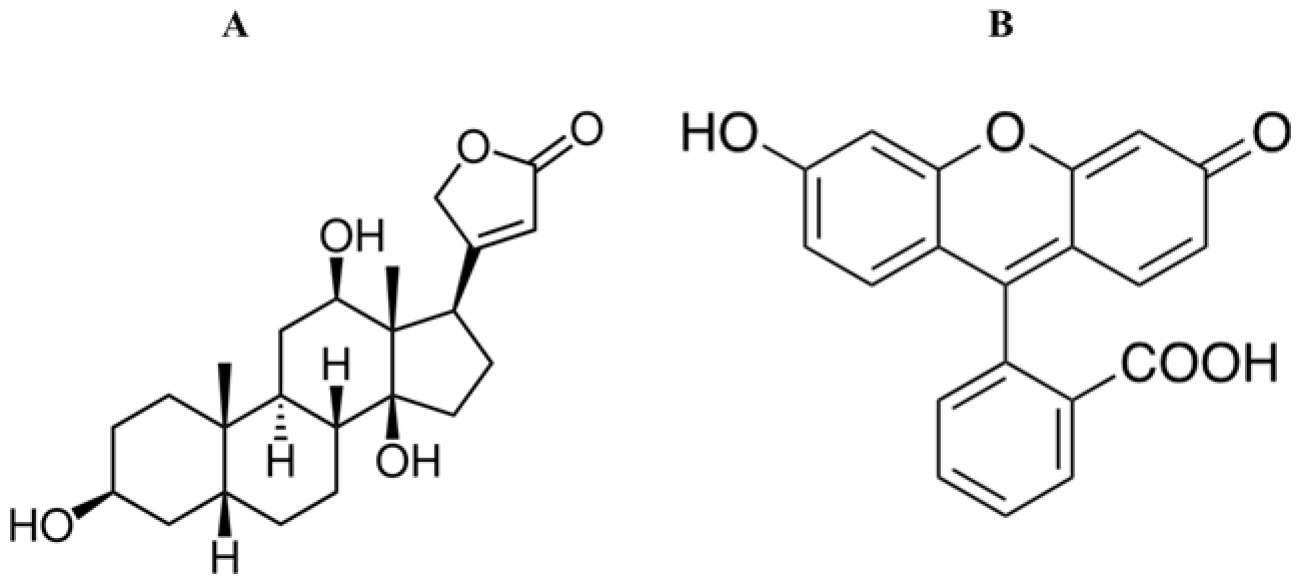

Figure 8A: Digoxigenin molecule, B: Fluorescein molecule(modified from Wikipedia)

hapten.This molecule can be chemically introduced into biomolecules like proteins and nucleic acids, to be detected further by using a specific antibody. Because naturally occurring DIG is limited to certain plants, there should be no cross reaction between anti DIG antibody and all other molecules in eukaryotic cells. Nucleotide molecules labeled with digoxigenin can be detected with anti-digoxigenin antibodies with high affinities. These antibodies can be labelled with dyes, enzymes, or fluorescence to visualize the site of expression directly. Using the secondary antibody can amplify the signal indirectly. Digoxigenin is linked to the C-5 position of the uridine nucleotide (Figure 9A) which is then incorporated into RNA (a "riboprobe") as it is synthesized by the enzymatic machinery [33]

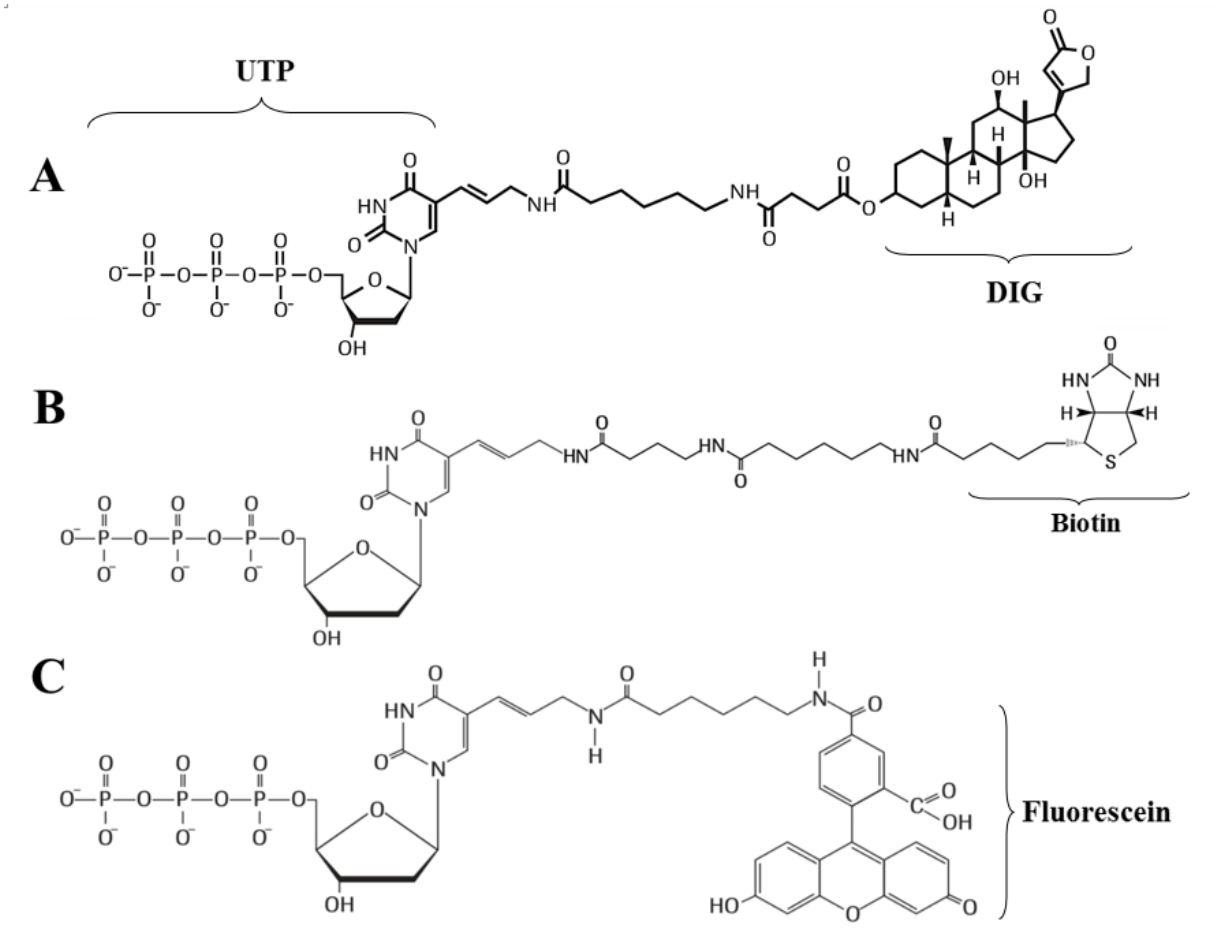

Figure 9 A: Uridine nucleotide conjugated with Digoxigenin (digoxigenin-UTP) B: Uridine nucleotide conjugated with Biotin (Biotin-dUTP) C: Uridine nucleotide conjugated with Fluorescein (Fluorescein –dUTP) (Figures modified from Wikipedia)

Fluorescein (Figure 8B) and Biotin labeled nucleotides were also introduced to the market by Roche in 1991 (Figure 9B and C). The mixture of nucleotides can be used for indirect and direct *in situ* hybridization [34, 35].

There are two types of nonradioactive labeling for *in situ* hybridization: direct and indirect. In the direct method, the detectable molecule is bound directly to reporter nucleic acid, and the hybridization of the target with this probe can be visualized immediately after hybridization, under the microscope. The fluorochrome labeled RNA probe developed by Bauman et al in 1980 [36], and the direct enzyme labeled nucleic acids described by Renz and Kurz in 1984 [37]. If antibodies against labeled nucleotides are available, the direct method can converted to the indirect method (see Hopman et al. 1986) [38].

3.2.3 Staining:

In this method, the reporter molecule should be accessible for the antibody and should not participate in any other reactions during the different steps of the method. Using Anti-DIG or fluorescein conjugated with alkaline phosphatase was developed by Roche. This staining is based on precipitation of soluble and colorless molecules during the interaction with an enzyme (mostly Alkaline phosphatase), perecipitated molecules accumulate in the cells and producing colour in the place of hybridized RNAs. As long as the enzyme is active and interacts with the substrate, the staining will be continue and get stronger, using this method for low expressed genes is profitable and staining can be amplify by enzyme substrate reaction prolonging. In this study two different NBT(Nitro blue tetrazolium chloride yellowish, soluble) /BCIP (5-Bromo-4-chloro-3-indolyl phosphate colorless, soluble) for violet staining and (Figure 10) INT(2-[4-iodophenyl]-3[4-nitrophenyl]-5phenyl-tetrazolium chloride)/BCIP for yellow staining were used

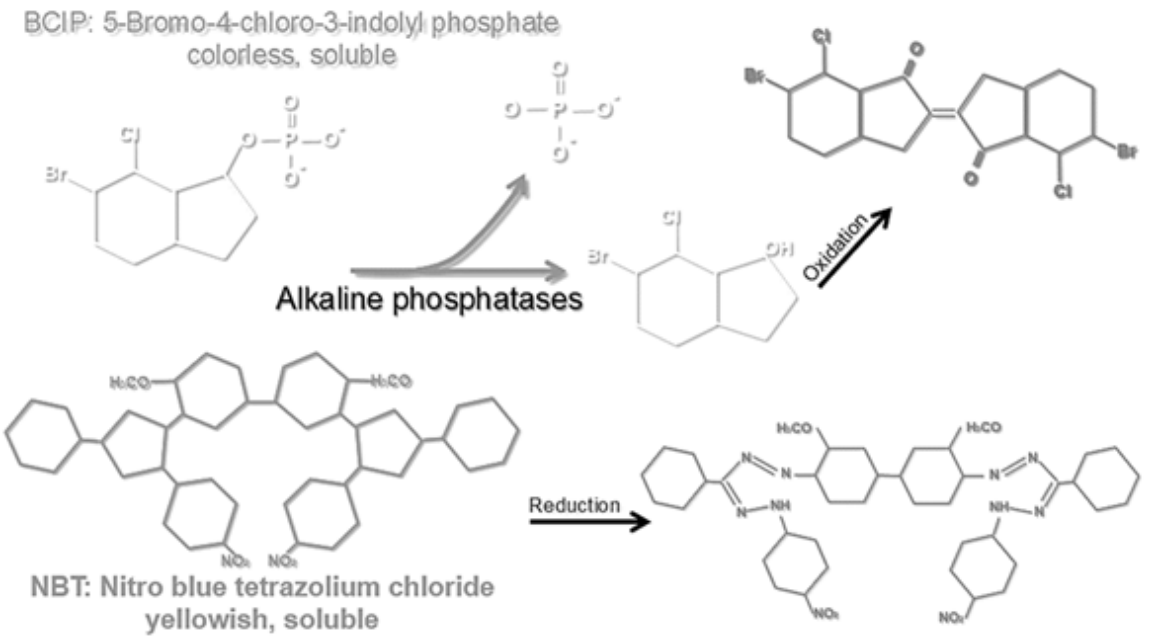

Figure 10: The chemical reactions between alkaline phosphatase as an enzyme and BCIP as the substrate, at the end the violet color is emerged

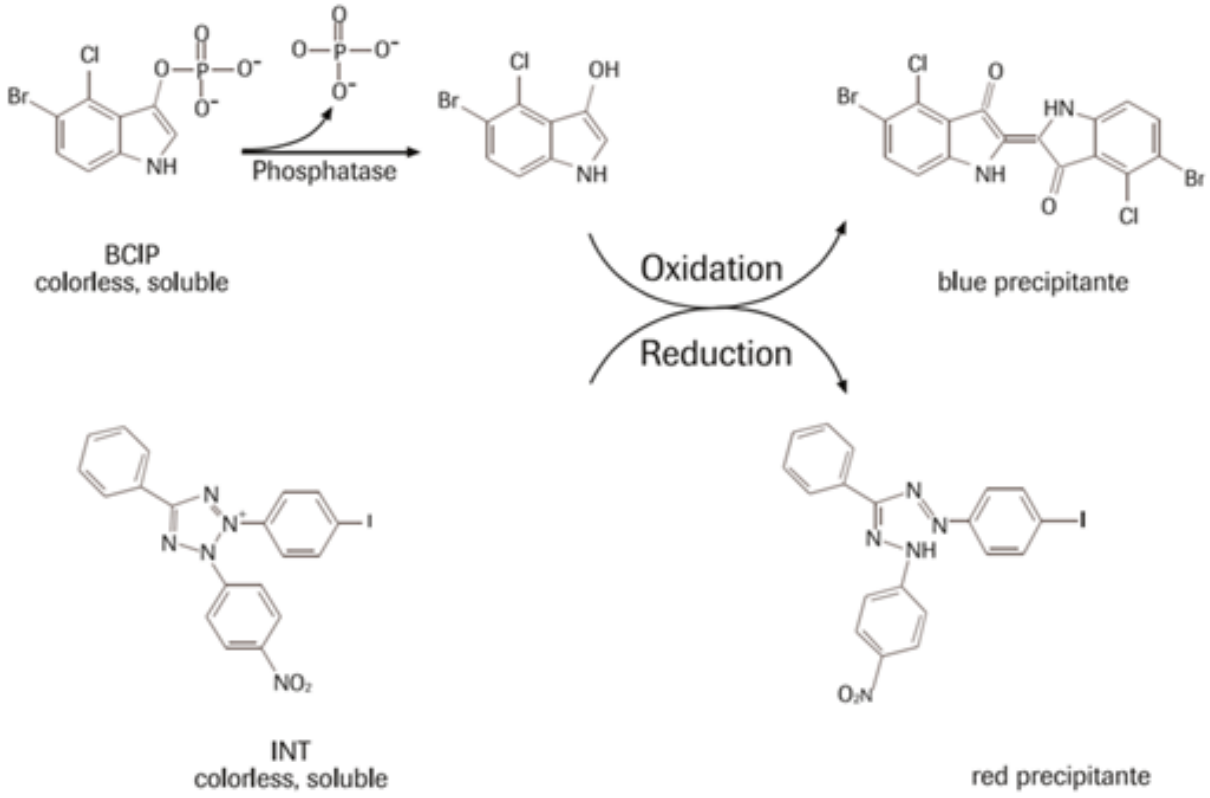

Figure 11: The chemical reactions between alkaline phosphatase as an enzyme and BCIP as the substrate, at the end the orange color is emerged

(Figure 11). In both staining BCIP is the alkaline phosphatase substrate, removing one phosphate group from BCIP induce it to interact with NBT or INT in the solution and new molecules forms new molecules which are not soluble anymore .

3.2.4 Probes (cRNA) preparation:

The first step of *in situ* hybridization is probe preparation. Normally, the researcher spends a great deal of time on this complicated procedure. Classic primer design and a standard PCR set-up for DNA amplification should be the first step. Following this, PCR products should run on an agar gel and DNA fragments be extracted from it. During this process, DNA fragments will be purified and prepared for vector insertion. In the next step, choosing the right vector and restriction enzymes are important (vectors should have one RNA polymerase sequence upstream or downstream from the insertion site). Following this step, the amplified DNA should be inserted in the vector which designed to amplify in bacteria, this process is referred to as "bacterial transformation" and is generally done by using *Escherichia coli* (*E. coli*). Vectors should have another important characteristic: they should contain the antibiotic resistant gene, such that only the colonies that pass transformation completely can grow on the agar plate. These colonies should be selected and cultured to amplify the vector and the DNA fragment inside it. After DNA extraction from the cultured colony, sequencing the DNA is necessary. If the DNA sequencing shows the vector contains a DNA fragment and it is in right direction for transcription, the transformed colony can be used and should be cultured in a bigger volume of media. At this step DNA extraction and purification should be done for transformed colonies in the culture. Purified vectors extracted from these colonies have to treat with a pair of restriction enzymes in order to separate target DNA from the vector. Restriction enzymes should cut and aim at RNA polymerase upstream and downstream from the inserted DNA fragment. The whole digested DNA mixture should then be separated by running it on an agar gel. Extraction and

subsequent purification of these fragments are the final steps in DNA preparation. These DNA fragments can then be used for antisense RNA (cRNA) synthesis.

3.2.5 New Method:

Unnecessary steps for cRNA preparation were made *in situ* hybridization as a complicated method for gene expressions study and synthesis a variety of antisense RNAs in a short period of time was not possible. Unnecessary steps for cRNA preparation made *in situ* hybridization a complicated method for gene expressions study, and synthesis a variety of antisense RNAs in a short period of time was not possible. Skipping many unnecessary steps for cRNA preparation was therefore necessary both to conserve materials, and to save time. In order to reach these goals, the new method was designed based on DNA amplification and primer design [39].

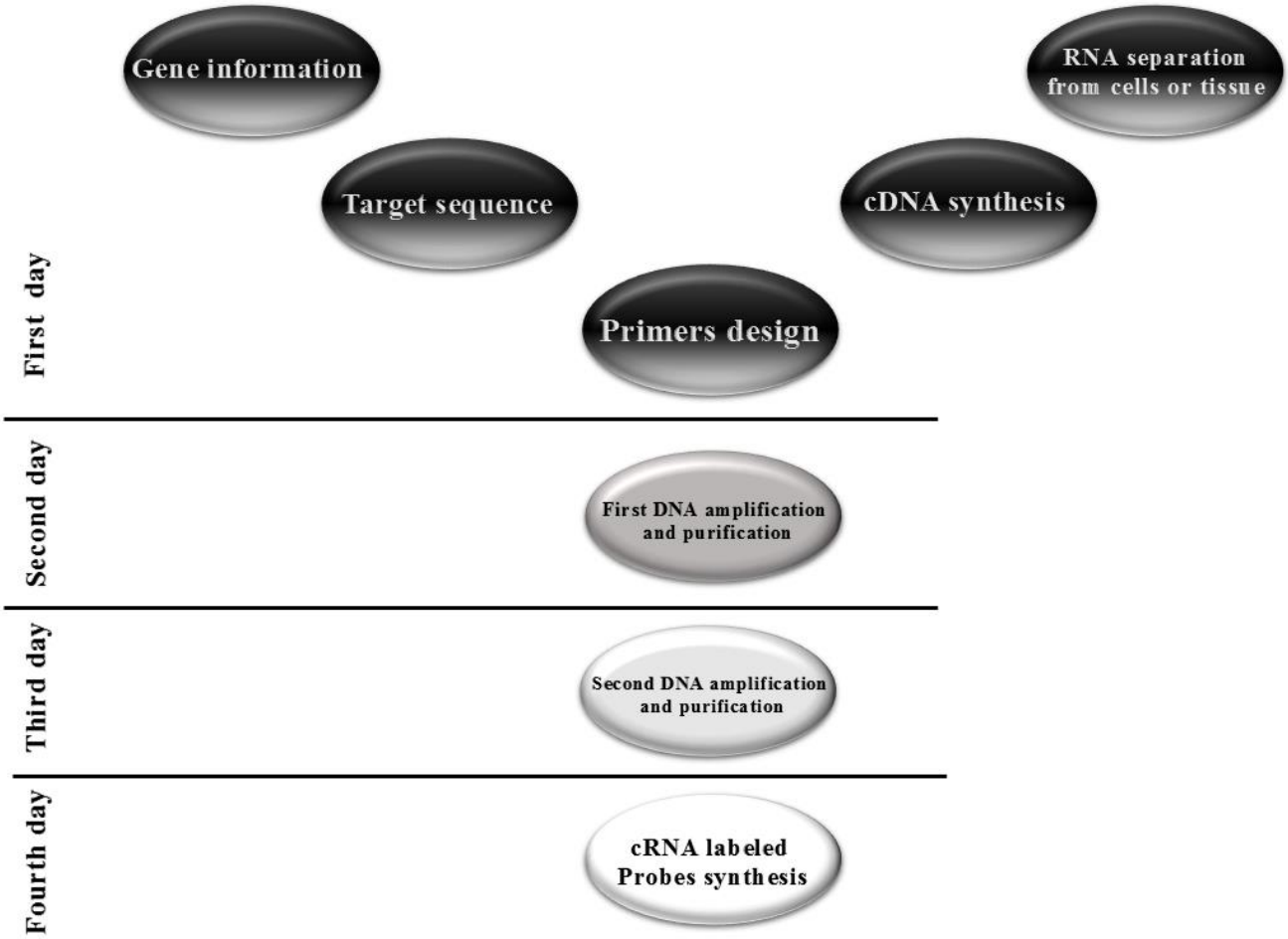

Figure 12: Schematic cRNA labeled preparation

The new method has the sufficient ability for digoxigenin or fluorescein labeled cRNA probes preparation in a few days, it makes *in situ* hybridization more readily for large scale gene expression analysis(Figure12).The protocol is based on two-steps Polymerase chain reaction (PCR) amplification and purification. By using extended PCR primers included the RNA-polymerase promoters, without time consuming for cloning and many purification and gene extraction steps, the protocol practically is reviled the fast method for any cRNA preparation [39]. Hybridized mRNA in tissue cells with antisense labeled cRNAs can be visible after precipitate formation (enzymatic reaction between alkaline phosphatase enzyme (conjugated with digoxigenin or fluorescein specific antibodies) and its substrate).

3.3 Aim of the study:

Recovery from acute toxic injury in the liver is a problem many people are daily confronted with. Such damage to hepatocytes can be induced by different molecules and medicines like ethanol or Acetaminophen. One of the most frequently used model to study acute liver injury is a single injection of CCl_4 as a toxic agent in mice or rats. In order to explore liver damage post CCL_4 injection and to study consequent gene expression patterns in liver cells, *in situ* hybridization was chosen. With this method the local pattern of gene expression in tissue samples was analyzed at the single cell level.

The following questions were addressed in this study:

1- Are hepatocytes massively dying under conditions of damage?

2- Which zone in the liver is targeted by CCl_4-mediated toxicity?

3- Is Cyp2e1 the key enzyme that triggers liver damage post CCl_4 injection?

4- Are the gene expression patterns related to nitrogen and carbohydrate metabolism changes in the liver during recovery from injury?

4 Materials and methods:

4.1 Chemicals and reagents:

Table 2:

Name	Company, Address
NaOH	Carl Roth GmbH+Co.KG, Karlsruhe Germany
KCl	Sigma-Aldrich Chemie GmbH, Munich, Germany
KH_2PO_4	Carl Roth GmbH+Co.KG, Karlsruhe Germany
NaCl	Applichem GmbH, Ottoweg 4 D-64291 Darmstadt, Germany
$MgCl_2$	Carl Roth GmbH+Co.KG, Karlsruhe Germany
Na_2HPO_4	Sigma-Aldrich Chemie GmbH, Munich, Germany
Na_2CO_3	Carl Roth GmbH+Co.KG, Karlsruhe Germany
$NaHCO_3$	Applichem GmbH, Ottoweg 4 D-64291 Darmstadt, Germany
NaOH	Carl Roth GmbH+Co.KG, Karlsruhe Germany
H_3BO_3	Carl Roth GmbH+Co.KG, Karlsruhe Germany
CH_3COOH	Merck, Darmstadt, Germany
HCl	Merck, Darmstadt, Germany
EDTA	Calbiochem, Darmstadt, Germany
Glutaraldehyde	Sigma-Aldrich Chemie GmbH, Munich, Germany
Sodium Citrate	Carl Roth GmbH+Co.KG, Karlsruhe Germany
Formamide	Carl Roth GmbH + Co Kg, Karlsruhe, Germany
Ethanol	Merck, Darmstadt, Germany
Xylol	Merck, Darmstadt, Germany
tRNA	Sigma-Aldrich Chemie GmbH, Munich, Germany
Chaps	Sigma-Aldrich Chemie GmbH, Munich, Germany
Tween 20	Carl Roth GmbH + Co Kg, Karlsruhe, Germany
Phenol	Carl Roth GmbH+Co.KG, Karlsruhe Germany
Chloroform	Sigma-Aldrich, Munich, Germany

Name	Company, Address
Heparin	Sigma-Aldrich Chemie GmbH, Munich, Germany
Isoamylalkohol	Sigma-Aldrich, Munich, Germany
Sodium acetate	Carl Roth GmbH+Co.KG, Karlsruhe Germany
Glycin	Applichem GmbH, Darmstadt, Germany
Proteinase K	Sigma-Aldrich, Munich, Germany
Penicillin/Streptomycine	Biochrom KG, Berlin, Germany
Paraformaldehyde	Sigma Aldrich, Munich, Germany
Ethidium Bromide	Sigma, Munich, Germany
Agasrose	Agarose Neeo ultra-quality, Carl Roth GmbH+Co.KG, Karlsruhe Germany
Boehringer Block	Roche/Boehringer, Mannheim, Germany
Tris-HCl	Carl Roth GmbH+Co.KG, Karlsruhe Germany
Fat pen	Vector Laboratories, Loerrach, Germnay
Boehringer Block	Roche/Boehringer, Mannheim, Germany
Trypsin	gibco by life technologies,Paisley, England
FCS	Fetal calf serum,Invitrogen, Karlsruhe, Germany
Goat serum	Invitrogen, Karlsruhe, Germany
Aquatex	mounting medium ,Merck, Darmstadt, Germany
SP6 RNA polymerase	20 U/µl, Fermentas, St. Leon-Rot, Germany
T7 RNA polymerase	20 U/µl, Fermentas, St. Leon-Rot, Germany
Oligo dt primer	Fermentas St. Leon-Rot, Germany
Random Hexamer	Fermentas St. Leon-Rot, Germany
Reverse Transcriptase	AMV Reverse Transcriptase, Promega, Madison, USA
DreamTaq	5 u/µl, Fermentas St. Leon-Rot, Germany
DIG RNA Labeling	DIG RNA Labeling mix, 10x conc, Roche, Mannheim, Germany
Fluorescein RNA Labeling	Fluorescein RNA Labeling mix,10x conc, Roche, Mannheim, Germany
Anti-Digoxigenin-AP	Fab Fragments**,** Roche, Mannheim, Germany

Name	Company, Address
Anti-Fluorescein-AP	Fab Fragments, Roche, Mannheim, Germany
RNA isolation kit	NucleoSpin® TriPrep purification system, Macherey-Nagel, Düren, Germany
DNA extraction kit	NucleoSpin® Extract II, Macherey-Nagel, Düren, Germany
NBT/BCIP	Roche/Boehringer, Mannheim, Germany
INT/BCIP	Roche/Boehringer, Mannheim, Germany
β-Mercaptoethanol	Sigma Aldrich, Munich, Germany

4.2 Buffers and reagents:

Table 3:

Buffers and reagents	Preparation
10x PBS	dissolve 1.37 M NaCl (80.1 g), 0.027 M KCl (2.0 g), 0.015 M KH_2PO_4 (2.0 g), 0.065 M Na_2HPO_4 x $2H_2O$ (11.6 g in) 1000 m Milipore-water l, adjust pH to 7.2-7.4
5x TBE	54 g Tris, 27.5 g Boric Acid(H_3BO_3), 20 ml EDTA 0.5M adjust the PH at 8.3 final volume with Milipore-water 500ml.
Buffers and reagents	Preparation
0.5x TBE	dilute50 ml 5x TBE buffer in 950 ml Milipore-water
1x TAE	dilute 20 ml 50x TAE buffer in 980 ml Milipore-water
Sodium acetate 3M	246 gram of Sodium acetate dissolve in 1L of Milipore-water
0.2% Glycin,	dissolve 0.4 g Glycin in 200 ml 1x PBS.
Proteinase K	Dissolve 100mg of Proteinase K in 10ml 1xPBS (10mg/ml)
Penicillin/Streptomycine	Stock solution 10000 U/ml, dilute with DMEM, working solution 100 U/ml
Ethidium Bromide	Dissolve 30mg of Ethidium Bromide in 10ml Milipore-water
Agarose gel	dissolve Agasrose Neo Ultra Qualität 1.0 g in 100ml 0.5x TBE buffer (or 100 ml 1x TAE buffer) in the microwave for 5min, add 10 µl Ethidium Bromide solution 3 mg/ml
2N NaOH	Dissolve 4 gram in 50 ml Milipore-water
4% PFA	heat 150 ml Milipore-water to 60°C. Add 8 g PFA (Paraformaldehyde), 1 ml 2N NaOH and 20 ml 10x PBS. Wait till the solution is clear, and adjust the pH to 7.4 with 30% HCl (ca. 161 µl). Fill up to 200 ml with Milipore-water and let it cool down.
4% PFA + 0.2% Glutaraldehyde	dilute 0.8 ml Glutaraldehyde in 200 ml 4% PFA
1x PBS+Tween	add 1ml Tween20 to 1 ml 1x PBS

Buffers and reagents	Preparation
B-Block	dissolve 2 g Boehringer Block in 90 ml 1x PBS +Tween in a water bath at 65°C. After cooling add 10 ml goat serum. Aliquots are stored at -20°C.
20x SSC	87.65 g of NaCl and 44.1 g of sodium citrate were dissolved in 400 ml distilled water. (pH 4.5) adjusted to 500 ml with Milipore-water.
2x SSC	add 20 ml 20x SSC pH 4.5 to 180 ml Milipore-water.
50% Formamid/2x SSC	mix 40 ml 20x SSC pH 4.5 with 200 ml 100% Formamide, then add Milipore-water to 400 ml.
0.5 M EDTA pH 8.0	Dissolve 18,6 gram in 100ml Milipore-water
10% CHAPS	Dissolve 10 gram in 100ml Milipore-water
Heparin (50 mg/ml)	Dissolve 50mg in 1 ml Milipore-water
tRNA (50 mg/ml)	Dissolve 50mg in 1ml Milipore-water
1mM EDTA	dilute 0.372 g EDTA in 1000ml Milipore-water
HYBmix	mix 25 ml Formamide, 12.5 ml 20x SSC pH 4.5, 500 mg Boehringer Block and 10 ml Milipore-water in a water bath at 65°C, add 500 µl 0.5 M EDTA pH 8.0, 50 µl Tween20, 500 µl 10% CHAPS, 20 µl Heparin (50 mg/ml) and 1 ml tRNA (50 mg/ml)
Tris-HCl pH 9.5 1M	Dissolve 60,5 gram in 500 ml Milipore-water, adjust pH at 9,5
NaCl 5M	Dissolve 29,25 gram in 100 ml Milipore-water
$MgCl_2$ 1M	Dissolve 40,66 gram in 200 ml Milipore-water
NTM pH9.5	mix 20 ml 1 M Tris-HCl pH 9.5, 4 ml 5 M NaCl with 10 ml 1 M $MgCl_2$ and add Milipore-water to 200 ml.
NBT/BCIP	Dissolve 20µl of stock solution in 980µl NTM pH9.5
INT/BCIP	Dissolve 7,5µl of stock solution in 980µl NTM pH9.5

4.3 Primers and sequences

4.3.1 Mouse Primers for *In situ* hybridization:

Table 4:

Mouse Genes	NCBI Reference		Primers
Albumin (S.Albu)	NM_009654.3	F	CAGTGAATTGATTTAGGTGACACTATAGAAGTGCTGTATCCCTGTTGCTGAGACTTGC
		R	CAGTGAATTGTAATACGACTCACTATAGGGAGAGTGCTTTCTGGGTGTAGCGAACTAG
Albumin (L.Albu)	NM_009654.3	F	CAGTGAATTGATTTAGGTGACACTATAGAAGTGCCTGCAACACAAAGATGACAACCCC
		R	CAGTGAATTGTAATACGACTCACTATAGGGAGAGGGATCCACTACAGCACTTGGTAAC
Arginase (Arg1)	NM_007482.3	F	CAGTGAATTGATTTAGGTGACACTATAGAAGTGGAGCTCCAAGCCAAAGTCCTTAGAG
		R	CAGTGAATTGTAATACGACTCACTATAGGGAGACGAAGCAAGCCAAGGTTAAAGCCAC
Glutaminase 2 (Gls2)	NM_001033264.3	F	CAGTGAATTGATTTAGGTGACACTATAGAAGTGCTTAGGCACTGACTACGTGCACAAG
		R	CAGTGAATTGTAATACGACTCACTATAGGGAGACCGAGACATCTCCACTATATGCAGC
Glutamine synthetase	NM_008131.3	F	CAGTGAATTGATTTAGGTGACACTATAGAAGTGCTCCATCCTGTTGCCATGTTTCGAG
		R	CAGTGAATTGTAATACGACTCACTATAGGGAGAGAGAGGGATCACTGGAAGTCTAGTC
Glucose-6-phosphatase (G6pc)	NM_008061.3	F	CAGTGAATTGATTTAGGTGACACTATAGAAGTGCCCATCCCAGGTTGAGTTGATCTTC
		R	CAGTGAATTGTAATACGACTCACTATAGGGAGAGAGAGAAGAATCCTGGGTCTCCTTG
Glycogen synthase 2 (Gys2)	NM_145572.2	F	CAGTGAATTGATTTAGGTGACACTATAGAAGTGCTGGGTTCATGTGACCTCAGATTGC
		R	CAGTGAATTGTAATACGACTCACTATAGGGAGACCTCGATGGCTGTGATTTCTGACAC
Gapdh	NM_008084.2	F	CAGTGAATTGATTTAGGTGACACTATAGAAGTGGAGTATGTCGTGGAGTCTACTGGTG
		R	CAGTGAATTGTAATACGACTCACTATAGGGAGAGGTTTCTTACTCCTTGGAGGCCATG
Cytochrome P450 (Cyp2e1)	NM_021282.2	F	CAGTGAATTGATTTAGGTGACACTATAGAAGTGCAAGGAGGTGCTACTGAACCACAAG
		R	CAGTGAATTGTAATACGACTCACTATAGGGAGAGATGACATATCCTCGGAACACGGTG
aSMA	NM_007392.2	F	CAGTGAATTGATTTAGGTGACACTATAGAAGTGGAAGAGCATCCGACACTGCTGACAG
		R	CAGTGAATTGTAATACGACTCACTATAGGGAGACAGTTGTGTGCTAGAGGCAGAGCAG
Gss	NM_008180.1	F	CAGTGAATTGATTTAGGTGACACTATAGAAGTGCTTCCTGGAGCAAACACTGTCTAGC
		R	CAGTGAATTGTAATACGACTCACTATAGGGAGACTCCAGAGCTTGTACCATTTCCTCC
Gpx4	NM_008162.2	F	CAGTGAATTGATTTAGGTGACACTATAGAAGTGGCTTACTTAAGCCAGCACTGCTGTG
		R	CAGTGAATTGTAATACGACTCACTATAGGGAGAGCTGGTTTTCAGGCAGACCTTCATG

4.3.2 Human Primers for *In situ* hybridization:

Table 5:

Human Genes	NCBI Reference		Primers
Albumin	NM_000477.5	F	CAGTGAATTGATTTAGGTGACACTATAGAAGTGGGTGAGACCAGAGGTTGATGTGATG
		R	CAGTGAATTGTAATACGACTCACTATAGGGAGACACACATAACTGGTTCAGGACCACG
Alpha-Fetoprotein (AFP)	NM_001134.2	F	CAGTGAATTGATTTAGGTGACACTATAGAAGTGGAGATAGCAAGAAGGCATCCCTTCC
		R	CAGTGAATTGTAATACGACTCACTATAGGGAGAGGGGGCTTTCTTTGTGTAAGCAACG

4.3.3 QRT-PCR primers

Table 6:

Gene	5' Primer	3' Primer
Alb	GTCTTAGTGAGGTGGAGCATGACAC	GCAAGTCTCAGCAACAGGGATACAG
Arg1	GGAGGCCTATCTTACAGAGAAGGTC	CGAAGCAAGCCAAGGTTAAAGCCAC
Gys2	CCTCGATGGCTGTGATTTCTGACAC	CTTGGGCGTTATCTCTGTGCAGCAA
Gcgr	CACAGTGATCATGCAGTACGGCATC	CAAACAGACACTTGACCACCACCCA
Gapdh	CTTCAACAGCAACTCCCACTCTTCC	GGTTTCTTACTCCTTGGAGGCCATG
Gls2	CTTCTGCCAGAAGTTGGTGTCTCTC	CCGAGACATCTCCACTATATGCAGC
Gs	GCCAGGAGAAGAAGGGCTACTTTGA	GAGAGGGATCACTGGAAGTCTAGTC
G6pc	TCCTCCTCAGCCTATGTCTGCATTC	GAGAGAAGAATCCTGGGTCTCCTTG
Cyp2e1	CACCGTGTTCCGAGGATATGTCATC	ACACACGCGCTTTCCTGCAGAAAAC

4.4 Total RNA isolation:

Total RNA was isolated from C57BL/6 mouse liver or HepGII cells using Total RNA isolation (Macherey-Nagel, Germany), for tissue RNA extraction, 30 mg of liver was cut from mouse liver and disrrupted in a tube and hemogenized it with 350µl of buffer RA1(+3.5µl β-Mercaptoethanol), for cell line RNA extraction, $5x10^6$ cells counted from culture and lysed with 350µl of buffer RA1(+3.5µl β-Mercaptoethanol). After mixing and complete homogenizing, the lysates were filtered through NucleoSpin (violet ring), it placed in a collection tube and centrifuged for 1 min at 11000 rpm.

Flow-throughs were collected in new 1.5 ml microcentrifuge tubes and 350µl EtOH(70%) were added to all filtered cell or tissue lysates. For RNA isolation, NucleoSpin® RNAII columns (light blue ring) were placed in a collection tubes and lysates loaded to the columns. Columns were centriguged for 30sec at 11000 rpm at this step total RNA were binded to the memberane. 350µl of MDB buffer were added to membrane (desalting memberane) and centrifuge columns at 11000 rpm for 30 sec.

95µl Dnase reaction mixture (10µl of reconstitute rDNase + 90µl reaction buffer) was added directly to the membrane and columns were incubated at RT for 15min. Digested DNAs were removed by adding 200µl of RA2 buffer to columns (centrifuged at 11000 rpm for 30sec), and RNAs were washed by adding 500µl of RA3 2 times (centrifuged at 11000 rpm for 30sec), membranes were dried at high speed centrifugation for 4 min, columns placed in new collection tubes and total RNAs were eluted from columns by adding 50µl Rnase free water. Total RNAs were collected with high speed spinning down. Total RNA concentrations were mesured by using Thermo scientific NANODROP 2000.

4.5 PCR Clean-up gel extraction:

The position of PCR products were excised from the 1% agarose gel (without ethidium bromide), for

each 100mg of agaroase gel 100µl NTI buffer was added and incubated at 50°C for 10min(till gell completely dissolve in the buffer), NucleoSpin® Gel and PCR Clean-up Column were placed into a collection tube, samples loaded and centrifuges them at 11000 rpm (DNA binding), membrane were washed with 700µl NT3 buffer and dried at high speed centrifugation. DNAs were eluted by adding 50µl pure water and their concentration were mesured with Thermo scientific NANODROP 2000.

4.6 Cell lines:

10^6 HepG2 cells (Hepatocellular carcinoma cell line) were suspended in 15ml media (DMEM with penicillin/streptomycin and 10% (v/v) FCS L-glutamine and penicillin/Streptomycin) and seeded in medium size flasks. Flasks were incubated in a standard tissue culture incubator at 37°C, 5% CO_2, and 95% humidity until 80–90% confluence(48h) were reached (10^7 cells). Cells were trypsinized and suspended in 10ml DMEM, after counting cells, the suspension centrifuged at 1000 rpm for 3min. The supernatant was removed and the pellet was resuspend with cold PBS to reach a final 5 x10^6/ml cell density, they were centrifuged at 1000 rpm for 3min and the lysate buffer was added to the pallet (the procedure was continued as mentioned for total RNA isolation.

4.7 RNA isolation from tissue:

RNA was isolated from C57BL/6 mouse liver and HepG2 cells using NucleoSpin® Total RNA isolation (Macherey-Nagel, Germany) as mentioned before, measured for total RNA concentration and used for cDNA synthesizes.

4.8 First cDNA synthesis:

First-strand cDNA was synthesized with 3µg total RNA using 1µl random hexamer primers and 1µl Oligo-dt primers (Fermentas) final volume 15µl with milipore-water in microptube. The mixture incubated for 5 min at 70°C and placed on ice after, 2µl dNTPs, 2µl AMV Reverse Transcriptase, 5µl 5x buffer (Promega, Madison) and 1µl RNase inhibitor were added when it completely cold(with the final 25µl volume). Microtubes were incubated at 42°C for 2h.

4.9 Primer Design:

"The key element in the protocol is primer design with additional RNA polymerase promoters which during PCR cycles are added in the template (Figure 13).The designed primers contained a short terminal 5' sequence followed by SP6 or T7-RNA-polymerase promoter sequences and target DNA specific primer sequences and sense and antisense cRNA probes can transcribed from the same amplified target DNA (PCR product) . To make it easy for sense and antisense RNA synthesis the SP6 promoter was combined with the upstream gene specific primer and the T7 promoter with the downstream primer, then using T7-RNA-polymerase with amplified target DNA generates antisense cRNA probes, while *in vitro* transcription by SP6-RNA-polymerase yielded sense cRNA probes. Primers were designed (listed in Fig13, tables 4 & 5) to synthesize cRNA probes against mouse albumin (LA-1202nt corresponding to nucleotide 423 to 1559 and SA-288nt corresponding to nucleotide 1143 to 1364 NM_009654.3), human albumin (Alb-

1108nt, nucleotide 490 to 1531 NM_000477.5) and human AFP mRNA (AFP-894nt, nucleotide 540 to 1367 NM_001134.1).

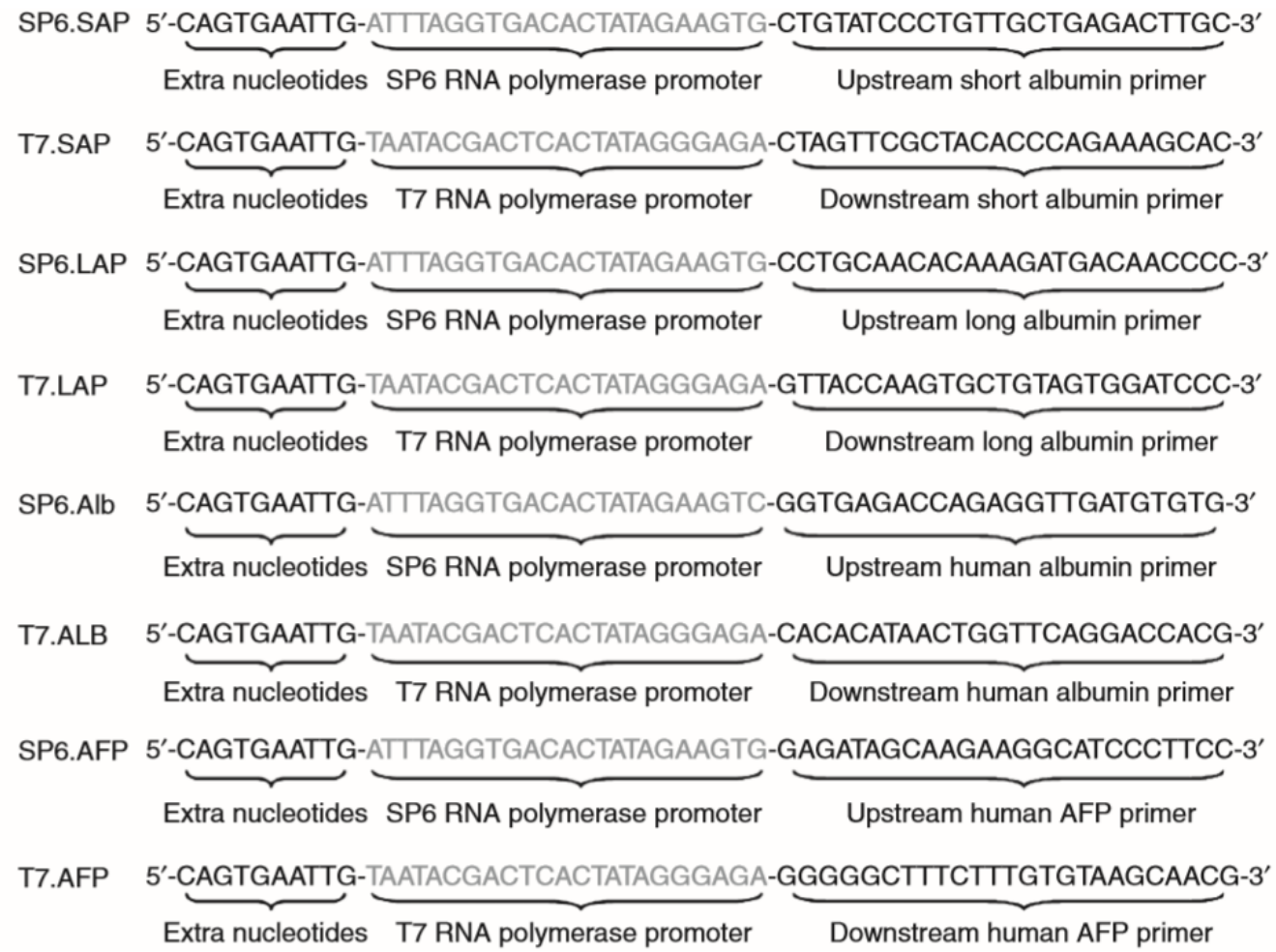

Figure13: Template cDNA synthesis by PCR (modified from Ghafoory et al 2012)

Template DNAs for ISH probes were prepared through two PCR amplification steps using SP6 or T7-RNA-polymerase promoter containing primers.

4.10 Template cDNA synthesis by PCR:

PCR templates were performed as follows: 1µg cDNA, 1µl dNTPs 10 mM, 0.5µl of DreamTaq 5 u/µl (Fermentas), 0.5µl upstream (Sp6) primer and 0.5µl downstream (T7) primer (each 100 pmol/µl) in a total volume of 50µl were used for the first PCR reaction. Primers detailed in figure 1 were used to synthesize mouse albumin (LA-1202nt, SA-288nt), human albumin (Alb-1108nt) and human AFP (AFP-894nt) cDNA fragments. Amplifications were performed with 2 min at 95°C, followed by 30 cycles with 30sec at 95°C, 2min at 60°C and 1min at 72°C.

Following PCR, complete samples were run on 1% agarose gel without ethidium bromide with a small aliquot of the reaction in a separate lane. This lane together with size standard was cut from the gel and stained to visualize PCR reaction products. The position of the PCR fragment in ethidium bromide stained lane was measured with a ruler and used to define the position of the corresponding non-stained gene specific cDNA PCR fragments. These were excised from the gel and extracted with DNA extraction kit (NucleoSpin® Extract II, Macherey-Nagel, Germany) as mentioned before. The remaining gel may be stained to ensure that the band was excised properly.

4.11 Second round of PCR amplification:

Purified PCR fragments were then used for a second round of PCR amplification in larger volume (e.g. 400µl) scaled up from the above protocol in parallel 50µl PCR reactions. The resulting template PCR fragments were purified and concentrated by phenol-chloroform extraction and ethanol precipitation. Concentrated PCR fragments were again purified using agarose (1%) gel electrophoreses and PCR fragments excision (without UV exposure) and recovered with DNA extraction kit (NucleoSpin® Extract II). Purified PCR fragments were used directly for *in vitro* transcription of cRNA probes.

4.12 Phenol-chloroform extraction and ethanol precipitation:

400µl of each PCR sample directly added to 200µl Phenol, 192µl of chloroform and 8µl of isoamylalkohol added to the mixture and mixed it completely, spin it for 20min (4°C) at 11000 rpm.The upper phase (contains cDNA) was collected in a new microtube . 400µl of chloroform was added to the collected sample and mixed well, mixtures was spined for 20min at 11000 rpm. The upper phase was collected and mixed with 40µl sodium acetate 3M, 3µl glycogen, 1200µl of pure EtOH and incubated at RT for 20min.

The mixture spined at high speed for 10min and the white pallet washed with %70 Ethanol. Washed pallet dried at RT and was dissolved completely in 50µl of Milipore-water. Following this step concentrated PCR fragments were again purified using agarose (1%) gel electrophoreses and PCR fragments excision (without UV exposure) and recovered with DNA extraction kit (NucleoSpin® Extract II). Purified PCR fragments were used directly for *in vitro* transcription of cRNA probes.

4.13 ISH riboprobe synthesis:

Digoxigenin (DIG) or Fluorescin labeled cRNAs were synthesized using 1µg of purified PCR fragments (template DNA), 1µl DIG or Fluorescin 10x nucleotide mix (Roche, Mannheim), 1µl SP6 or T7 RNA polymerase (20 u/µl, Fermentas) in 10µl total volume. SP6 RNA polymerase was used for sense labeled cRNA preparation and T7 RNA polymerase for antisense labeled cRNA preparation. The labeled cRNA probes were precipitated with absolute ethanol and the pellet was dissolved in 50% Formamide/ 2x SSC. Probes which were later hydrolyzed in order to modulate fragment length were dissolved in RNase free water.

4.14 Regulation of RNA probe length by alkaline hydrolysis:

Probe fragment length can be adjusted by alkaline hydrolysis to obtain smaller cRNA fragments (e.g. 200nt) which may penetrate tissue more efficiently [40].

1µg of the long cRNA probe (LA-1202nt) was dissolved in RNase free water to obtain a final volume of 50µl and was hydrolyzed by adding 30µl of Na_2CO_3 200 mM, 20µl of $NaHCO_3$ 200 mM and incubated for 37 min at 60°C [40]. The appropriate size distribution was controlled by gel electrophoresis.

4.15 Animal experiments:

4.15.1 Mouse treatment and liver resection:

CCl_4 injection in mice was regarded as a widely accepted model to study liver injuries and/or liver regeneration in vivo. 28 male (8-week-old) Balb/c mice weighing 20–25g were used. Acute liver injury was induced by intraperitoneal injection of CCl4 mixed with mineral oil 1:8 (1ml⁄kg body weight). All animals received humane care and all animal protocols were in full compliance with the guidelines for animal care and were approved by the government of Baden-Württemberg's Animal Care Committee, Regierungspräsidium Karlsruhe, Germany. Mice were sacrificed at 3 h, 6 h, day 1, day 2, day 3, and day 6 post injection and livers were used for *in situ* hybridization, immunohistochemistry and total RNA isolation. A portion of liver samples were fixed in 4% buffered paraformaldehyde for histological examination and immunostaining. The left were snap frozen in liquid nitrogen. 4 - 6 mice were used for every time point.

4.15.2 Mouse liver paraffin embedded block preparation:

Pieces of removed mouse liver tissues were rapidly rinsed in PBS and fixed with 4% PFA at 4°C overnight. Fixed tissue was washed with PBS (60min at RT) and dehydrated with 50%, 70%, 80%, 96% and pure EtOH (each of them 60min at RT). Dehydrated tissues were immersed in Aceton/EtOH (1:1) 90min RT and pure Aceton 60min RT, prepared tissues were embedded with prewarmed paraffin (62°C) for 3h, and cooled in tissue cassettes at room temperature.

4.16 Human liver Paraffin embedded tissue preparation:

Human liver paraffin-blocks were prepared from HCC patients at the Department of Laboratory Medicine, Eastern Hepatobiliary Surgery Hospital, Second Military Medical University, Shanghai, China. The study protocol conformed to the ethical guidelines of the Declaration of Helsinki (1975). The study was approved by the ethics committee of the Second Military Medical University, Shanghai, China. All patients provided an informed consent before the study.

4.17 Section preparation:

Sections were cut at a thickness of 4 μm (with microtom) and placed on poly-L-Lysine-covered slides. Paraffin sections were deparaffinized with pure xylene 3 × 7min, xylene/ethanol(1:1) 2 min and rehydrated in EtOH decreasing concentration 2 × 2 min pure EtOH and 96%, 90%, 70%, 50% (each of them 1 min) followed by PBS (5min). Sections were then incubated with 20

µl/ml proteinase K for 8 min at 37°C, with 0.2% glycin for 6 min and post-fixed with 4% PFA supplemented with 0.2% glutaraldehyde for 20 min.

4.18 *In situ* Hybridization (ISH):

After 'post-fixation' in 4% PFA-glutaraldehyde, slides were washed with PBS and sections were encircled with a fat pen (ImmEdge, Vector Laboratories). Mouse liver sections were covered with hybridization mix (5ml Formamid, 2.5ml 20x SSC, pH 4.5, 100mg Boehringer Block, 2ml Milipore-Water, 100µl 0.5 M EDTA, pH 8.0, 100µl Tween 20 (10%), 100µl 10% CHAPS, 4µl Heparin (50 mg/ml), 200µl tRNA (50 mg/ml)) and prehybridized for 1h at 69°C. The hybridization mix was denatured at 95°C for 5 min and chilled on ice immediately before it was added to tissue sections. After prehybridization, specific probes were added to 200-300µl hybridization mix in order to obtain a final concentration of 2 ng/µl. The probe containing hybridization mix was denatured at 95°C for 5 min and chilled on ice. For hybridization the hybridization mix was added to tissue sections and sections were incubated O/N at 70°C. Subsequently, tissue sections were washed with 2x SSC, incubated with 50% Formamide/ 2x SSC 30 min at 65°C, and washed with PBS containing 0.1% Tween at RT. The sections were then incubated for 1h at 37°C with 1% blocking reagent (Roche, Mannheim) in PBS (B-Block) and 2h at 37°C with alkaline phosphatase-coupled anti-digoxigenin antibody (Roche, Mannheim) diluted 1:1,000 in B-Block. Excess antibody was removed by washing for 8 min twice with PBS containing 0.1% Tween, then sections were equilibrated for 10 min in NTM Buffer (Tris-HCl 100mM, NaCl 100mM, and $MgCl_2$ 50mM, pH 9.5). Color development was performed at 37°C O/N in NTM buffer containing NBT/BCIP 20µl/ml (Roche, Mannheim). Staining was stopped washing twice with PBS.

For double staining, slices were again fixed 10 min at RT with 4% PFA/PBS. Tissue sections were washed with PBS containing 0.1% tween 3 times and then incubated for 1h at 37°C with 1% blocking reagent and 2h at 37°C with alkaline phosphatase-coupled anti-Fluorescein antibody (Roche, Mannheim) diluted 1:1,000 in B-Block. Excess antibody was removed by washing 3 times 15 min with PBS containing 0.1% Tween, then sections were equilibrated 10 min in NTM Buffer. Color development was performed at 37°C O/N in NTM buffer containing INT/BCIP 7.5µl/ml (Roche, Mannheim). Staining was stopped washing twice with PBS**.** Tissue sections were analyzed and recorded using a digital microscope (Biozero 8000, KEYENCE).

4.19 Immunohistochemistry (done by Qi Li):

4.19.1 Deparaffinization:

Immunohistochemistry for alpha-smooth muscle actin (aSma) was performed on paraffin embedded mouse liver tissue sections following standard protocols, first deparaffinization was done by incubating tissue sections at 60° C for 60 min. They were dewaxed with xylene for 5 min 3 times. Sections were dehydrated through descending ethanol: 100% ethanol for 5 min twice and 95%, 70% and 50%ethanol for 5 min once, at the end sections were incubated in distilled water 1 × 5 min, followed by being rinsed in PBS 1 × 5 min.

Antigen demaskingwas done for sections using microwave, they were heated up to 95° C (2 - 3 min 200 W) in 10 mM EDTA pH 8, then 50 sec-off-10 sec-on of the microwave were performed for 10 min. Then sections were cooled for 35 - 40 min to reach a temperature of 37° C and washed with PBS 3 × 5min.Tissues were covered with some drops of Dual Endogenous enzyme block in a humid atmosphere for 15 min in order to endogenous peroxidase blocking(DAKO, Glostrup, Denmark). Signal was visualized using 3,3'- diaminobenzidine (DAB) staining. After sections were washed with PBS 3 × 5min, they were incubated with the diluted α-SMA antibody

(DAKO, Glostrup, Denmark) at 4° C overnight. Afterwards, they were re-warmed at room temperature for 1 hour and washed with PBS 3 × 5 min before incubation with secondary goat anti-mouse antibody (DAKO, Glostrup, Denmark).

4.19.2 Preparation and application of peroxidase substrate DAB:

1 tablet of DAB was dissolved in 15 ml 0.05 M Tris (hydroxymethyl) aminomethane, pH 7.6 (keep in dark) which was filtered with filter paper. 12 µl H_2O_2 was added to the filtrate. Sections were washed with PBS 3 × 5 min and covered with 200 µl of the substrate. The color development was observed under the microscope (maximally incubation time: 10 min) and the reaction was stopped by immersing the sections in distilled water for 5 min.

4.19.3 Counterstaining, clearing and mounting:

Sections were immersed in Mayers Hämalaun solution for several seconds and then rinsed with water for 10 min, followed by being dehydrated through ascending ethanol: 95% ethanol 2 × 10 sec and 100% ethanol 2 × 10 sec. Clearing was performed in xylene 2 × 10 sec. Finally sections were mounted with malin oil and covered with glass.

4.20 Quantitative real time reverse transcription PCR:

775 ng of total RNA isolated from C57BL⁄6 mouse liver was reverse transcribed using Roche first strand cDNA synthesis kit with Oligo dT primers. Quantitative real-time PCR was performed on a LightCycler® 480 (Roche Applied Science) using 2 µl cDNA (1:10 dilution of transcribed cDNA), LightCycler® 480 SYBR Green I master mix (Roche) and respective PCR primers. Primer pairs used for qRT-PCR are listed in following Table 2.

qPCR was performed using the following protocol: 1 cycle pre-incubation: 5 min at 95°C, followed by 40 amplification cycles: 10s at 95°C, 10s at 60°C 20s at 72°C. For all samples a

melting curve analysis was performed in order to monitor the generation of expected unique PCR products.

For statistical analysis, relative expression (RE) levels were calculated with the function ($RE = 2^{-\Delta\Delta Ct}$), where $\Delta\Delta Ct$ is the normalized difference in threshold cycle (Ct) number between the control sample and the CCl4- treated sample. Each Ct value was calculated from triplicate replicates of any given condition. All samples were normalized to the corresponding expression level of albumin. The mean of relative expression levels were calculated from the individual RE values from 2 independent experiments, and the standard error of the mean (SEM) was calculated from the standard deviation. In order to evaluate the statistical significance the Student's T-test was employed, comparing control sample to CCl_4- treated samples.

5 Results:

5.1 Primer design:

Primer design is the most important step in our protocol (Fig.13). In addition to gene specific sequences, an SP6 RNA polymerase promoter sequence was included in the upstream and a T7 RNA polymerase sequence in the downstream primer. Thus, templates for *in vitro* transcription were directly generated by PCR and antisense cRNA probes were synthesized using T7-RNA-polymerase, while *in vitro* transcription by SP6-RNA-polymerase yielded sense cRNA probes [39]. To test this method, the PCR primers listed in figure 13 and tables 4&5 were designed. These primers were used to prepare mouse albumin sense and antisense cRNAs [Long Albumin(LA)-1202nt corresponding to nucleotides 423 to 1559, and SA288nt corresponding to nucleotide 1143 to 1364 NM_009654.3], human albumin antisense cRNA (Alb-1108ntnucleotide 490 to 1531 NM_000477.5), and human AFP antisense cRNA (AFP-894nt, nucleotide 540 to 1367 NM_001134.1) [39].

5.2 Template synthesis, first PCR:

Template cDNAs for ISH probes were prepared through two PCR amplification steps using SP6 or T7-RNA-polymerase promoter containing primers. PCR templates were performed as mentioned in the materials and methods section. Primers detailed in Figure13 were used to synthesize and amplify mouse albumin (LA-1202nt, SA-288nt), human albumin (Alb-1108nt), and human AFP (AFP-894nt) cDNA fragments by using the PCR method (Figure 14). Components which participated in the PCR reaction are explained schematically in Figure 14A. The first cycle of the PCR reaction begins with DNA denaturation at 95°C (DNA melting). Reaction then continues with the cooling down of the system to an annealing temperature (60-65°C). At this temperature, primers (that are complementary to the 3' ends of each of the

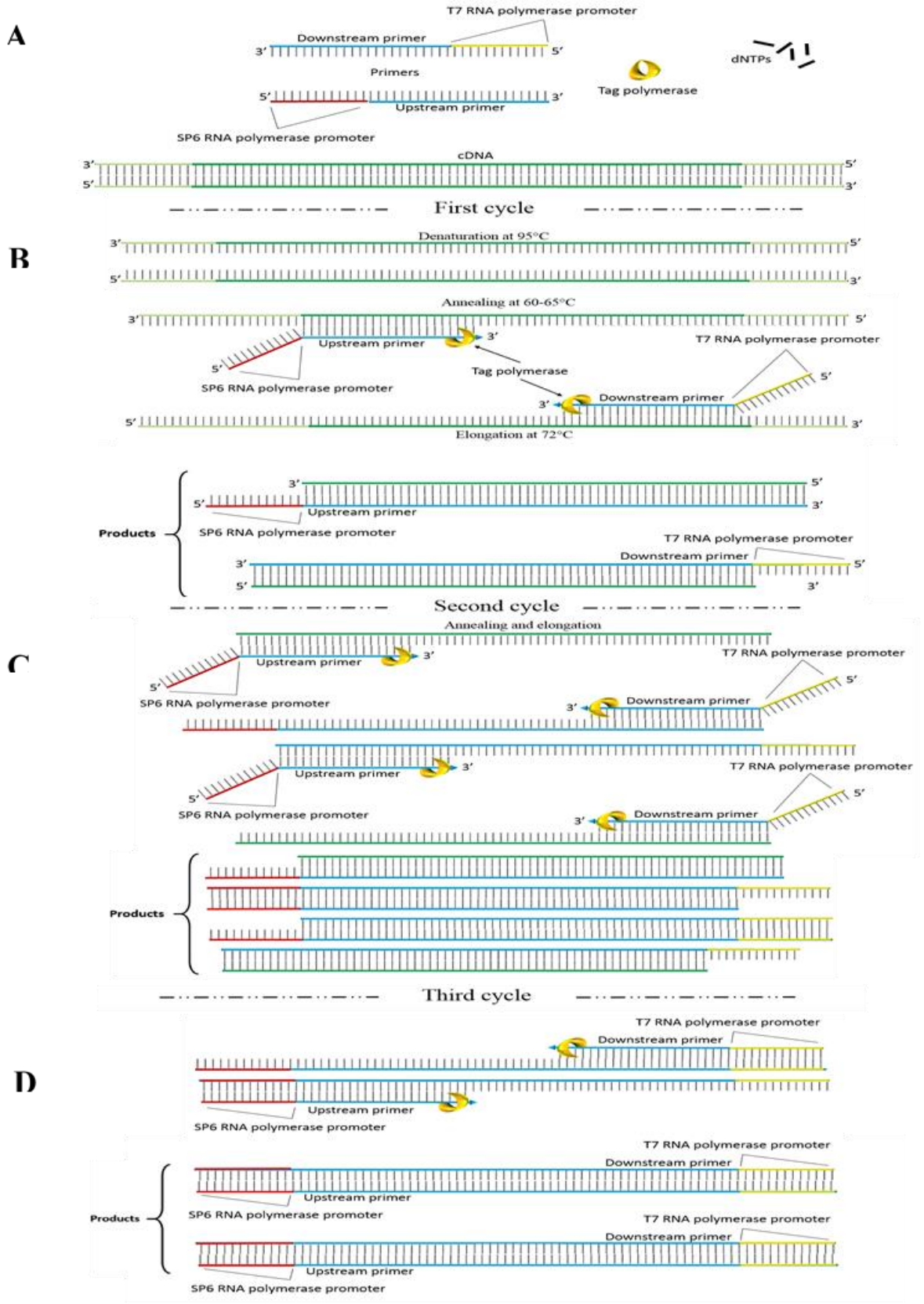

Figure 14: Schematically explanation for producing target DNA with two additional RNA polymerase promoter by PCR amplification

sense and anti-sense strands of the target DNA) can bind to their target sequences. After this step, the system is reheated to the elongation temperature (72°C). At this temperature, tag DNA polymerase enzymatically assembles and synthesizes a new single strand DNA complementary to the DNA strand by adding dNTPs (1000nt per min) in a 5' to 3' (condensing the 5'-phosphate group of the dNTPs with the 3'-hydroxyl group at the end of the nascent DNA strand) direction [41] (Figure 14B). At the end of the first cycle, all of the synthetized DNA molecules have at least one SP6 or T7 RNA polymerase promoter in their upstream side (Figure 14B). In the second round of PCR, new cDNA templates with new extra sequences use DNA as a template and, at the end of this cycle, most of the copied DNA has both promoters (Figure 14D). By the end of the third cycle, both promoters are included in the cDNA sequences (Figure 14F). By increasing PCR cycles, the number of cDNA fragments with two promoters is increased exponentially and, at the end, dominant cDNA copies have both promoters.

5.3 The Important method problem:

The interaction between two primers during the PCR procedure is a major drawback to this method, since it can lead to primer dimer formation. These cDNA fragments are smaller and, by increasing primer size, amplify faster than the PCR target product. Therefore, the chance of unwanted binding between two primers increases (Figure 15). In the method previously explained, these cDNA fragments have both RNA polymerase promoters. Using target cDNA templates contaminated with primer dimers (for *in vitro* transcription) induces unspecific sense or antisense cRNA formation. In the case of using a contaminated cRNA-labelled probes mixture, the chance of false positives or strong background result in sections will increase. This concentration of byproducts in a PCR reaction is dependent on primer sequences and the original cDNA template concentration in the PCR reaction buffer [42, 43]. In order to solve the problem,

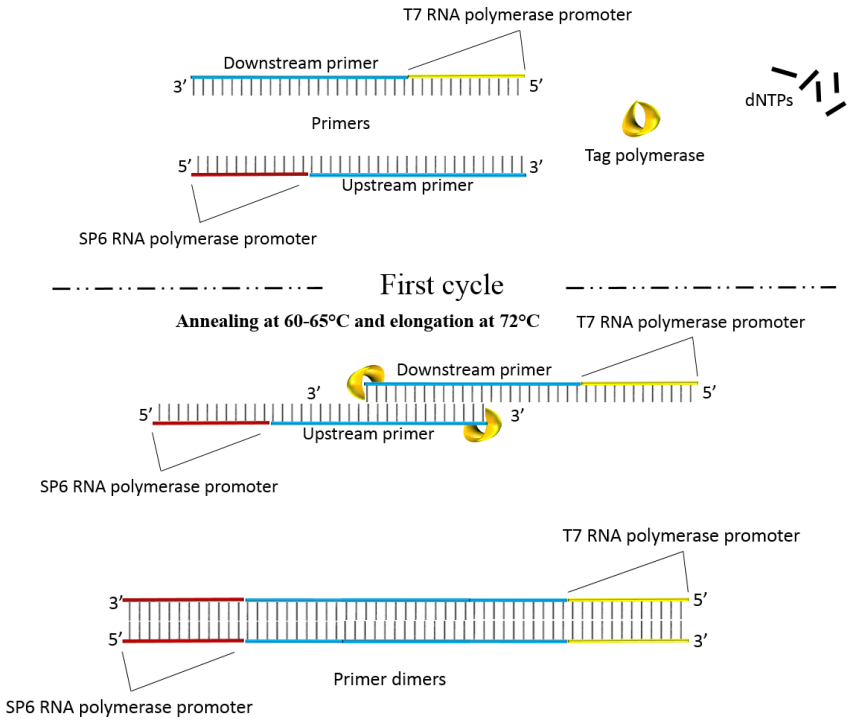

Figure 15: Primer dimers synthesis during first PCR cycle

gel purification was completed after the first PCR amplification and small size DNA fragments were separated from the PCR target products (running them through 1% agarose gel, as mentioned in the materials and methods section). Introducing purified cDNAs as template DNA in the second round of PCR amplification not only increased the amount of cDNA but decreased primer dimers formation, as well (Figure 16). Long and short albumin cDNAs in the first and second round of PCR are compared in Figure 16. It is clear that, in the second round of PCR, primer dimers disappeared completely and the amount of target cDNAs increased. To reach the highest target cDNA concentration, final PCR products were concentrated using phenol-chloroform extraction and ethanol precipitation, as well as agarose gel electrophoresis purification. Purified DNA (minimal concentration: 200 ng/µl) was then used for labelled cRNA synthesis. Both of the PCR fragments shown in Figure 16 have the expected size and comprise gene-specific cDNA and RNA polymerase promoter sequences incorporated at both sides of the

target DNA fragment. The *in vitro* transcription for generation of sense or antisense probes (depending on the use of SP6 or T7 RNA polymerase, respectively) was completed by using the purified DNA fragments [39].

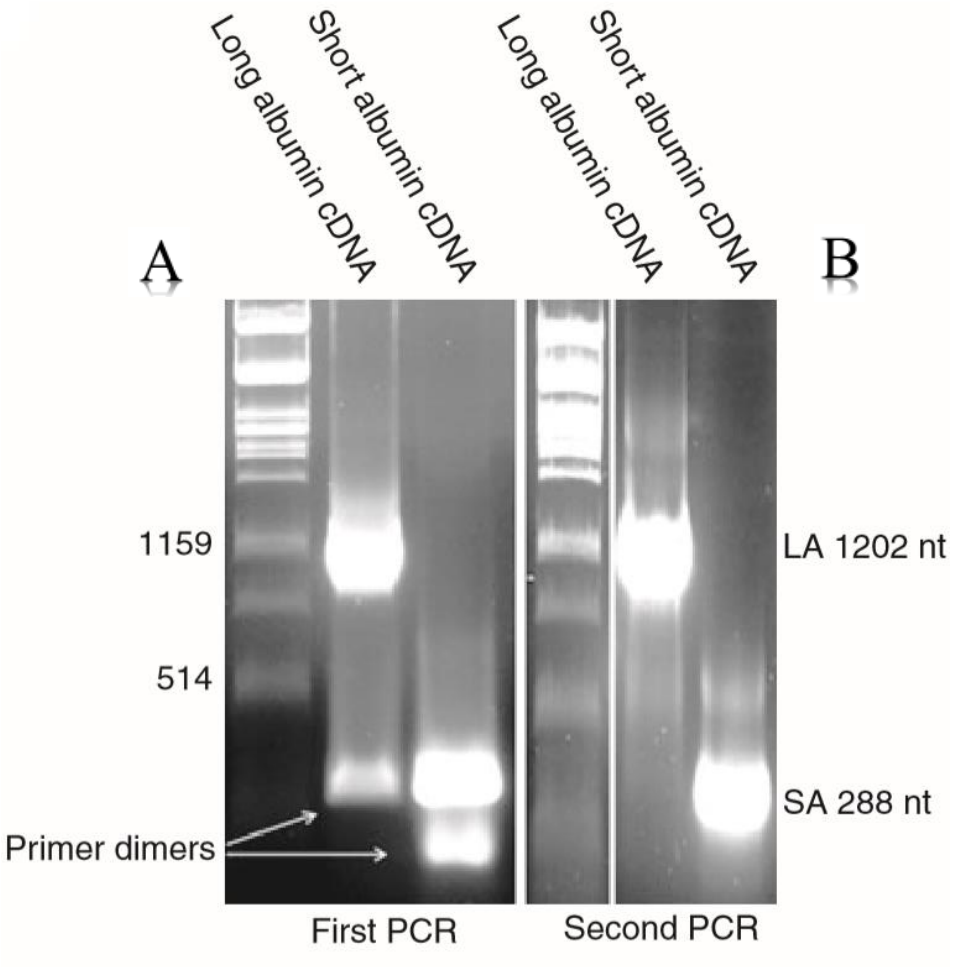

Figure 16: Comparison between first PCR amplified products A and second PCR amplified products B (modified from Ghafoory et al 2012) demonstrating the elimination of primer dimers.

5.4 *In vitro* cRNA transcription:

The purified cDNAs are easy to use for mRNA transcription (sense or antisense labelled cRNA preparation) and the location and direction of promoters designed by this method allow sense and antisense labelled cRNAs from one target DNA fragment to be generated. A mixture of SP6 or T7 RNA polymerase enzyme, buffer, RNase free water, nucleotides (digoxigenin or

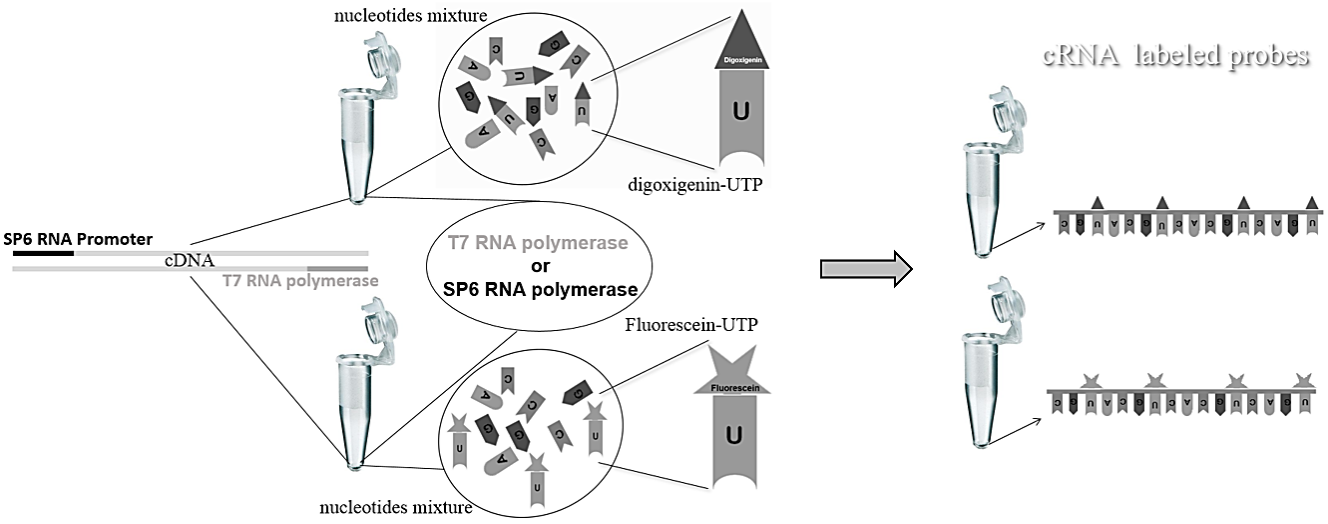

Figure 17A: Sense and antisense labelled cRNA preparation from purified cDNA

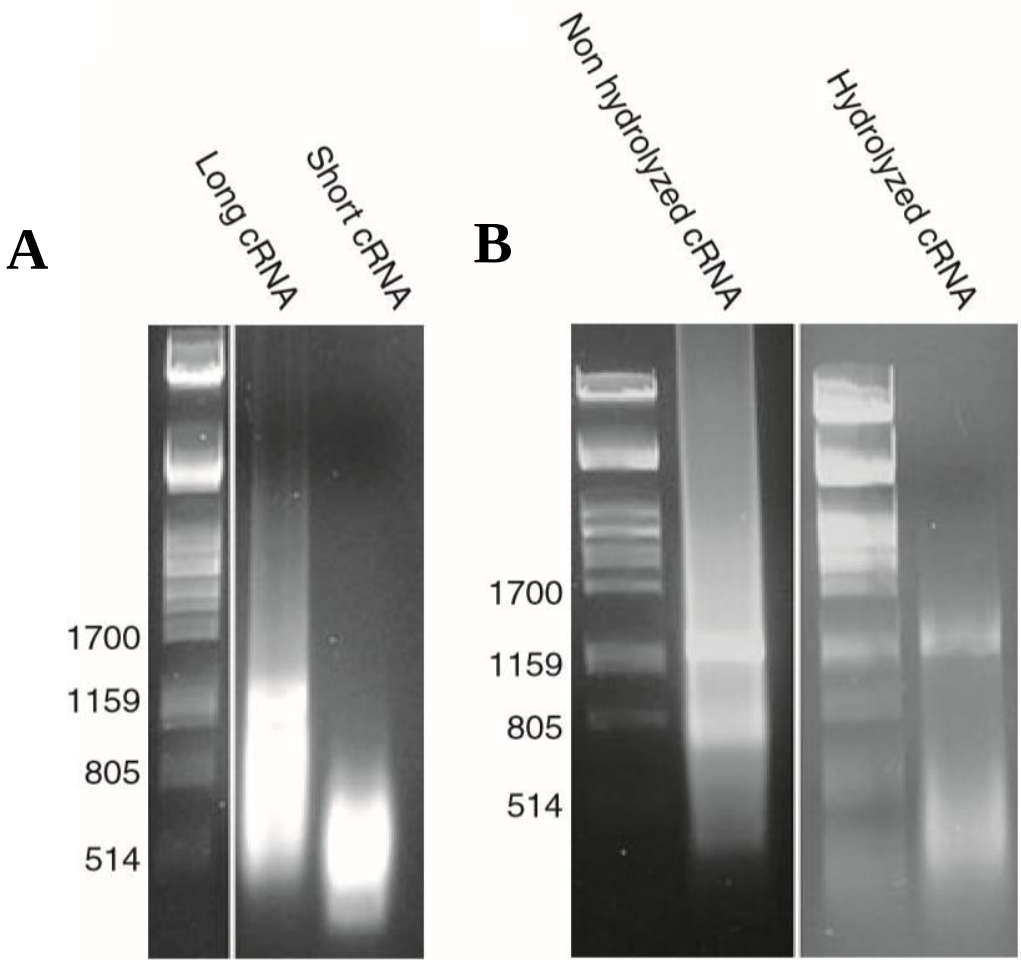

Figure 17B: A, in vitro transcribed cRNA probes (long and short mouse albumin); B, alkaline hydrolysis: non-hydrolyzed (1202nt) and hydrolyzed (200nt) long mouse albumin probe. (modified from Ghafoory et al 2012)

fluorescein labelled UTP with CTP, ATP, and GTP), and the purified cDNA with promoters (SP6 and T7 RNA polymerases) were used for *in vitro* sense or antisense cRNA probe generation (Figure 17A), changing UTR labelled nucleotide (digoxigenin or fluorescein) in the nucleotide mixture, thus generating different cRNAs labelled for ISH co-staining.The quality of mouse albumin (short and long) antisenses are shown in Figure 17A [39]**.**

5.5 *In situ* hybridization of mouse liver sections:

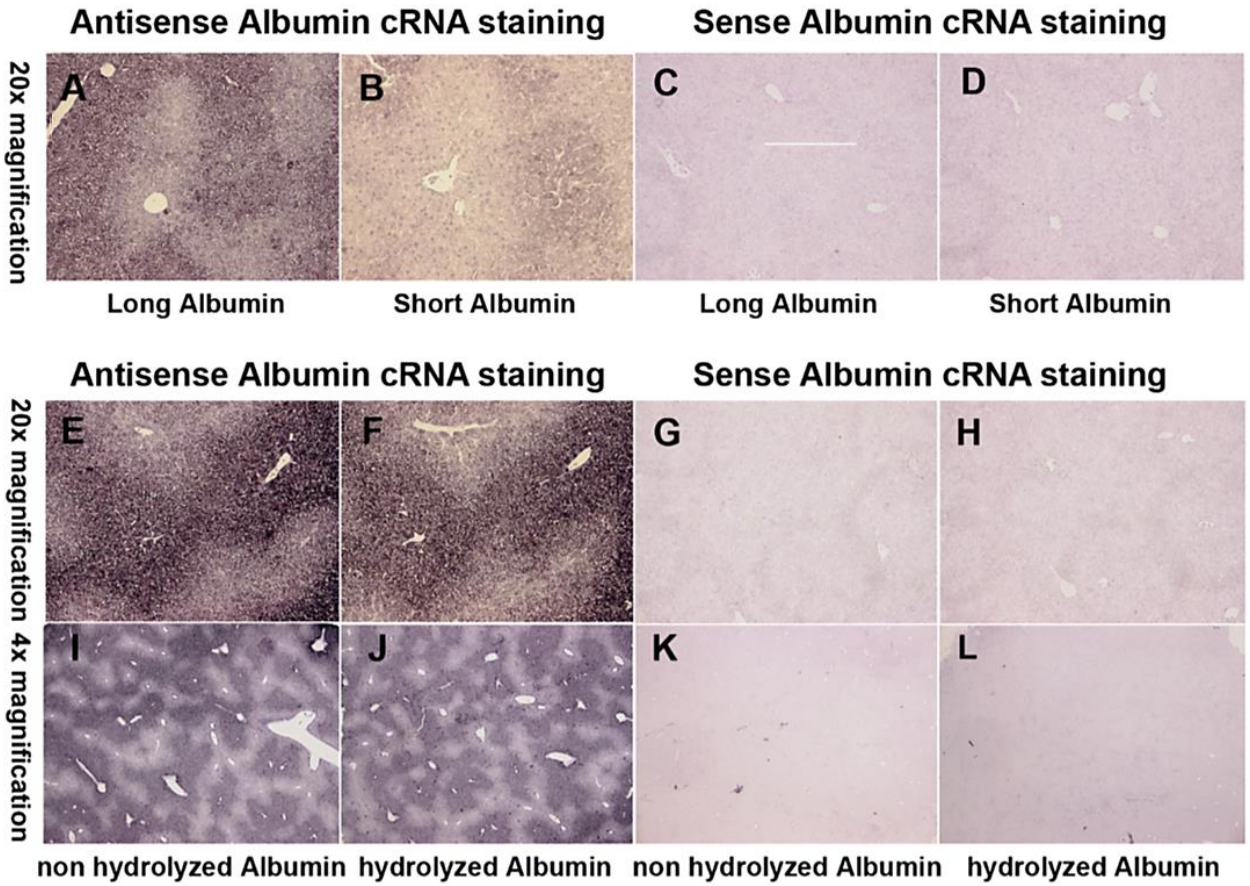

Figure 18: In situ hybridization of albumin mRNA in mouse liver sections; Role of the riboprobe length for sensitivity. Sections were hybridized with antisense (A) and sense (C) long albumin (1202nt) or antisense (B) and sense (D) short albumin cRNA (200nt). Images were captured with 20- or 4-fold magnification as indicated. Sensitivity of hydrolyzed and non-hydrolyzed long albumin copy RNA (cRNA) was compared; sections were hybridized with non-hydrolyzed (E,I) and hydrolyzed (F,J) probes. Hybridization with non-hydrolyzed (G,K) and hydrolyzed (H,L) sense long albumin cRNA probe is shown as control (modified from Ghafoory et al. 2012)

The relationship between size and peneteration of probes in to the tissue was studied: after cRNA probes were synthesised, mouse albumin cRNA long probe was hydrolyzed into smaller fragments (around 200nt) by using alkaline hydrolysis [40]. The change of fragment size of the hydrolyzed cRNA is presented in Figure 17B. Mouse antisense albumin probes (digoxigenin labelled) were used for detecting transcribed albumin in paraffin sections of adult mouse livers. Microscopic images of *in situ* hybridization results in liver sections are presented in Figure18. Both long (LA-1202nt, Figure 18A) and short (SA-288nt, Figure 18B) DIG-labeled antisense cRNAs, as well as albumin mRNA specific hybridization were validated by absence of signals in control of consecutive sections hybridized with sense probes (Figure 18C, D).

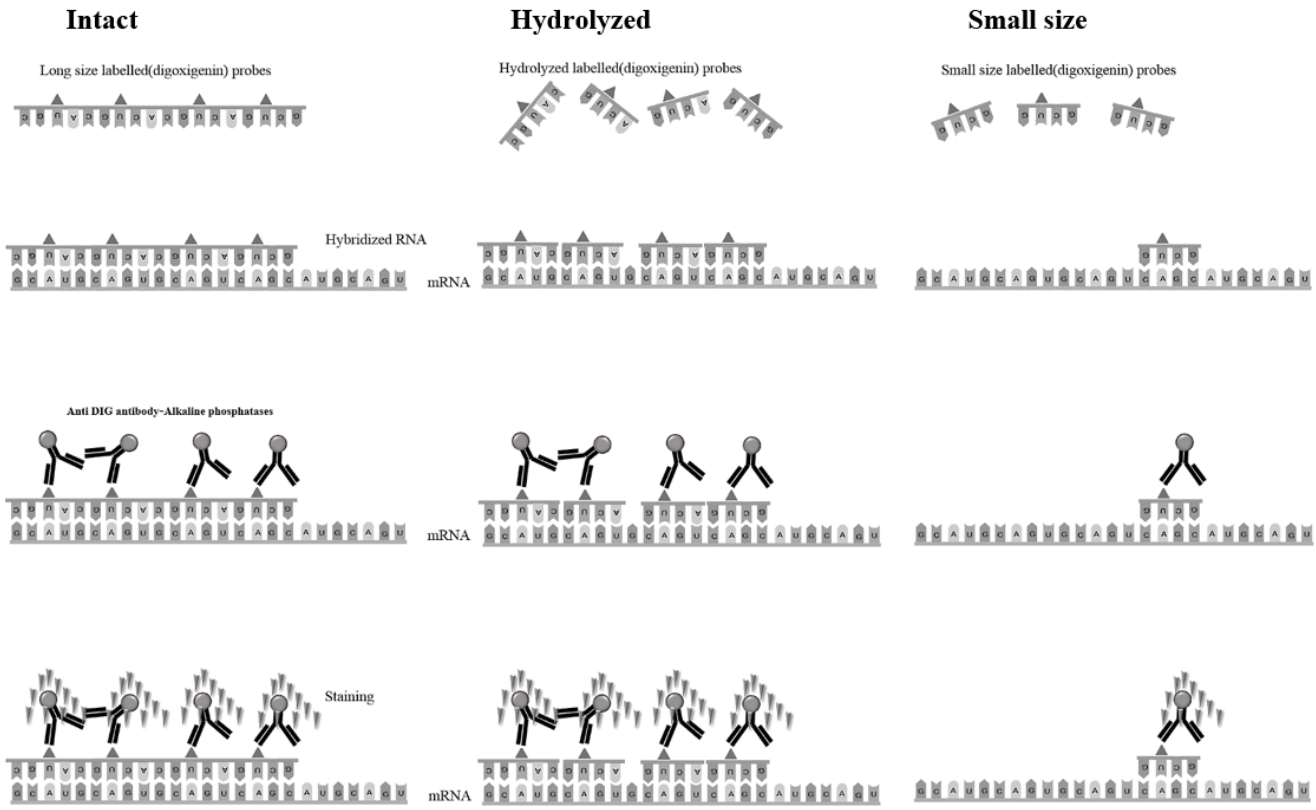

Figure 19: A comparison of staining for different antisense cRNA prepared for *in situ* hybridization

Interestingly, the longer probe had a stronger signal than the short albumin cRNA probe, which could provide greater detection sensitivity (Figure 18A, B). Both probes were applied in equally large excess during hybridization. Thus, the larger number of incorporated UTR in the longer albumin cRNA probe explains the stronger signal obtained with it. In another study, hydrolyzed and non-hydrolyzed probes were used for detection of albumin transcripts in consecutive mouse liver sections (Figure 18E, F, I, and J)[39]. Comparable signals were observed with both hydrolyzed and non-hydrolyzed probes.Sense probe hydrolysis did not increase unspecific background staining in the control section (Figure 18G, H, K and L). In an attempt to explain the obtained results (albumin *in situ* hybridization) schematically is shown in Figure 19. Using intact antisense cRNA probes (maximum UTP-DIG number) for hybridization, increased anti-DIG antibody (conjugated with Alkalin phosphatase) numbers bound to albumin mRNA in the section (in comparison to short cRNA probes). Colour intensity is also dependent on the precipitation rate of the changed substrate (by enzyme reaction) in the section. Equal intensity staining obtained from hydrolyzed antisense albumin cRNA (from different parts of the intact probe) and intact long albumin cRNA hybridization in consecutive liver sections revealed that the number of UTP-DIG in hydrolyzed and intact albumin cRNAs was almost equal. Small size cRNA, which generated from a small part of target cDNA template, has less UTP-DIG than the intact and hydrolyzed cRNA. The concomitant section hybridized with short probe (for the same duration) has less color intensity than others[39].

5.6 Pathological changes in mouse and human liver sections:

The protocol's applicability was shown by analysing albumin mRNA expression in human and mouse liver hepatocytes. Albumin mRNA expression in mouse liver hepatocytes was studied

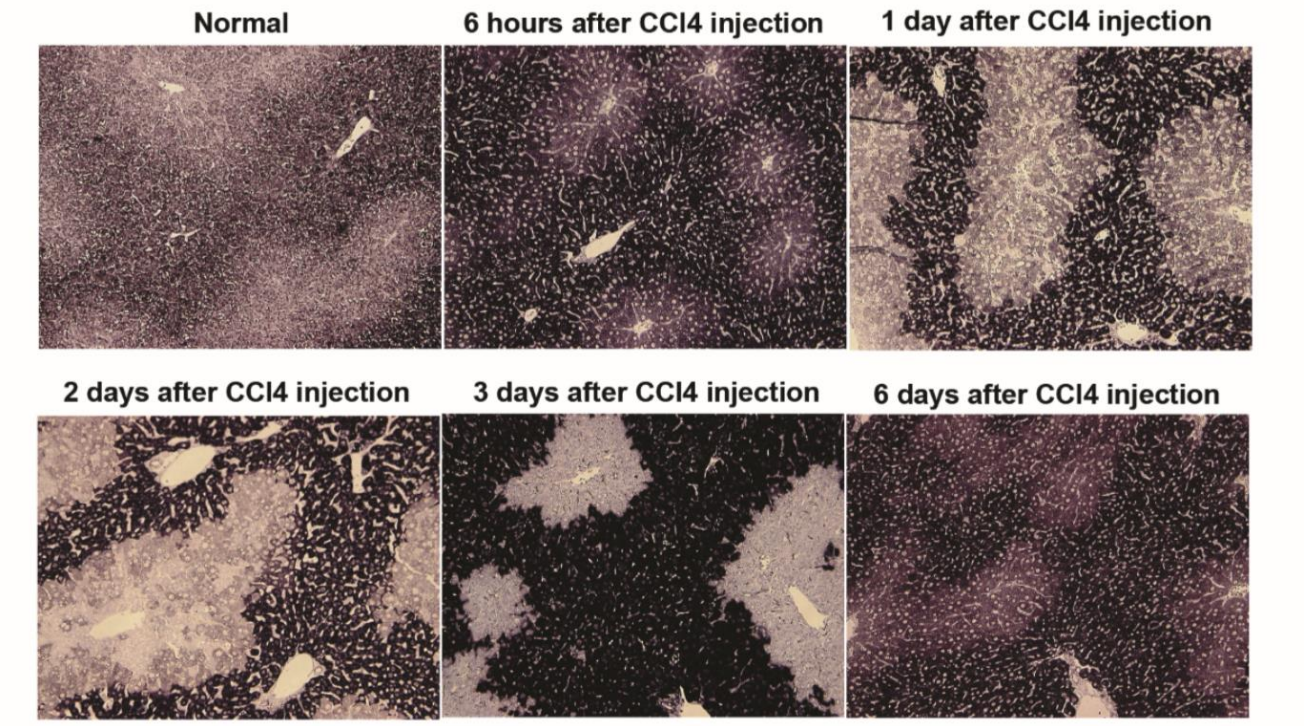

Figure 20A: Visualization of carbon tetrachloride (CCl4)-mediated mouse liver damage using in situ hybridization (ISH) for albumin in paraffin sections (A). Staining for albumin mRNA expression revealed progression of damage until day 2 and subsequent recovery to days 3 and 6. (modified from Ghafoory et al. 2012)

during an induced injury by carbon tetrachloride (CCl_4) and compared with healthy liver hepatocytes [39]. In another experiment, albumin and alpha-fetoprotein (AFP) mRNA expression in human hepatocellular carcinoma (HCC) was studied. Sections from different parts of the tumor (cancerous and noncancerous areas) that had been hybridized with human albumin antisense cRNA (Fluorescein labelled) and human AFP antisense cRNA (DIG labelled) were co-stained [39]. In the first study, liver damage induced by CCl_4 was revealed. In late time points post injection, the hepatocytes around the central vein lost albumin expression (albumin staining) when compared to the adjacent periportal areas (Figure 20A). The albumin expression was only marginally changed after 6 hours, but visible liver damage had occurred on days one and two post-CCl_4 injection. Albumin expression was also strongly reduced in the pericentral hepatocytes. Expansion of the albumin expressing area on day three provided signs of recovery

from liver damage. By day six, recovery was completed and albumin expression returned to healthy liver expression patterns.

In the second study, human mRNA specific probes for albumin and AFP (alpha-fetoprotein, a major plasma protein produced by the yolk sac and the liver during fetal development, is considered the fetal form of serum albumin) were prepared and used in liver sections from HCC patients as a marker for HCC progression.

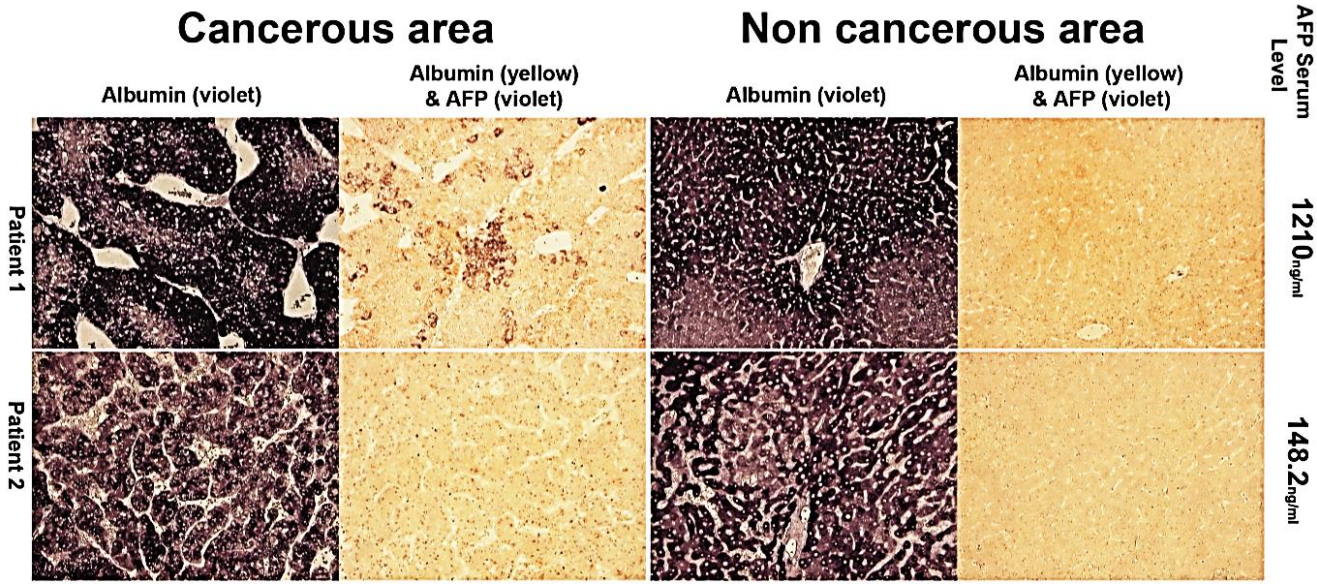

Figure 20B: Albumin and alfa-fetoprotein (AFP) mRNA expression in paraffin liver sections from human hepatocellular carcinoma (HCC) patients (B). Sections were stained with antisense copy RNA (cRNA) for albumin or double-stained with antisense cRNAs for both albumin and AFP as indicated. Strong AFP expression in cancerous area correlated with high AFP blood levels indicated on the right. (modified from Ghafoory et al. 2012)

Images taken from noncancerous areas showed much more similarity to albumin expression patterns in healthy mouse livers. Interestingly, AFP expression was found specifically in

cancerous areas. Elevated AFP levels in patient serum directly correlated with increased color intensity in HCC-cells (Figure 20B) [39].

5.7 Liver CCl_4 damage:

In the first part of this study, the new method proved its practicality for cRNA preparation in a short period of time. In the second part of this study, key enzymes and receptors related to neutralization and recovery (Cyp2e1, Glutathione synthetase and Glutathione peroxidase 4), ammonia detoxification and urea synthesis (Glutaminase2, Glutamin synthetase, and Arginase1), and carbohydrate metabolism (Glycogen synthase2, Glucose-6-phosphatase c, Glucagon receptor, and Glyceraldehyde-3-phosphate dehydrogenase) were chosen and antisense cRNAs were prepared to visualize gene expression changes during acute liver damage.

CCl_4 mixed with mineral oil (1ml⁄kg body weight) and introduced to mouse livers by intraperitoneal injection, induced acute liver damage in two groups of Balb⁄c mice, with seven mice in each group. Mice from each group were sacrificed at different time points (3h, 6h, 1d, 2d, 3d, and 6d) post injection and their livers compared with healthy livers. The livers were removed immediately and divided into two parts. The first part was used in paraffin-embedded block preparation (for ISH or IHC staining) and the second part was used for tissue RNA extraction. cDNAs were synthesized and quantitative real-time PCR measurements (to compare changes in gene expression during CCl_4 treatment) were taken [44].

Tissue sections from all groups (different time points) were arranged on one slide to ensure equal conditions during *in situ* hybridization with one or two gene specific probes. The expression of two chosen genes was visualized in one section using digoxigenin and fluorescein labelled antisense cRNAs, with yellow stain for probes labelled with fluorescein and violet stain for probes labelled with digoxigenin. All *in situ* hybridization results were visualized using a digital microscope at 2-3 magnification levels to obtain an overview of region specific gene expression

patterns in the sections (4x), as well as higher resolution gene expression patterns (20x or 40x). For optimal comparison, pictures from complementary areas of subsequent slices (complementary areas of the liver tissues sections are shown for all hybridizations whenever possible) were taken.

The results of our ISH experiments, which show gene expression pattern changes, are presented in seven figures (Figures 21, 22, 23, 24, 25, 26, and 27). Albumin gene expression in different time points with three different magnifications and in comparison with DAPI staining is shown in Figure 21. Key enzymes of nitrogen metabolism and ammonia detoxification (Figure 22), glucose storage and release, and other genes involved in detoxification and basic cellular metabolism (Figure 23) are also shown. In Figure 24, higher magnification ISH images of most of genes analyzed in tissue sections from days 1, 2, and 3 post CCl_4 injection are presented together to facilitate a comparison of tissue distribution of all genes in a more detailed view. Cyp2e, Gpx4 (Glutathione peroxidase 4), and Gss (Glutathione synthetase) co-stained with albumin and gene expressions are shown in Figure 26. In most sections, albumin expression was used as a marker for the periportal area. To give further evidence of the validity of gene expression staining with antisense cRNAs, the gene expression and related synthetized protein stain in consecutive mouse liver sections with respect to aSMA protein (Figure 27A) were compared. In Figure 27B, gene expression and DAPI staining for both the same and consecutive sections were compared. Since ISH only provides relative gene expression values elucidating areas of high and low expression of respective genes, overall mRNA levels was also analysed by RT-qPCR (Figure 25) [44].

5.8 Albumin expression:

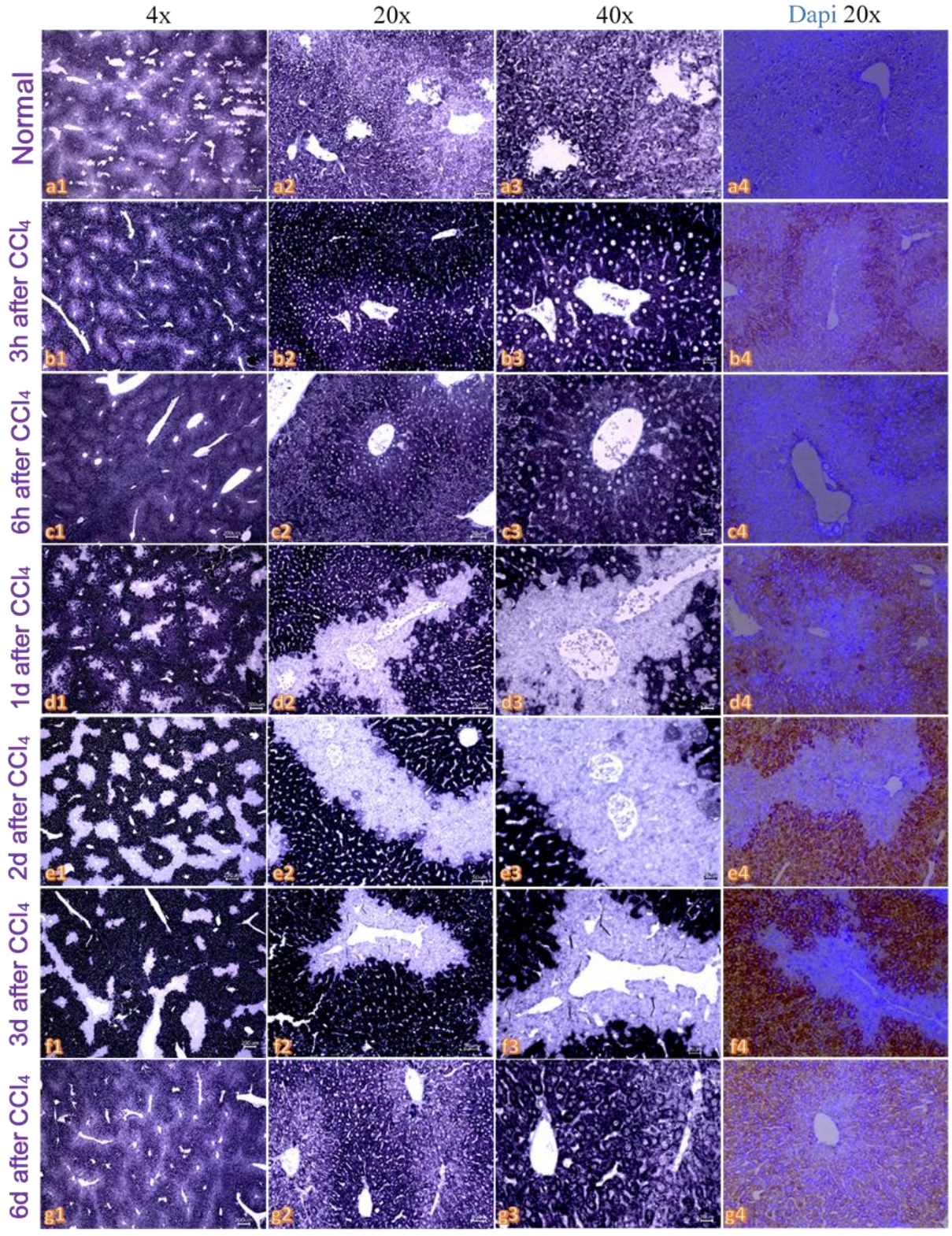

Figure 21: Albumin expression in mouse liver sections during different time points post CCl_4 treatments with an overlay with DAPI staining.

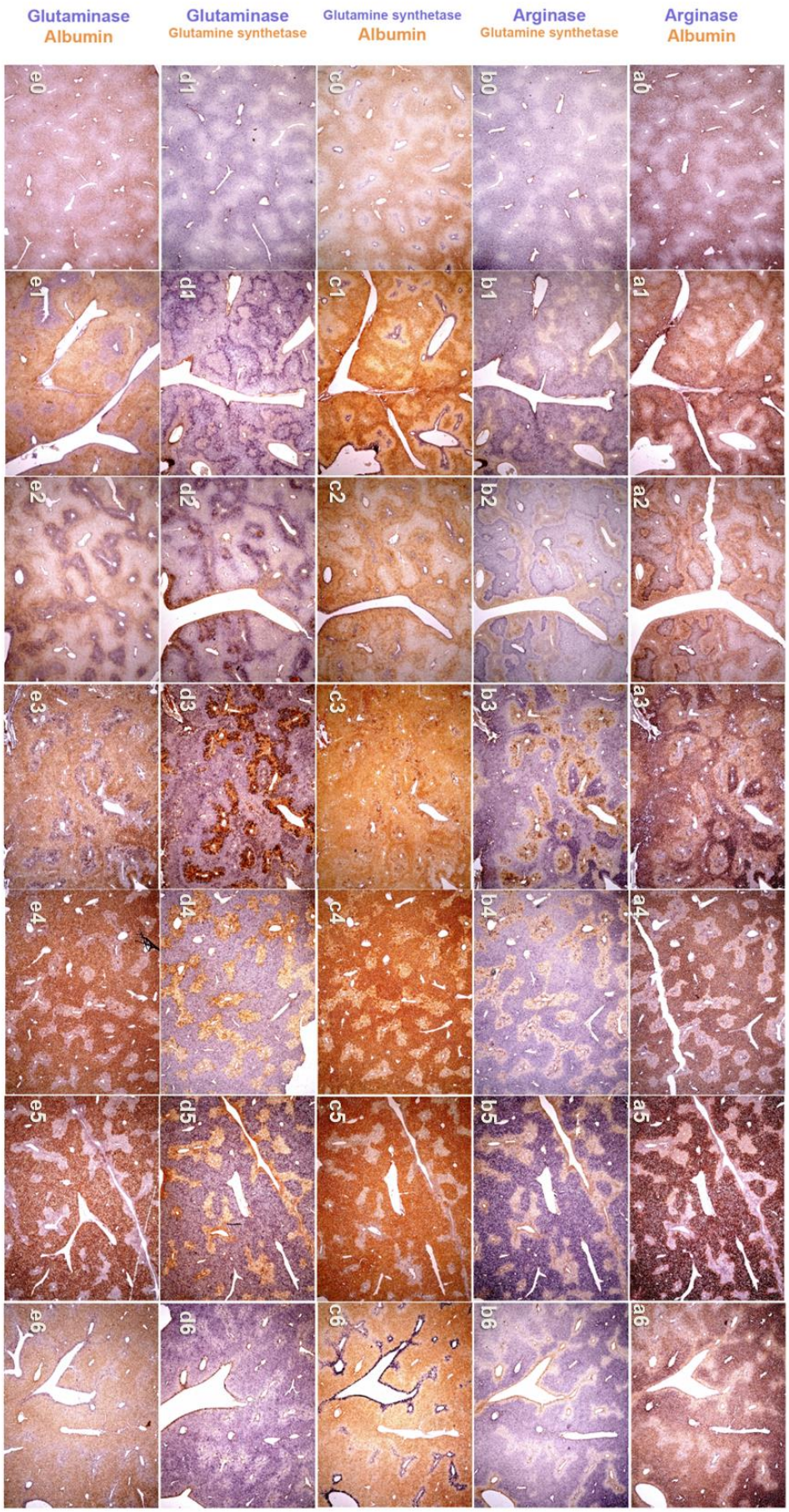

Figure 22: ***In situ*** **hybridization for genes from nitrogen metabolisms.** ***In situ*** **hybridization of mouse liver sections with probes for selected genes involved in nitrogen metabolism at different time points post CCl_4 injection in each panel, genes were visualised by dual staining with yellow and violet dye precipitation . Gene names are indicated on the left in the respective color. Co-staining for both genes in the same area resulted in dark brown staining. Pictures were captured with 4x objective(modified from Ghafoory et al 2013)**

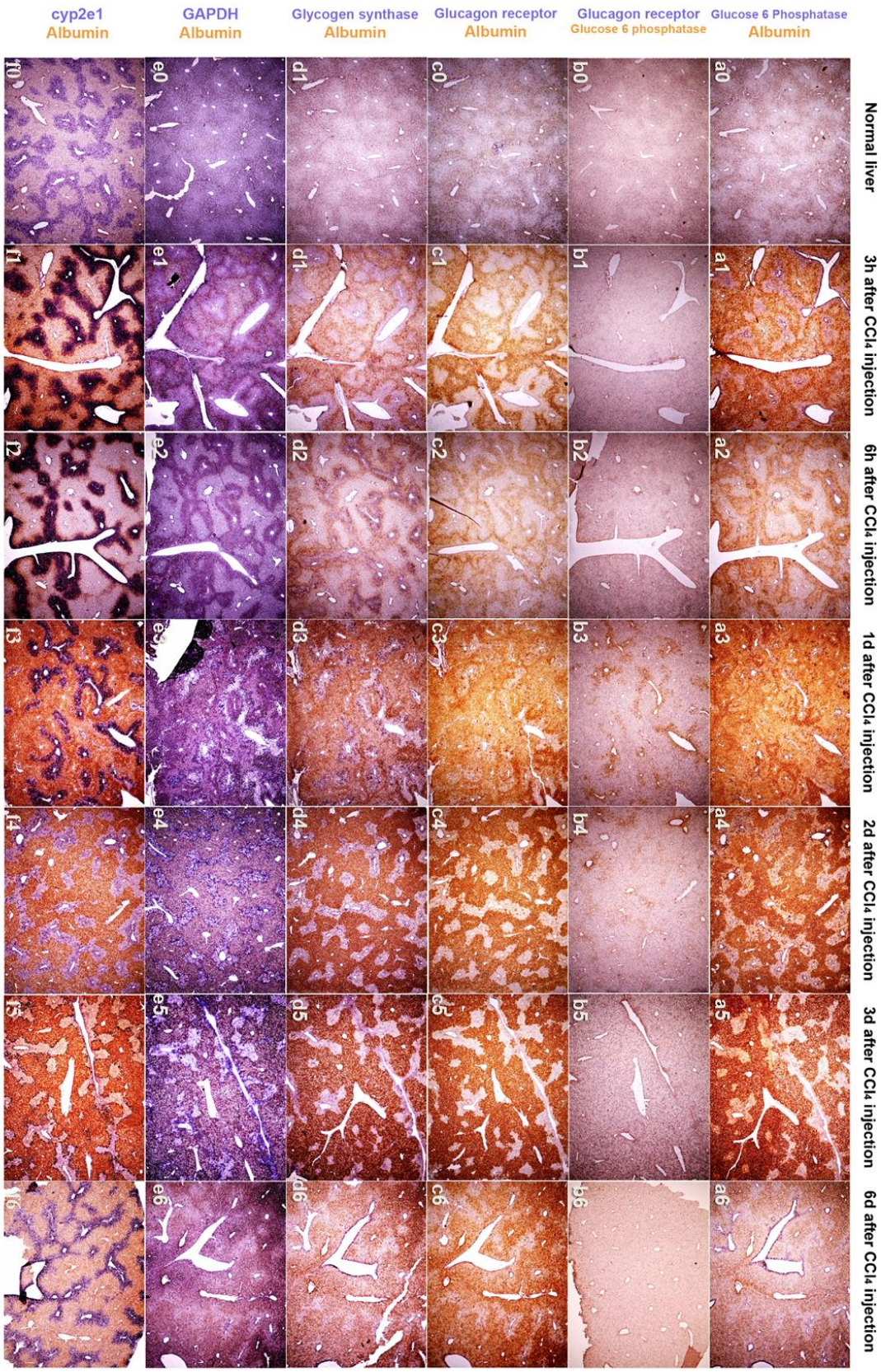

Figure 23.*In situ* hybridization for carbohydrate metabolism genes.
***In situ* hybridization of mouse liver sections with probes for selected genes of carbohydrate metabolism at different time points post CCl_4 injection. Genes were visualised by dual staining with yellow and violet dye precipitation. Gene names are indicated on the left in the respective color. Co-staining for both genes in the same area resulted in dark brown staining. Pictures were captured with 4x objective. (modified from Ghafoory et al 2013)**

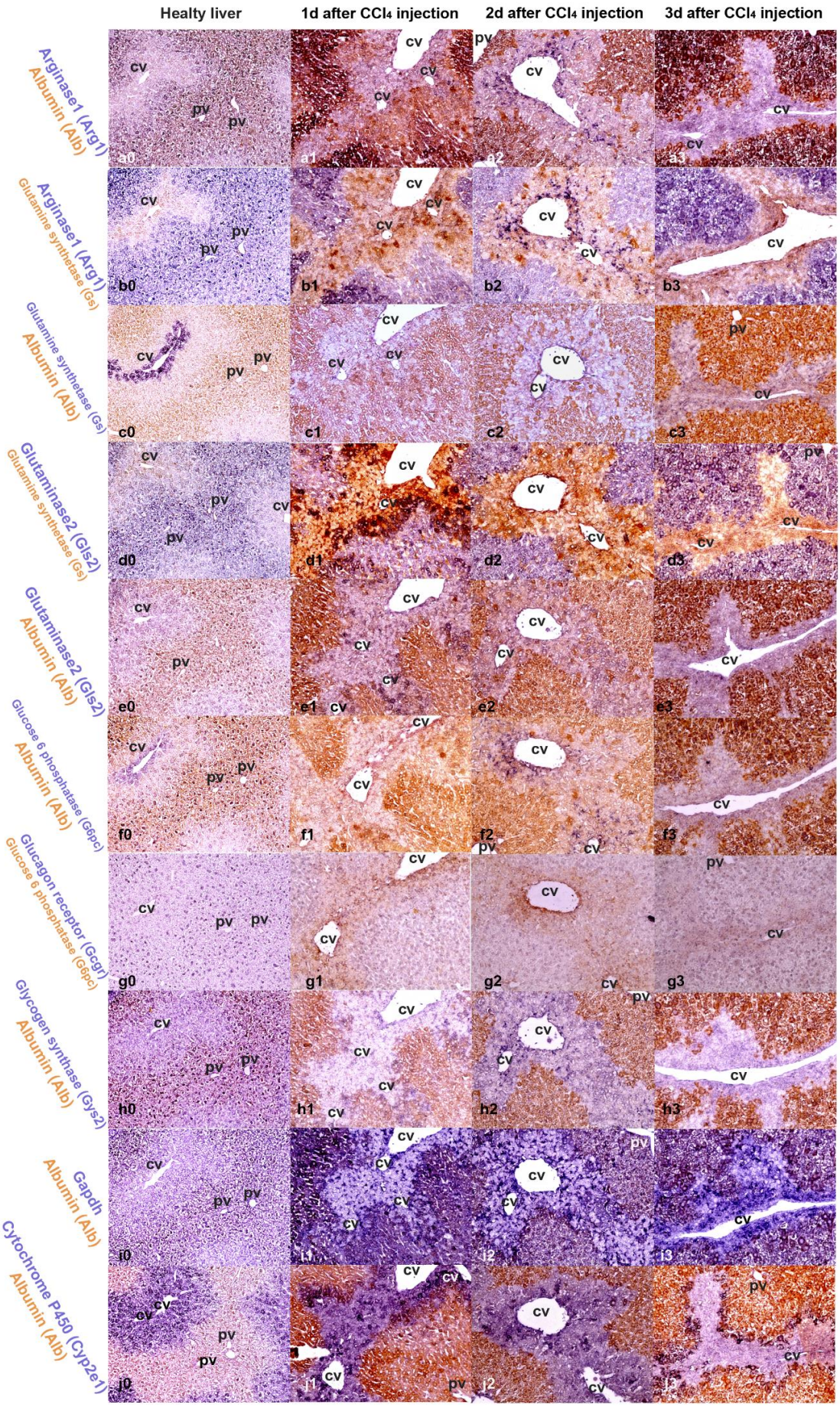

Figure 24: Higher resolution *in situ* hybridization images.
In situ **hybridization of mouse liver sections from untreated animals and form days 1 to 3 after CCl_4 injection, with higher magnification (20x objective). Genes analyzed are indicated at the left in the respective color for each row. Co-staining for both genes in the same area resulted in dark "brown" staining. Specific areas of the liver tissue (acini) are marked: central vein (cv), portal vein/area (pv). (Modified from Shahrouz etal 2013)**

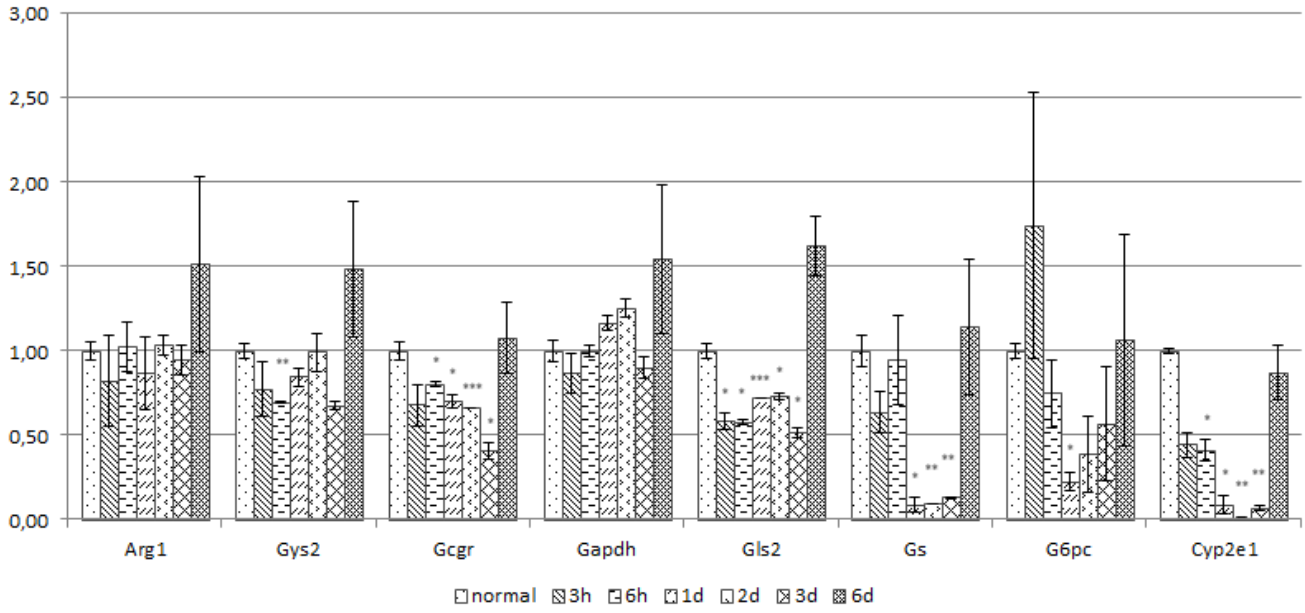

Figure 25: Quantitative real time PCR
Total RNA was extracted from mouse liver at different time points after administrating CCl_4. cDNA was analyzed using primers recognizing the following genes: Arg1, Gys2, Gcgr, Gapdh, Gls2, Gs, G6pc, Cyp2e1. Primer recognizing Albumin was used for normalization. Values shown represent the mean (+/- SEM) of two individual experiments. * = p<0.05, ** = p<0.01, *** = p<0.001, Student's T-test. (modified from Ghafoory et al 2013)

The most important protein secreted by hepatocytes in to the blood circulation is albumin. In healthy livers, albumin is synthesized more in PPH than in PCH, which leads to a specific pattern of hepatic albumin expression visualizing the liver acini, [39, 45] (Figure 21 a1, a2 and a3). In response to CCl_4 treatment, albumin expression was even lower in PCH (conversely, in PPH, the albumin gene expression increased during CCl_4 treatment), which can be seen by the increased signal difference between PPH and PCH for albumin mRNA. In contrast, on post CCl_4 injection day 6, albumin expression was more equally distributed than in normal (untreated) livers.

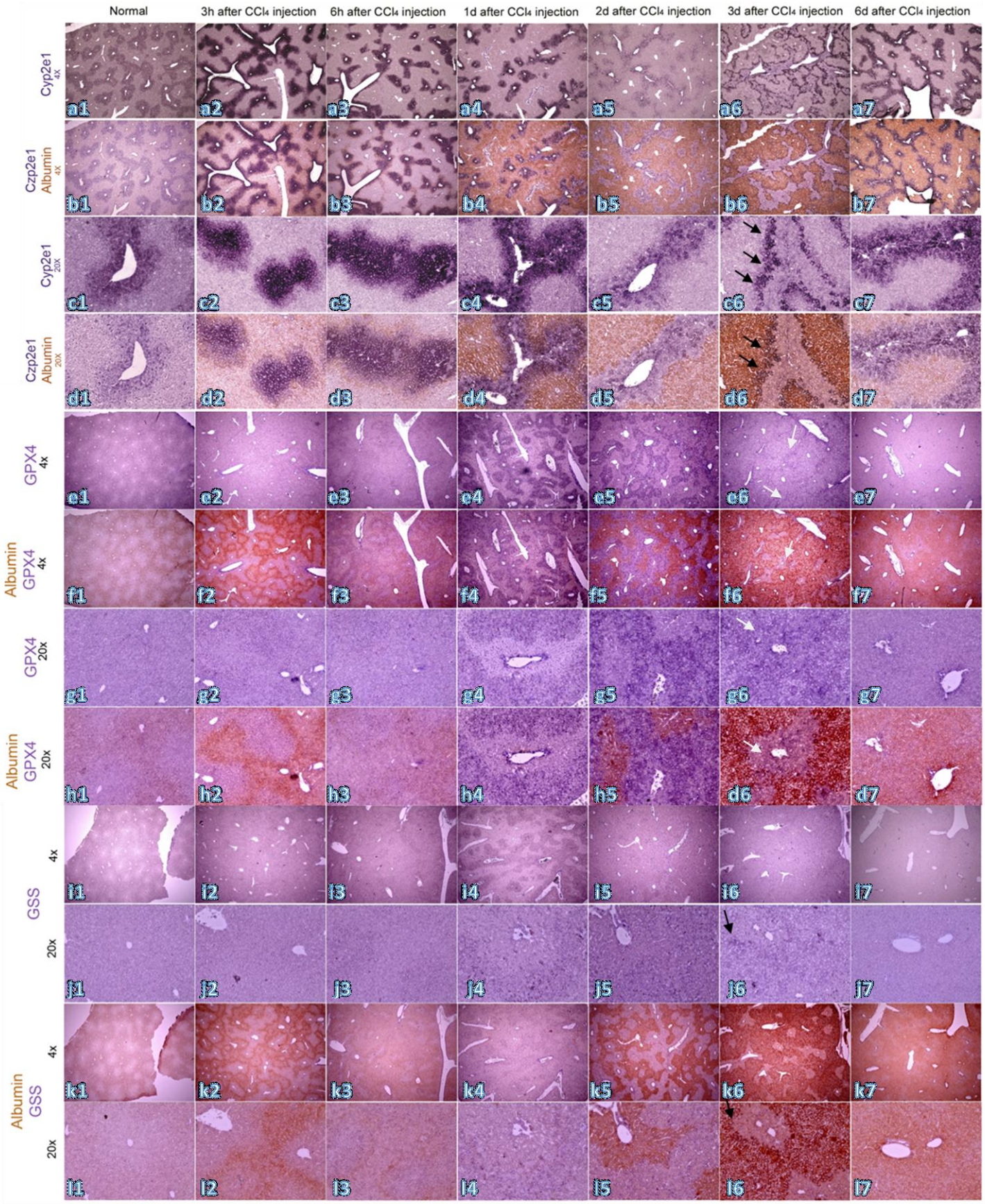

Figure 26: Mono and co-staining of the expression of three key enzymes in damaged liver and during recovery from CCl_4 -induced damage at different time points post injection. Monostaining picture were taken after the first staining for Cyp2e1, Gpx4 and Gss, then in situ procedure was continued for second staining (Albumin) and the last pictures were taken (co-stained pictures).Pictures of mono and co-staining were taken from the same area.

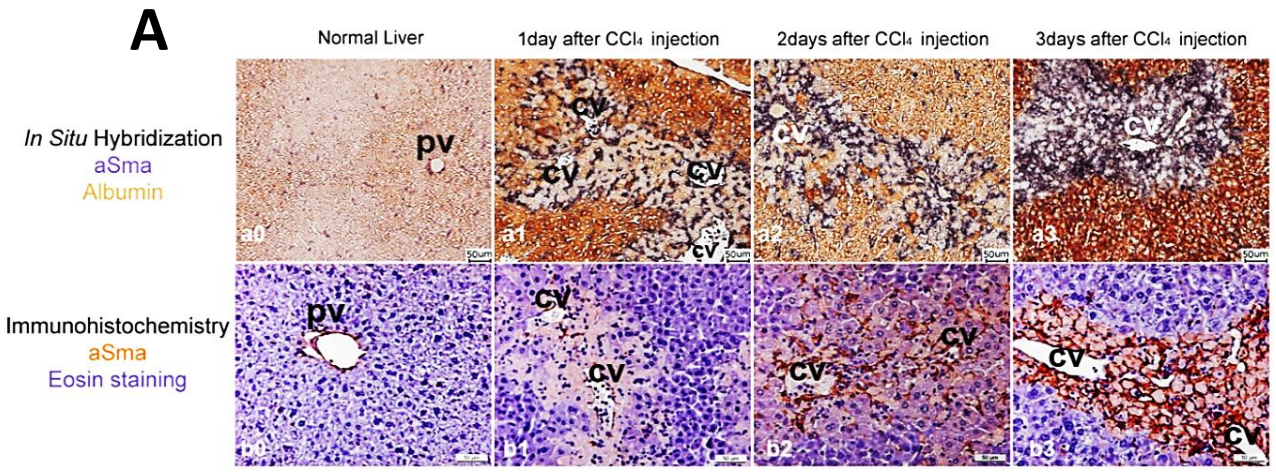

Figure 27A: comparison between *in situ* Hybridization and immunohistochemistry staining, *In situ* hybridization with Asma and Albumin antisense probes in different time pointsafter CCl_4 treatment. Immunohistochemistry staining with anti Asma antibody and eosin staining (modified from Ghafoory et al 2013)

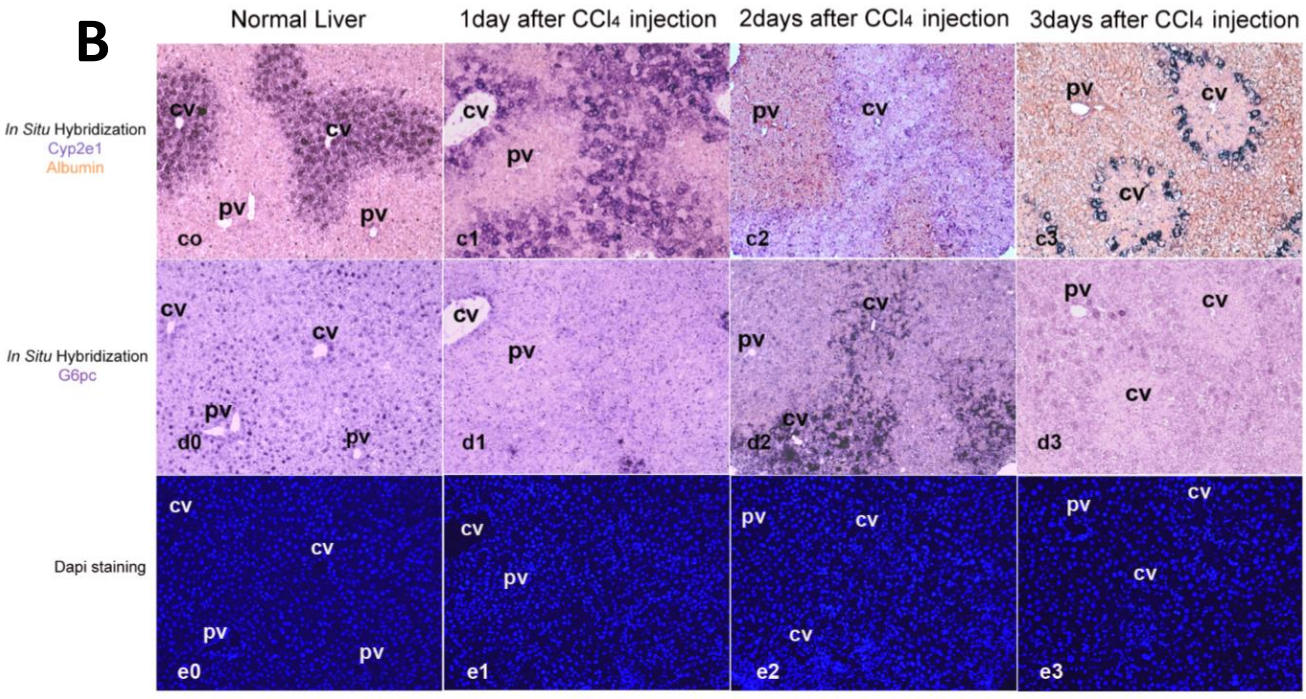

Figure 27B: comparison between gene expressions and DAPI staining with 20x magnification (modified from Ghafoory et al 2013)

In this study, albumin expression was used as a marker for HPPs. Albumin was expressed in different time points post injection, and at different magnification levels (Figure 21). DAPI staining and albumin expression (Figure 21a4, b4, c4, d4, e4, f4 and g4) revealed many cell nuclei in the pericentral area at all the time points measured, indicating that most of the cells in the damaged area were still alive.

In healthy livers, the expression of enzymes involved in nitrogen metabolism and ammonia detoxification has been assigned to defined areas [9] (Figure 7). *In situ* hybridization signals for arginase (Arg1) and glutaminase (Gls2) show a zonation similar to that of albumin in normal livers (Figure 22 a0, b0, d0 and e0), a finding that fits within the established functions of periportal hepatocytes[44, 46] (Figure 7). Glutamine synthetase is expressed in 2 or 3 layers of hepatocytes around the pericentral vessel (Figure 22 c0), these results are in line with the previously published findings on Gs zonation activity [47, 48]. At early time points (3h and 6h) post CCl4 treatment, Arg1 and Gls2 mRNAs were detected throughout tissue sections, with very specific high expression in hepatocytes located in the boundary between the periportal and pericentral areas (Figure 22). At day 1, a more selective expression of Arg1 and Gls2 was observed, and sharp expression spots in the pericentral area became completely visible. These Arg1 signals in the pericentral area became stronger on day 2, in particular when analyzed with higher magnification (Figure 24 a2 and b2). The total levels of Arg1 in mRNA analyzed by RT-qPCR did not change relative to albumin until day 3, and had increased only marginally on day 6 specifically, they increased only marginally (Figure 25). In contrast, Gls2 mRNA levels immediately decreased and remained lower from 3h through post injection day 3 and increased at day 6 (Figure 25) [44]. It should be noted that Arg1 is only expressed by hepatocytes and kupffer cells [48]. Therefore the speckled signals in the pericentral area observed on day 2 (Figure 24 a2 and b2) could also belong to infiltrated macrophages that moved into the

pericentral area during liver recovery. Gs expression was also changed significantly during CCl4 treatment. At early time points post injection, strong expression around the pericentral vein was visible (Figure 22 c0-2). This signal was missed on days 1, 2, and 3 (Figure 22 c3-5), but was clearly visible again by day 6 (Figure 22 c6). Quantitative analysis of Gs mRNA from total RNA extracted from livers showed a parallel change that mirrored the changes observed for Gs expression in the *in situ* hybridization. A significant decrease in Gs expression at days 1, 2, and 3, as well as a clear recovery by day 6 (Figure 25), confirmed that damage (after CCl_4 injection) is restricted to the pericentral area. Thus, while enzymes involved directly in the control of glutamine levels and ammonia producing were decreased, the total capacity for removing ammonia and generating urea remained active throughout the toxicity period[44].

Storage and mobilization of glucose is another important role of hepatocytes (Figure 8). The enzyme glycogen synthase 2 (Gys2) is responsible for glycogen synthesis and glucose-6-phophatase (G6pc) is needed for glucose release. In total, mRNA level Gys2 (like Arg1) shows marginal changes after injection (Figure 25). In contrast, G6pc expression was induced 3h post injection, reduced significantly by day 1, and returned to normal levels at late time point (Figure 25). Gcgr, the receptor for glucagon hormone (which is involved in increasing circulated glucose levels), appears to be down regulated until day 3 and restored by day 6 (Figure 25). Looking at the spatial Gcgr distribution in liver tissue shows a quite uniform expression of the Gcgr observed during treatment (Figure 23 b and c) that is also clearly visible at higher magnification (Figure 24 g). Albumin-strong expression obscures this homogenous signal, which is, however, clearly visible in co-staining with G6pc (Figure 23 b). Gys2 mRNA (like Gcgr) is also distributed equally (Figure 23 d0, and 4 h) in periportal and pericentral hepatocytes, producing identical hybridization pictures when co-stained with albumin. The sequence used for antisense G6pc cRNA preparation in this study belongs to a very specific isoform only expressed in liver hepatocytes and does not detect other glucose-6-phosphatase isoforms[44]. The very distinct

G6pc1 expression pattern are visible on days 1, 2, and 3 (Figure 23 b3-5). Higher resolution (Figure 24 f1-3 and g1-3) clearly showed G6pc1 expression in the “damaged” pericentral area. Gapdh has a basic function in cells: it is considered a housekeeping gene and gene expression reference. In fact, total mRNA levels for Gapdh did not significantly change during treatment (only a slightly higher expression relative to albumin was detected on day 6) Figure 25, and were similar to Arg1 and Gys2 expression[44].

While Gapdh plays a central role in energy generation, its ability to identify in cells with high energy requirements should also be considered. In healthy, untreated mice, Gapdh is homogeneously expressed in the pericentral and periportal areas of the liver. The distribution of Gapdh mRNA in mice livers treated with CCl_4 adheres to the albumin pattern in the first 6h, but at later time-points, such as from days 1 to 3, Gapdh showed an increased expression in the damaged areas (Figure 23 e3-5, and 24 i0-3), clearly reflecting continuous Gapdh expression. Interestingly, some cells in the damaged pericentral area expressed Gapdh with high intensity (Figure 23 e3-5, and 24 i1-3) [44]. This staining clearly shows cells with high metabolic activity present in the damaged area by day 3. When all these data are taken together, the following picture emerges: Gys2 expression does not change significantly and remains uniform at different time points. While Gcgr expression is uniformly reduced, G6pc shows the most dynamic pattern. After an immediate induction at 3h post injection, its expression is significantly reduced on day 1 and is followed by a continuous increase until day 6. Interestingly, while overall expression is reduced (Figure 25), ISH clearly shows that G6pc1 expression is not uniformly lost and a high level of expression is retained in the damaged area (Figure 23, 24, and 27B). This high metabolic activity is further reflected by associating with Gapdh expression in the damaged area (Figure 23e, and 24i) [44].

This research built upon our previous studies by considering other enzymes responsible for cell recovery after damage by free radicals. In an oxidative stress condition, Glutathion is used as an

electron donor by Glutathione peroxidase 4 enzyme (Gpx4) to protect hepatocytes against peroxides such as hydrogen peroxide (H_2O_2) and organic hydroperoxides (ROOH). In this process, toxic molecules are neutralized and two glutathione molecules form the disulfide bond glutathione disulfide (GSSG). GSSG is also a substrate for Glutathione reductase (GSR) and can change GSSG to producer molecules (Figure 10) [49]. Measuring the GSH/GSSG ratio shows cell toxicity, a ratio that is close to 90% in healthy cells. Gss, Gpx4, and Gsr are considered strategic enzymes for healthy cells [50].

Glutathione synthetase (Gss) as the Glutathion (GSH) producer and peroxidase 4 enzyme (Gpx4) were chosen. To study Gss and Gpx4 expression during CCl_4 treatment, ISH was completed for all liver sections. Gene expression is shown separately in figure 26 for Gss and Gpx4 (violet) when co-stained with albumin as PPHs marker (orange). To compare mono- and co-staining with albumin, pictures were taken with two magnifications after the initial staining (violet), and ISH was continued for the next staining (Figure 26). Gpx4 were expressed higher in PPHs [24, 51] than PCHs in normal livers, and our staining for normal liver section showed that PPHs expressed Gpx4 more than HPCs, and that Gss expression had the same pattern as Gpx4 (Figure 26). Three hours post CCl_4 injection, both genes were almost equally expressed in both areas. Gene expression patterns were changed and shifted to the PCHs at 6 hours post injection and continued to reach the maximum levels in PCHs during days 1 and 2 Expression of both genes decreased in PCHs on day three, Gss high expression was completely lost but Gpx4 expression was sill detectable in PCHs. Both genes' expression had returned to normal on day 6. It is clear that Gpx4 and even Gss expression are raised in response to increased toxic Cyp2e1 by-product molecules in PCHs. Interestingly, at day three post injection, Cyp2e1 and Gss were expressed only in a mono layer of cells between PPHs and PHCs; these cells are also the last cells in the PPH area which expressed albumin (Figure 26 c6, d6, j6 and l6). At the same time, since Gpx4 is expressed within the cells in the PCHs, this may indicate the co-expression of Cyp2e1 and Gss at

the same time and in the same cells, because of the activity and toxic by-products of Cyp2e1 activity. Gpx4 expression, however, continues simultaneously in cells located in the inner layer of the pericenteral area. Examining Cyp2e1 expression required for CCl4 metabolism also clearly showed the specific gene expression response to the toxic challenge. While overall expression of Cyp2e1 is immediately down regulated post CCl_4 exposure (the lowest levels occurred on days 1 to 3 and were followed by a recovery on day 6), the specific Cyp2e1 gene expression stained with ISH clearly showed a local and specific increased expression pattern in the pericentral area (Figure 23 f). At higher magnification (Figure 24 j), strong signals for Cyp2e1 mRNA are clearly visible in the damaged areas, which define a boundary along the area with higher albumin expression.

ISH reliability was shown by comparing Alpha-smooth muscle actin (aSMA is considered the gene expressed by activated stellate cells) at the gene and protein levels and by using ISH and IHC methods (Figure 27A). It is therefore clear that protein and gene expression exhibit the same patterns at different time points.

6 Discussion:

The first part of the results demonstrates the introduced method for cRNA preparation is sensitive and specific, at least for albumin transcript detection in sections of adult mouse liver, as well as albumin and AFP transcripts, in human liver cancer sections. Upon staining with albumin-specific probes, the heterogeneously distribution of albumin mRNA expression in the liver sections were seen. This result is in keeping with the published results of traditional probe preparation protocols [39]. The traditional preparation of cRNA includes five established protocols, target cDNA amplification, cloning of cDNA in a plasmid vector with appropriate RNA polymerase promoters upstream and downstream of the cloned cDNA fragment, large-

scale preparation of the plasmid vector, restriction digest of the template vector and a final purification step before in vitro transcription of the labelled cRNA.

In contrast, rapid and efficient of new protocol for labelled cRNA probe synthesis proves that cRNA preparation begins during the equivalent of what was the 5^{th} step of the old method. Further, using purified PCR fragments does not require cloning, plasmid selection, and preparation. The cRNA probes generated by the new protocol are ideally suited to detect specific mRNAs in paraffin sections or cultured cell lines in media (*in vitro*) and enable visualization of specific mRNAs comparable to previously published results [39, 44, 52]. The AFP and BMP9 specificity staining [52] in the cancerous area of human HCC sections showed the general applicability of the new protocol for histological analysis. Taken together, the major advantages of the new simple protocol are the short time required for cRNA labelled preparation. To follow up the liver injury in animal model during recovery from CCl_4 injection, the new method was developed for different antisense cRNAs preparation. Mice treated with an acute toxic dose of CCl4, which leads to massive changes in the liver, including a possibility of necrotic cell death in the pericentral area and subsequent regeneration involves degradation and removal of the remaining cell debris and repopulation of the necrotic area by proliferating hepatocytes from adjacent unaffected areas [17, 53-56]. This step is conducted based on the assumption that CCl4 treatment leads to strong changes in liver enzyme serum levels and liver tissue morphology. The induced changes are mostly in the pericentral area (damaged zone) [17, 57], visualizations of apoptotic cell nuclei, and transient caspase activation [58]. In this study, enzyme expressions involved in nitrogen (ammonia) metabolism, glucose storage and release were analysed. These are responsible for cell recovery from damage induced by CCl_4 in mouse liver (a well-established model for liver cell damage [59]). Obtained results clearly show continuous gene expression (Fig 22, 23, 24 and 26) and intact nuclei (Fig 21). Such ongoing gene expression

requires de novo synthesis of mRNA, in the area around the pericentral vein (considered the damaged area) throughout the time course analyzed. De novo synthesis of mRNA can occur only in living cells and reflects gene expression in the specific area. The correlation between mRNA expression and protein synthesis during CCl4 treatment has also been shown for alpha-smooth muscle actin (aSma) (Figure 27 A), [44]. Time dependent results obtained from ISH (the changes in gene expression patterns) indicate that large numbers of cells in the pericentral area survived and contributed to regeneration and recovery from damage. Nevertheless, CCl4 treatment induced visible tissue damage with a loss of cell-cell interactions, and infiltration of blood cells into the damaged area around the pericentral vein (Fig 28). RBCs infiltration in the space between damaged pericentral hepatocytes may be the key reason for the increase in aSMA expression at the protein and mRNA level in some cells in pericentral area (Fig 27A) [60, 61]. The analysis of total gene expression levels by quantitative real time PCR and using primers recognizing arginase (Arg1), glycogen synthase (Gys2), glucagon receptor (Gcgr), Gapdh, glutaminase (Gls2), glutamine synthase (Gs), glucose-6-phosphatase (G6pc), cytochrome p450 2E1 (Cyp2e1), and Albumin (Alb) (which was used for normalization and as a reference gene) is presented in Figure 25 [44]. The combination of RT-qPCR data with gene specific staining revealed, unlike the previously published results which showed cell death around the central vein after CCl4 treatment [34], a more complex response should be considered in the damaged area. These responses include cell survival and neutralization of the toxic effect of new by-products. One of the clear indicators of liver parenchymal cell viability is G6pc expression, the glucose-6-phosphatase isoform is expressed only in hepatocytes [44]. In the damaged pericentral area, despite a strong reduction of total G6pc mRNA levels as analyzed by RT-qPCR (Figure 25), G6pc was expressed increasingly by some pericentral hepatocytes even as late as 3 days post CCl_4 injection. The increased expression of G6p (hepatocyte specific isoform) was complemented by high Gapdh mRNA signals in the same

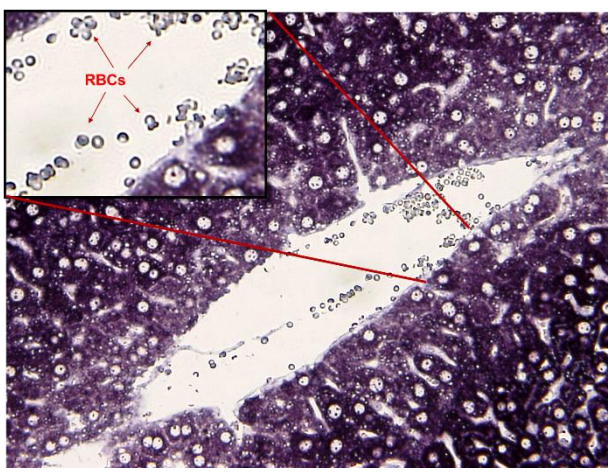

3h

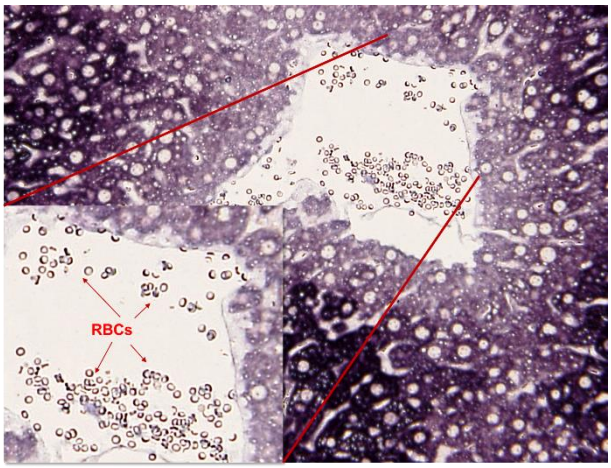

6h

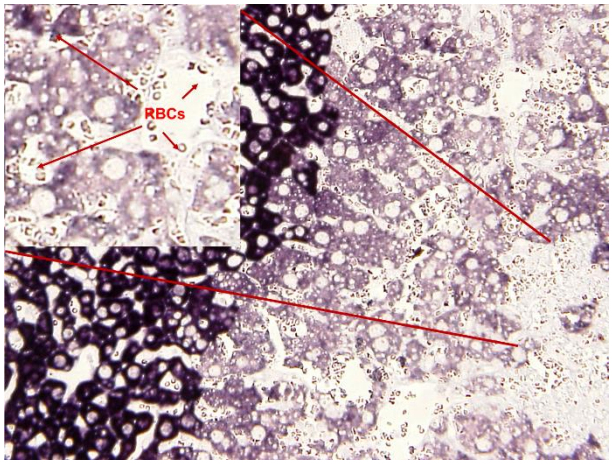

1d

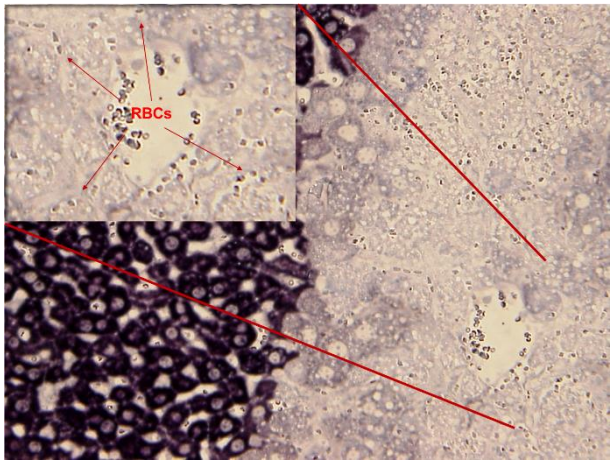

2d

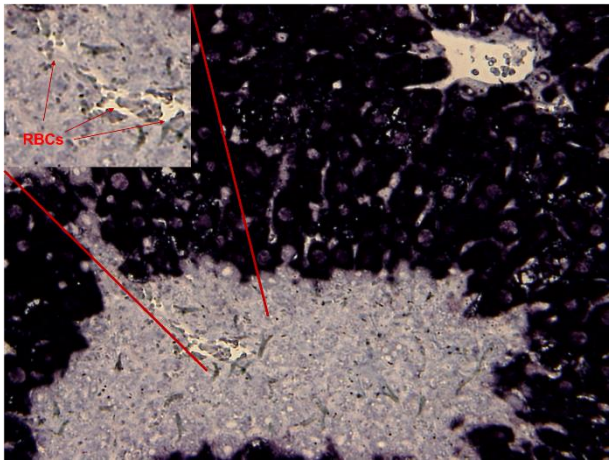

3d

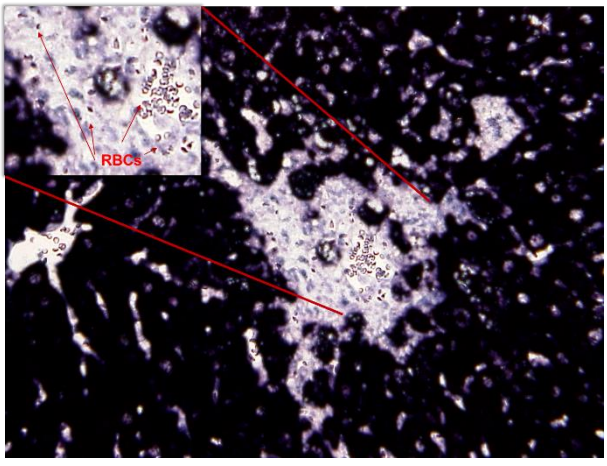

6d

Figure 28: RBCs (red blood cells) penetration and depletion from the damaged area post CCl_4 injection, during different time points. Albumin gene expression was used as a marker for periportal area

area, albeit not necessarily in the same cells. Another selective expression for genes required for ammonia elimination and glutamine level maintenance was also observed. While RT-qPCR results show that the total expression of Arg1 did not significantly change, its expression increased in some damaged area cells at later time points (Fig 24 a&b). The reorganization of Arg1 expression in the pericentral area not only has a very specific pattern of tissue distribution during the time course but also exhibits a late recovery [44].While the expressions of albumin and arginase mRNAs overlap at early and late time points, indicating that expression is specific to periportal hepatocytes, a quite different picture is observed at day 2 post CCl_4 injection, where Arg1 is expressed in a speckled pattern in the damaged area. Since Arg1 is not expressed in hepatocytes alone, and can appear in many other cell types, this signal could also come from non-parenchymal cells. Such cells include stellate cells and infiltrating blood monocytes which have both been described to express Arg 1 [62, 63]. On days 1 and 2, glutamine synthase also showed a speckled expression in the pericentral zone. These speckled stainings do not overlap, which indicates that arginase and glutamine synthase expressions occur in different cell populations in the damaged area. Cyp2e1, Gpx4, and Gss expression over time are the most compelling adjustments of gene expression upon CCl4. Cyp2e1 was expressed throughout the liver but expression was much higher around the pericentral vein in healthy liver mice, and after recovery at day 6. Three hours post CCl_4 injection, and at early time points, Cyp2e1 expression increased locally, in the pericentral area, although overall expression in total liver lysates was reduced (perhaps because of reduced expression in the periportal hepatocytes). This change continued at later time points and zonation of Cyp2e1 expression reached a sharp and clear boundary-like expression pattern which separated the albumin producing periportal area and the damaged pericentral region (Figures 23f, 22j, 25, 26, and 27B). Cyp2e1 mono staining at day 3 (Fig 26) showed a sharp expression in a rim of hepatocytes around the pericentral area, which seems to be the last frontline for CCl_4 neutralization. Co-staining with Alb revealed that these

cells are the first hepatocytes around the pericentral area to express Alb (at day 3). Gss also showed the same weaker expression pattern. Gpx4, as the key enzyme for free radical molecule neutralization, was generated during all time points (Fig 26). Although activation of CCl4 by Cyp2e1 contributes to the observed severe damage, the very specific pattern of Cyp2e1 and Gpx4 expressions could ensure efficient transformation and detoxification of CCl4 and its by-products in the pericentral area to neutralize and prevent further spread of the toxic agent into other areas, thereby limiting overall tissue damage and ultimately supporting regeneration. The gene expression pattern during treatment was summarized in figure 29.

7 Conclusion:

The detialed analysis of the expression of genes, required for detoxification, nitrogen metabolism, and glucose utilization, in the liver upon damage induced by CCl_4, revealed a rapid adjustment of gene expression patterns on both the spatial distribution and the overall level. The changes and local shifts of gene expression patterns confirmed that CCl4 mediated damage occured specifically around the central vein. The key observations were: (I) while the initial pattern of Cyp2e1 expression around the centrail vein is responsible for the strong local damage, the readjustment of the Cyp2e1 gradient with very high expression just aroung the damage array could confine damage and ensure rapid detoxification; (II) shortly after induction of Gss and Gpx4 occured in the damaged pericentral area, providing enhanced metabolic capacity, required to further neutralize CCl_4 by-products and damage; (III) this is followed by increased local mobilization of glucose from hepatocytes in the damaged area, reflected in local higher levels of

G6pc expression, which can provied glucose for the intense metabolism required for repair and recovery and elimination of infiltrated RBCs by Kupffer or other immune cells in the damaged area; (IV) importantly this also confirmed, that CCl_4 damage didn't immediately induce cell death but rather leads to a rapid response and adjustment of expression patterns against the toxic effects. Thus, it can be assumed that CCl_4 toxicity didn't lead to complete necrotic, massive cell death in the damaged liver tissue, but rather resulted at least in part in a functional transition supporting recovery. The results presented here clearly show that hepatocytes in the damaged area did not undergo massive necrotic or induced cell death but rather a clear adaptive response that can support the recovery from damage and formation of new hepatic tissue in the damaged area [44]. Liver cells remained viable in the damaged area and adjusted gene expression accordingly, to orchestrate protection from further damage and to enable efficient recovery in this area. In the end after repair and regeneration, normal gene expression patterns are reestablished, e.g. Cyp2e1 transcription, on day 6 post CCl_4 injection [44]. Liver zonation is of uppermost importance for orchestrating the biochemical metabolism of the liver, as it not only plays an important role for the maintenance of basic liver functions, but is also needed for overall health. It also helps the liver to cope with damage caused by toxins by limiting the damage to smaller areas. In addition, adjusted gene expression patterns and sustained viability of all liver cell types in response to damage should enable the observed efficient recovery of the damaged region [44]. To visualize these contributions the gene expression patterns observed in liver sections representing damage, damage response and recovery are summarized in Figure 29.

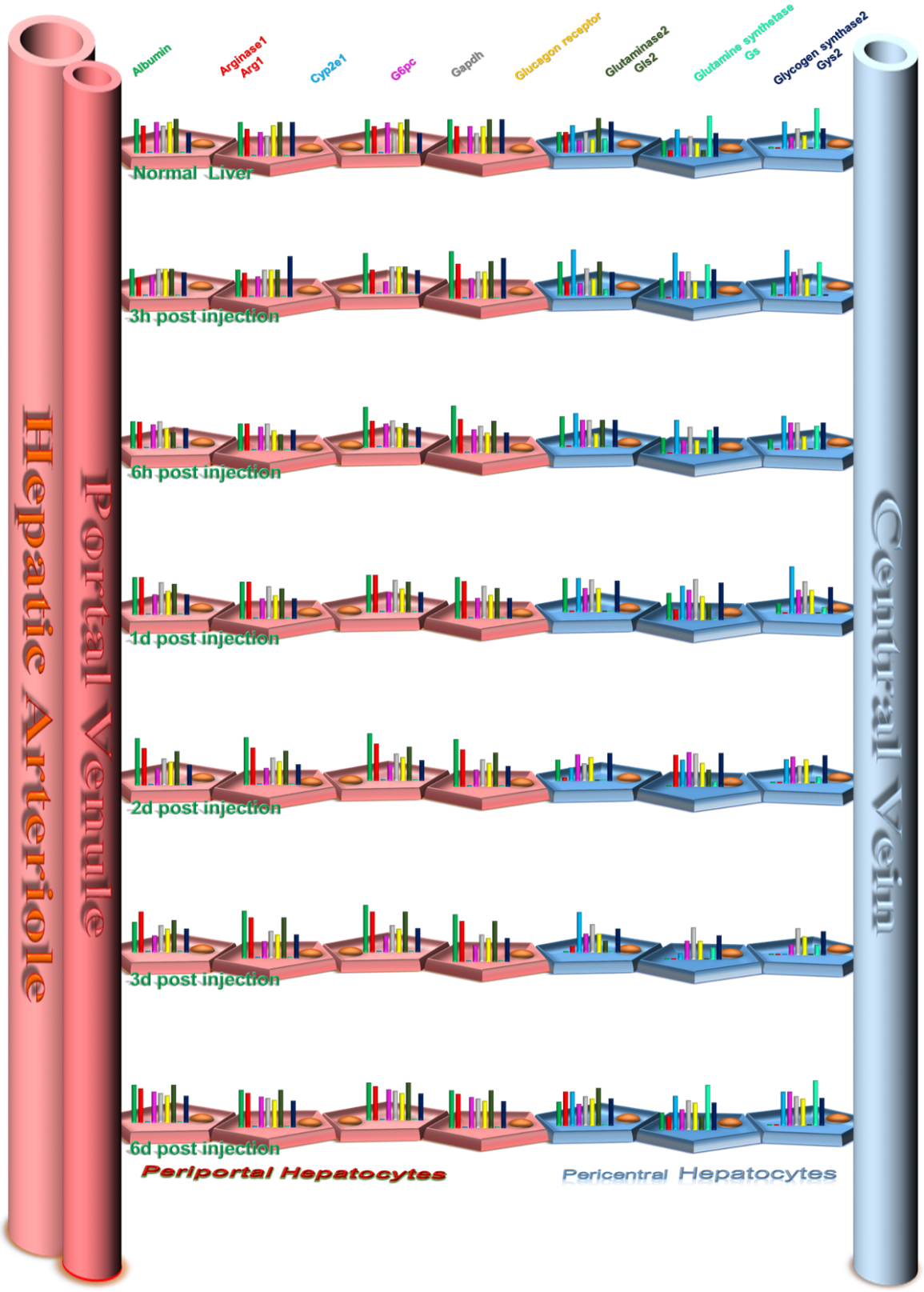

Figure 29. Graphical summary of the area specific gene expression patterns. Results from the ISH analysis are summarized as 7 conditions. Healthy liver (normal), 3h, 6h, 1 day(1d), 2 days (2d), 3 days (3d), and 6 days (6d) after CCl4 treatment. Column size reflects the relative intensity of expression for each gene and different colours are used: dark green for Albumin, red for Arginase1, light blue for Cyp2e, violet for G6pc, grey for Gapdh, yellow for Glucagon receptor, brown for Glutaminase, light green for Glutamine synthetase, and dark blue for Glycogen synthase expression.

8 References

[1] Si-Tayeb K, Lemaigre FP, Duncan SA. Organogenesis and development of the liver. Dev Cell 2010;18:175-189.
[2] Jenne CN, Kubes P. Immune surveillance by the liver. Nat Immunol 2013;14:996-1006.
[3] Crispe IN. Liver antigen-presenting cells. Journal of hepatology 2011;54:357-365.
[4] Jungermann K, Kietzmann T. Oxygen: modulator of metabolic zonation and disease of the liver. Hepatology 2000;31:255-260.
[5] Jungermann K. Zonation of metabolism and gene expression in liver. Histochem Cell Biol 1995;103:81-91.
[6] Haussinger D, Schliess F. Glutamine metabolism and signaling in the liver. Front Biosci 2007;12:371-391.
[7] Haussinger D. Hepatocyte heterogeneity in glutamine and ammonia metabolism and the role of an intercellular glutamine cycle during ureogenesis in perfused rat liver. Eur J Biochem 1983;133:269-275.
[8] Haussinger D. Liver glutamine metabolism. JPEN J Parenter Enteral Nutr 1990;14:56S-62S.
[9] Moorman AF, de Boer PA, Watford M, Dingemanse MA, Lamers WH. Hepatic glutaminase mRNA is confined to part of the urea cycle domain in the adult rodent liver lobule. FEBS Lett 1994;356:76-80.
[10] Moore MC, Coate KC, Winnick JJ, An Z, Cherrington AD. Regulation of hepatic glucose uptake and storage in vivo. Adv Nutr 2012;3:286-294.
[11] Jonges GN, Van Noorden CJ, Lamers WH. In situ kinetic parameters of glucose-6-phosphatase in the rat liver lobulus. The Journal of biological chemistry 1992;267:4878-4881.
[12] Bartels H, Vogt B, Jungermann K. Glycogen synthesis via the indirect gluconeogenic pathway in the periportal and via the direct glucose utilizing pathway in the perivenous zone of perfused rat liver. Histochemistry 1988;89:253-260.
[13] Jungermann K, Kietzmann T. Zonation of parenchymal and nonparenchymal metabolism in liver. Annu Rev Nutr 1996;16:179-203.
[14] Jungermann K, Kietzmann T. Role of oxygen in the zonation of carbohydrate metabolism and gene expression in liver. Kidney Int 1997;51:402-412.
[15] Ghosh A, Shieh JJ, Pan CJ, Sun MS, Chou JY. The catalytic center of glucose-6-phosphatase. HIS176 is the nucleophile forming the phosphohistidine-enzyme intermediate during catalysis. The Journal of biological chemistry 2002;277:32837-32842.
[16] Snider NT, Weerasinghe SV, Singla A, Leonard JM, Hanada S, Andrews PC, et al. Energy determinants GAPDH and NDPK act as genetic modifiers for hepatocyte inclusion formation. The Journal of cell biology 2011;195:217-229.
[17] Weber LW, Boll M, Stampfl A. Hepatotoxicity and mechanism of action of haloalkanes: carbon tetrachloride as a toxicological model. Crit Rev Toxicol 2003;33:105-136.
[18] Meunier B, de Visser SP, Shaik S. Mechanism of oxidation reactions catalyzed by cytochrome p450 enzymes. Chem Rev 2004;104:3947-3980.
[19] Guengerich FP. Cytochrome p450 and chemical toxicology. Chem Res Toxicol 2008;21:70-83.
[20] Sligar SG, Cinti DL, Gibson GG, Schenkman JB. Spin state control of the hepatic cytochrome P450 redox potential. Biochem Biophys Res Commun 1979;90:925-932.

[21] Poli G, Cheeseman K, Slater TF, Dianzani MU. The role of lipid peroxidation in CCl4-induced damage to liver microsomal enzymes: comparative studies in vitro using microsomes and isolated liver cells. Chemico-biological interactions 1981;37:13-24.
[22] Couto N, Malys N, Gaskell SJ, Barber J. Partition and turnover of glutathione reductase from Saccharomyces cerevisiae: a proteomic approach. J Proteome Res 2013;12:2885-2894.
[23] Teselkin YO, Babenkova IV, Kolhir VK, Baginskaya AI, Tjukavkina NA, Kolesnik YA, et al. Dihydroquercetin as a means of antioxidative defence in rats with tetrachloromethane hepatitis. Phytother Res 2000;14:160-162.
[24] Lindros KO. Zonation of cytochrome P450 expression, drug metabolism and toxicity in liver. General pharmacology 1997;28:191-196.
[25] Wong FW, Chan WY, Lee SS. Resistance to carbon tetrachloride-induced hepatotoxicity in mice which lack CYP2E1 expression. Toxicol Appl Pharmacol 1998;153:109-118.
[26] Lindros KO, Cai YA, Penttila KE. Role of ethanol-inducible cytochrome P-450 IIE1 in carbon tetrachloride-induced damage to centrilobular hepatocytes from ethanol-treated rats. Hepatology 1990;12:1092-1097.
[27] Haussinger D, Gerok W. Hepatocyte heterogeneity in ammonia metabolism: impairment of glutamine synthesis in CCl4 induced liver cell necrosis with no effect on urea synthesis. Chemico-biological interactions 1984;48:191-194.
[28] Mokuda O, Ubukata E, Sakamoto Y. Impaired glucose uptake and intact gluconeogenesis in perfused rat liver after carbon tetrachloride injury. Biochemical and molecular medicine 1995;54:38-42.
[29] Masuda Y, Yano I, Murano T. Comparative studies on the hepatotoxic actions of chloroform and related halogenomethanes in normal and phenobarbital-pretreated animals. Journal of pharmacobio-dynamics 1980;3:53-64.
[30] Coghlan JP, Aldred P, Haralambidis J, Niall HD, Penschow JD, Tregear GW. Hybridization histochemistry. Anal Biochem 1985;149:1-28.
[31] Gall JG, Pardue ML. Formation and detection of RNA-DNA hybrid molecules in cytological preparations. Proc Natl Acad Sci U S A 1969;63:378-383.
[32] Wilkinson DG. RNA detection using non-radioactive in situ hybridization. Current opinion in biotechnology 1995;6:20-23.
[33] Hart SM, Basu C. Optimization of a digoxigenin-based immunoassay system for gene detection in Arabidopsis thaliana. J Biomol Tech 2009;20:96-100.
[34] Dirks RW, Van Gijlswijk RP, Vooijs MA, Smit AB, Bogerd J, van Minnen J, et al. 3'-end fluorochromized and haptenized oligonucleotides as in situ hybridization probes for multiple, simultaneous RNA detection. Experimental cell research 1991;194:310-315.
[35] Wiegant J, Ried T, Nederlof PM, van der Ploeg M, Tanke HJ, Raap AK. In situ hybridization with fluoresceinated DNA. Nucleic acids research 1991;19:3237-3241.
[36] Bauman JG, Wiegant J, Borst P, van Duijn P. A new method for fluorescence microscopical localization of specific DNA sequences by in situ hybridization of fluorochromelabelled RNA. Experimental cell research 1980;128:485-490.
[37] Renz M, Kurz C. A colorimetric method for DNA hybridization. Nucleic acids research 1984;12:3435-3444.
[38] Hopman AH, Wiegant J, Tesser GI, Van Duijn P. A non-radioactive in situ hybridization method based on mercurated nucleic acid probes and sulfhydryl-hapten ligands. Nucleic acids research 1986;14:6471-6488.
[39] Ghafoory S, Breitkopf-Heinlein K, Li Q, Dzieran J, Scholl C, Dooley S, et al. A fast and efficient polymerase chain reaction-based method for the preparation of in situ hybridization probes. Histopathology 2012;61:306-313.
[40] Cox KH, DeLeon DV, Angerer LM, Angerer RC. Detection of mrnas in sea urchin embryos by in situ hybridization using asymmetric RNA probes. Developmental biology 1984;101:485-502.
[41] Chien A, Edgar DB, Trela JM. Deoxyribonucleic acid polymerase from the extreme thermophile Thermus aquaticus. Journal of bacteriology 1976;127:1550-1557.

[42] Chou Q, Russell M, Birch DE, Raymond J, Bloch W. Prevention of pre-PCR mis-priming and primer dimerization improves low-copy-number amplifications. Nucleic acids research 1992;20:1717-1723.
[43] Brownie J, Shawcross S, Theaker J, Whitcombe D, Ferrie R, Newton C, et al. The elimination of primer-dimer accumulation in PCR. Nucleic acids research 1997;25:3235-3241.
[44] Ghafoory S, Breitkopf-Heinlein K, Li Q, Scholl C, Dooley S, Wolfl S. Zonation of nitrogen and glucose metabolism gene expression upon acute liver damage in mouse. PLoS One 2013;8:e78262.
[45] Evarts RP, Nagy P, Marsden E, Thorgeirsson SS. In situ hybridization studies on expression of albumin and alpha-fetoprotein during the early stage of neoplastic transformation in rat liver. Cancer research 1987;47:5469-5475.
[46] Yu H, Yoo PK, Aguirre CC, Tsoa RW, Kern RM, Grody WW, et al. Widespread expression of arginase I in mouse tissues. Biochemical and physiological implications. The journal of histochemistry and cytochemistry : official journal of the Histochemistry Society 2003;51:1151-1160.
[47] Schols L, Mecke D, Gebhardt R. Reestablishment of the heterogeneous distribution of hepatic glutamine synthetase during regeneration after CCl4-intoxication. Histochemistry 1990;94:49-54.
[48] Pesce JT, Ramalingam TR, Mentink-Kane MM, Wilson MS, El Kasmi KC, Smith AM, et al. Arginase-1-expressing macrophages suppress Th2 cytokine-driven inflammation and fibrosis. PLoS pathogens 2009;5:e1000371.
[49] Holmgren A, Johansson C, Berndt C, Lonn ME, Hudemann C, Lillig CH. Thiol redox control via thioredoxin and glutaredoxin systems. Biochemical Society transactions 2005;33:1375-1377.
[50] Meister A. Glutathione metabolism and its selective modification. The Journal of biological chemistry 1988;263:17205-17208.
[51] Kera Y, Penttila KE, Lindros KO. Glutathione replenishment capacity is lower in isolated perivenous than in periportal hepatocytes. The Biochemical journal 1988;254:411-417.
[52] Li Q, Gu X, Weng H, Ghafoory S, Liu Y, Feng T, et al. Bone morphogenetic protein-9 induces epithelial to mesenchymal transition in hepatocellular carcinoma cells. Cancer science 2013;104:398-408.
[53] Sun F, Hamagawa E, Tsutsui C, Ono Y, Ogiri Y, Kojo S. Evaluation of oxidative stress during apoptosis and necrosis caused by carbon tetrachloride in rat liver. Biochimica et biophysica acta 2001;1535:186-191.
[54] Ichi I, Nakahara K, Fujii K, Iida C, Miyashita Y, Kojo S. Increase of ceramide in the liver and plasma after carbon tetrachloride intoxication in the rat. Journal of nutritional science and vitaminology 2007;53:53-56.
[55] Jaeschke H, Williams CD, Ramachandran A, Bajt ML. Acetaminophen hepatotoxicity and repair: the role of sterile inflammation and innate immunity. Liver international : official journal of the International Association for the Study of the Liver 2012;32:8-20.
[56] Godoy P, Hewitt NJ, Albrecht U, Andersen ME, Ansari N, Bhattacharya S, et al. Recent advances in 2D and 3D in vitro systems using primary hepatocytes, alternative hepatocyte sources and non-parenchymal liver cells and their use in investigating mechanisms of hepatotoxicity, cell signaling and ADME. Archives of toxicology 2013;87:1315-1530.
[57] Steup DR, Hall P, McMillan DA, Sipes IG. Time course of hepatic injury and recovery following coadministration of carbon tetrachloride and trichloroethylene in Fischer-344 rats. Toxicologic pathology 1993;21:327-334.
[58] Meng Z, Wang Y, Wang L, Jin W, Liu N, Pan H, et al. FXR regulates liver repair after CCl4-induced toxic injury. Molecular endocrinology 2010;24:886-897.
[59] Reynolds ES. Liver Parenchymal Cell Injury. I. Initial Alterations of the Cell Following Poisoning with Carbon Tetrachloride. The Journal of cell biology 1963;19:139-157.
[60] Grierson I, Lee WR. Further observations on the process of haemophagocytosis in the human outflow system. Albrecht von Graefes Archiv fur klinische und experimentelle Ophthalmologie Albrecht von Graefe's archive for clinical and experimental ophthalmology 1978;208:49-64.
[61] Tsui WM, Wong KF, Tse CC. Liver changes in reactive haemophagocytic syndrome. Liver 1992;12:363-367.

[62] Kasten J, Hu C, Bhargava R, Park H, Tai D, Byrne JA, et al. Lethal phenotype in conditional late-onset arginase 1 deficiency in the mouse. Molecular genetics and metabolism 2013;110:222-230.
[63] Weisser SB, Kozicky LK, Brugger HK, Ngoh EN, Cheung B, Jen R, et al. Arginase activity in alternatively activated macrophages protects PI3Kp110delta deficient mice from dextran sodium sulfate induced intestinal inflammation. European journal of immunology 2014;44:3353-3367.

Acknowledgments:

I would like to thank Prof. Dr. Stefan Wölfl for accepting me as his group member and giving me the chance to pursuit this project, I also thank him for his scientific support during my PhD studies.

I also thank Prof. Dr. Steven Dooley and PD. Dr. Katja Breitkopf-Heinlein for helping me in this research and Dr. Qi Li for an excellent cooperation. I appreciate the help from all colleagues working at the Institute of Pharmacy and Molecular Biotechnology at Heidelberg University with a nice working atmosphere specially Julia Lochead and Jannick Theobald. I would like to thank my wife, my son, my father and my mother for endless love and support and always encouraging me with great patience. At the end I would like to sincerely thank all my friends.